PROVENANCE OF A POLYDEFORMED METASEDIMENTARY SUCCESSION ON THE CANADIAN SHIELD: INSIGHTS FROM NEW U-PB, HF, AND O ISOTOPE ANALYSIS OF DETRITAL ZIRCON FROM THE PALEOPROTEROZOIC MURMAC BAY GROUP

A THESIS SUBMITTED TO THE COLLEGE OF GRADUATE AND POSTDOCTORAL STUDIES IN PARTIAL FULFILLMENT OF THE REQUIREMENTS FOR THE DEGREE OF MASTER OF SCIENCE IN THE DEPARTMENT OF GEOLOGICAL SCIENCES UNIVERSITY OF SASKATCHEWAN

Christine Shiels

COPYRIGHT STATEMENT

In presenting this thesis in partial fulfilment of the requirements for a Postgraduate degree from the University of Saskatchewan, I agree that the Libraries of this University may make it freely available for inspection. I further agree that permission for copying of this thesis in any manner, in whole or in part, for scholarly purposes may be granted by the professor or professors who supervised my thesis work or, in their absence, by the Head of the Department or the Dean of the College in which my thesis work was done. It is understood that any copying or publication or use of this thesis or parts thereof for financial gain shall not be allowed without my written permission. It is also understood that due recognition shall be given to me and to the University of Saskatchewan in any scholarly use which may be made of any material in my thesis. Chapter two is reproduced under the Geological Society of America "Fair Use" policy, see: http://www.geosociety.org/GSA/Publications/Info_Services/Copyright/GSA/Pubs/guide/copyright.aspx. This document has been reformatted from its original version for inclusion in this thesis.

Requests for permission to copy or to make other use of material in this thesis in whole or part should be addressed to:

Head of the Department of Geological Sciences

14 Science Place

University of Saskatchewan

Saskatoon, Saskatchewan

Canada S7N 5E2

ACKNOWLEDGEMENTS

I would like to express my deepest gratitude to my husband, Darcy Shiels, for convincing me to pursue higher education, for always believing in my abilities, and for being a pillar of both emotional and physical support, which was integral to my achievements. I would also like to thank my mother, Trudy Bartel, for her boundless support and encouragement.

My gratitude also goes out to Dr Sam Butler for encouraging me to try my hand at research while I was an undergraduate, and for all of his support and advice during both undergraduate and graduate studies. Thank you for believing in my potential, even though I didn't see it in myself.

I would like to thank my colleagues and friends from the University of Saskatchewan Department of Geological Sciences for all of their help, support, and sometimes their much-welcomed distractions, especially Victoria Stinson, Michael McConnell, Dr Jim Merriam, David Gebhardt, Josh Leland, Dr Yuanming Pan, Michael Cuggy, Stephanie Boulanger, Glecy Gamelin, Brayden McDonald, Chantal Strachan-Crossman, Michelle Howe, and Luc Chabanole.

I express sincere gratitude for assistance and guidance in the technical aspects of my research to Richard Stern, Rebecca Lam, and Bill Davis, and also to Natural Sciences and Engineering Research Council Canada (NSERC) and Natural Resources Canada Geo-Mapping for Energy and Minerals (GEM-2) for contributing funding for my project. I would also like to thank the members of my committee for their participation in my thesis, Drs Bruce Eglington, Kevin Ansdell, Ken Ashton, and my supervisor Dr Camille Partin.

ABSTRACT

The proximity and positions of the cratons that make up the Canadian Shield prior to and during the Rhyacian Period (2.30-2.05 Ga) are poorly known. The position of the Rae craton relative to the now proximal Slave, Hearne, and other microcontinents, such as the Buffalo Head-Chichaga domains, during this time period is not well defined. This is due in part to their boundaries having been overprinted by younger orogenic events. Sedimentary successions deposited near craton margins provide an opportunity to test hypotheses regarding nearest cratonic neighbors during deposition by reconstructing their sedimentary provenance using detrital zircon isotopic data. The polydeformed nature of the Murmac Bay Group, a metasedimentary succession deposited near the southwestern margin of the Rae craton in northern Saskatchewan, Canada, presents challenges in determining detailed stratigraphic relationships in the upper succession, which lacks distinct marker beds. Presented here is the first integrated detrital zircon U-Pb geochronology, Lu-Hf, and O isotope analysis of detrital zircon from these rocks in order to elucidate provenance, basin tectonic setting, and characterize crustal growth in the source regions. Previous U-Pb geochronology suggests the lower succession was deposited <2.32 Ga and the upper succession between <2.17 Ga and >1.93 Ga. New U-Pb detrital zircon ages for the upper succession define a new maximum depositional age constraint at <2.00 Ga. Analysis of published U-Pb detrital zircon age spectra suggest the tectonic setting for the upper Murmac Bay Group paleobasin was in the foreland of the Taltson orogeny. Integrating the U-Pb data with new Lu-Hf and O isotope data shows that the most probable source rocks, in addition to Rae crustal rocks, were granites that are currently buried under Phanerozoic cover in the Buffalo Head-Chinchaga domains of northern Alberta. Unique U-Pb age peaks that would point to the Hearne craton as a sediment source were not identified.

Hafnium model ages calculated from the upper Murmac Bay Group identify two periods of regional crustal growth at 2.83 Ga and 2.70 Ga, agreeing with Sm-Nd model ages from the western Churchill province.

TABLE OF CONTENTS

LIST OF TABLES

LIST OF FIGURES

CHAPTER 1: INTRODUCTION

The continental crust provides a record of the tectonic events and processes that have shaped our planet's evolution. Some of the oldest rocks and minerals known on Earth are the ~4.03 Ga to 4.00 Ga Acasta Gneisses located on the Slave craton of the northwest Canadian Shield (Bowring and Williams, 1999) and ~4.40 Ga detrital zircons from western Australia in the Jack Hills region (Wilde et al., 2001), which suggest that continental crust has existed on Earth for at least 4.40 billion years. In contrast the record preserved by oceanic crust extends only ~200 Ma (Hawkesworth et al., 2010). Crustal reworking through tectonic processes biases this record; as crustal material is recycled into the mantle, it is subject to increasing temperatures and pressures, which have the potential to reset the isotope systems that can be utilized for geochronological dating. Only the most robust minerals, such as zircon, are able to survive through some of these processes with the isotope ratios from their time of initial crystallization intact. Thus, there is a dearth of preserved material from Earth's earliest crust from which we can infer the timing and mechanisms of its generation and evolution.

There is considerable discussion as to what extent this preservation bias of continental crust affects our understanding of early Earth (e.g., Hawkesworth and Kemp, 2006; Hawkesworth et al., 2009, 2010, 2013; Condie et al., 2011; Lancaster et al., 2011; Roberts and Spencer, 2015; Spencer et al., 2015; Payne et al., 2016). Peaks and troughs in the detrital zircon record of modern sediments have been thought to represent either episodic crustal growth and magmatic activity during the peaks (e.g., Condie, 1998), or alternatively, this pattern has been interpreted as a function of crustal preservation. The volume of magma generated and preserved can vary widely by tectonic setting (Hawkesworth et al., 2009), for instance, in extensional settings, the magma generated is largely mafic, and thus is unlikely to contain substantial amounts of zircon. In contrast, magmatism in collision settings during supercontinent assembly tends to be granitic, derived from partial melting of existing crust and generally low in volume (Hawkesworth et al., 2010). The surrounding continental crust provides protection from tectonic recycling to these newly generated granitic rocks, and thus increases their potential for preservation. Peaks in the global detrital zircon record broadly coincide with periods of

supercontinent assembly, supporting the selective preservation interpretation (e.g., Campbell and Allen, 2008; Hawkesworth and Kemp, 2006; Kemp et al., 2006).

The timing of amalgamation of the cratons that make up the Canadian Shield (Figure 1.1) during the early Paleoproterozoic is still under investigation. Paleogeographic reconstructions, such as in Figure 1.2, require an abundance of stratigraphic, paleomagnetic, and isotopic data to accurately constrain relative craton positions. Much of the Canadian Shield has currently been mapped and dated only at a reconnaissance level, and the more detailed regional data that is published and available for analysis, the more robust these reconstructions can become. The southern Rae craton margin borders the Slave craton to the west, the Buffalo Head terrane to the south, separated by the Taltson magmatic zone, and also the Hearne craton to the east. The timing of amalgamation of these cratonic blocks to the Rae is widely debated, as discussed further in chapter two.

Isotope systems preserved in sedimentary rocks preserve a wealth of information regarding the Earth's history, including depositional environment, paleoclimate, timing of tectonic events and crustal growth, and the history of life. Older sedimentary successions can present a particular challenge in deciphering this information, as they have often been exposed to one or more episodes of metamorphism and deformation, thus careful analysis and interpretation of detrital zircons is necessary in order to distinguish between igneous zircons and zones within zircons, and those which formed as a result of metamorphism.

The Rae craton is host to several Paleoproterozoic sedimentary successions, many of which have been dated using U-Pb geochronology (e.g., Bostock and van Breemen, 1994; Van Breemen and Aspler, 1994; McDonough and McNicoll, 1997; Hartlaub et al., 2006; Martel et al., 2008; Bethune et al., 2010; Rainbird et al., 2010; Ashton et al., 2013; Partin et al., 2014a; Wodicka et al., 2014). This study expands on that approach by integrating U-Pb, Hf and O isotopes, and by utilizing DateView, an extensive database of U-Pb zircon crystallization and metamorphic ages (Eglington, 2004; Eglington et al., 2013) to investigate sediment provenance. This study centers on a polydeformed Paleoproterozoic sedimentary succession, the upper Murmac Bay Group, which was deposited in the Beaverlodge domain on the southwest margin of the Rae craton.

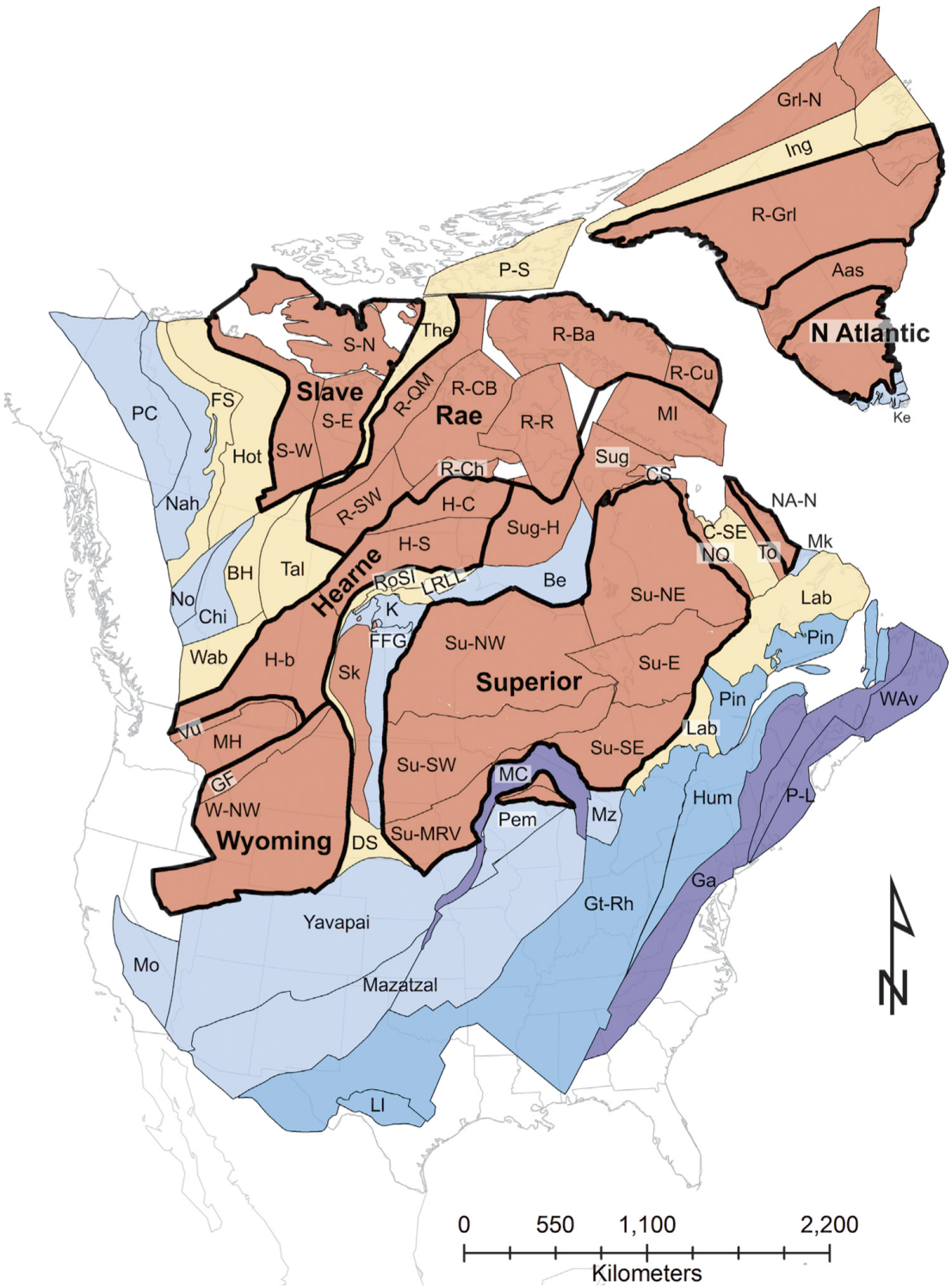

Figure 1.1 Map illustrating the domains and cratons in Canada and the northern United States from Eglington et al. 2013. Domains are broadly categorized with respect to age of their crust; oldest crust shown in brown, ranging to youngest in blue. Abbreviations used are Hearne (H-b = buried, H-C = central, H-S = south), North Atlantic (includes NA-N = Nain), Rae (R-Ba = Baffin Island, R-CB = Committee Bay, R-Ch = Chesterfield, R-Cu = Cumberland Peninsula, R-Grl = Greenland, R-QM = Queen Maud, R-SW = southwest), Slave (S-E = east, S-N = north, S-W = west), Superior (Su-E = east, Su-NE = northeast, Su-NW = northwest, Su-SE = southeast, Su-SW = southwest) and Wyoming (W-NW = northwest). Other abbreviated domains are: Aas = Aasiaat, Hum = Humber, BH

= Buffalo Head, Chi = Chinchaga, Ch-SE = southeast Churchill, CS = Cape Smith, DS = south Dakota, FFG = Flin Flon–Glennie, FS = Fort Simpson, GF = Great Falls, Ga = Gander, Grl-N = northern Greenland, Gt-Rh = Granite-Rhyolite, Hot = Hottah, Ing = Inglefield, K = Kisseynew, Ke = Ketilidian, Lab = Labrador, Ll = Grenville of the Llano area, LRLL = La Ronge–Lynn Lake–Rusty Lake–Leaf Rapids, MC = Mid-continent Rift, MH = Medicine Hat, Mk = Makkoviak, MI = Meta Incognita, Mo = Mojave, Mz = Mazatzal, Nah = Nahanni, No = Nova, NQ = New Quebec, PC = Pre-Cordillera of western Canada, Pin = Pinware, Pem = Pembine, P-L = Peri-Laurentia, P-S = Pearya south, RoSI = Rottenstone-Southern Indian, Sk = Sask, Sug = Sugluk, Sug-H = possible Hudson Bay extension of Sugluk, Tal = Taltson, The = Thelon, To = Torngat, Vu = Vulcan, Wab = Wabamun, Wav= West Avalonia.

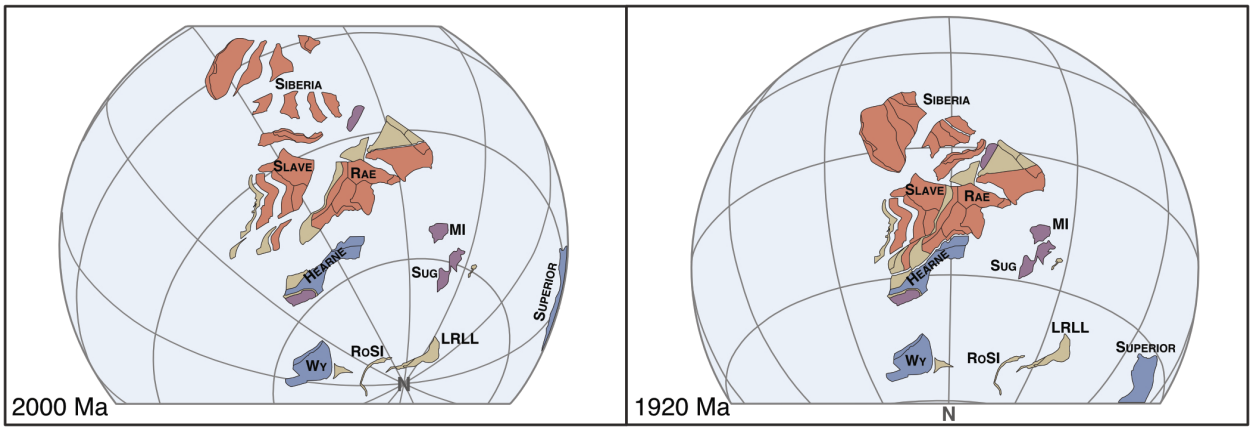

Figure 1.2 Palaeogeographic reconstruction of plates constituting Nuna at 2000 Ma (left), 1920 Ma (right) modified after Eglington et al. (2013). Plate positions are relative to that of present-day Slave craton. Plate abbreviations as in Fig. 1.1. Pehrsson et al. (2013) have correlated various crustal blocks into 'families', two of which are shown here: red = Rae 'family' and blue = Superia 'family'; purple polygons have not been grouped into 'families'; brown polygons are post-Archaean orogenic belts.

The purpose of this thesis is to provide insight into the tectonic setting of the upper Murmac Bay Group paleobasin and to provide evidence on the relative proximity of cratons neighboring the southwest Rae cratonduring the early Paleoproterozoic using detrital zircon provenance, and thus narrow constraints on the timing of their amalgamation. I will further constrain the depositional period of the upper succession of the Murmac Bay Group, and investigate the provenance of upper Murmac Bay Group sediments to elucidate their source. If sediments are found to have been sourced from a neighbouring craton, this will aid in deciphering the timing of regional tectonic events prior to and during their deposition.

In chapter two, new U-Pb detrital zircon geochronology results are reported, and a new maximum depositional age for the upper Murmac Bay Group is defined. These results are compared with published igneous crystallization ages from the DateView database to explore the provenance of upper Murmac Bay Group sediments in order to constrain relative craton positions

during deposition. This chapter has been previously published in the journal, *Lithosphere* (Shiels et al., 2016).

Chapter three expands on this approach by integrating Hf and O isotopic data in order to further constrain provenance by comparing the isotopic signatures of potential source rocks to that of the upper Murmac Bay Group detrital zircons. This chapter is currently in review in the journal, *Precambrian Research*. The appendices include full data tables and additional figures to clarify and support the findings of this study. Chapters four and five provide conclusions and recommendations for future study.

CHAPTER 2: PROVENANCE APPROACHES IN POLYDEFORMED METASEDIMENTARY SUCCESSIONS: DETERMINING NEAREST NEIGHBORING CRATONS DURING THE DEPOSITION OF THE PALEOPROTEROZOIC MURMAC BAY GROUP*

2.1 INTRODUCTION

The southwestern Rae craton of the Canadian Shield (Figure 2.1) is separated from the Hearne craton to the east by a geophysical boundary known as the Snowbird tectonic zone (Hoffman, 1988); together the Rae and Hearne cratons compose the western Churchill Province. The Snowbird tectonic zone has been variously interpreted as a late Archean (2.6 Ga) intracratonic shear zone (Hanmer et al., 1995a, 1995b) or an Archean suture (Regan et al., 2014) prior to the ~2.10 Ga breakup of a long-standing supercontinent, Kenorland (Aspler and Chiarenzelli, 1998). Alternatively, it has been hypothesized to represent a Paleoproterozoic (1.92 to 1.90 Ga) suture (Berman et al., 2007), possibly formed in the early stages of the Trans-Hudson orogeny (~1.92 to 1.80 Ga; Corrigan et al., 2009).

The southwestern Rae craton is bounded to the west by the ~2.00 to 1.90 Ga Taltson magmatic zone, which has been interpreted as the southern extension of the approximately coeval Thelon orogeny, resulting from amalgamation of the Slave and Rae cratons (Hoffman, 1988), and more recently as a separate entity (Card et al., 2010, 2014) resulting from either the amalgamation of the Slave-Buffalo Head and Rae cratons, or accretion of the Buffalo Head terrane to an already sutured Slave and Rae (Card et al., 2014). Card et al. (2014) have since reinforced the idea that the Taltson magmatic zone is a 1.99 to 1.96 Ga subduction-related magmatic arc emplaced into older rocks of the Taltson basement complex (e.g., McDonough et al., 2000) and that this arc (and related basement substrate) extends into Saskatchewan south of the Athabasca Basin. An alternative interpretation suggests emplacement in an intracontinental setting in the hinterland of a convergent plate margin (Chacko et al., 2000; De et al., 2000), requiring that the Slave and Rae cratons would have already been assembled by 2.00 Ga.

---

* Shiels, C., Partin, C.A., Eglington, B.M., 2016. Provenance approaches in polydeformed metasedimentary successions: Determining nearest neighboring cratons during the deposition of the Paleoproterozoic Murmac Bay Group. Lithosphere 8, 519–532. doi:10.1130/L537.1

Hence, there exists considerable debate as to the timing of amalgamation of the Rae and its neighboring cratons. Given the uncertainty regarding the interpretation of the late Archean to early Paleoproterozoic tectonic evolution of the Rae, Hearne, and Slave cratons, including their configuration and nearest cratonic neighbors during this time, these regions require further study to fully understand the origin of the Snowbird tectonic zone and Thelon orogeny (e.g., Pehrsson et al., 2013).

The relative paleogeographic positions of cratons and cratonic blocks during the earliest Paleoproterozoic Era (prior to the Trans-Hudson orogen) are difficult to constrain, owing, at least in part, to a paucity of reliable paleomagnetic data. However, provenance studies of Proterozoic sedimentary basins provide an opportunity to constrain

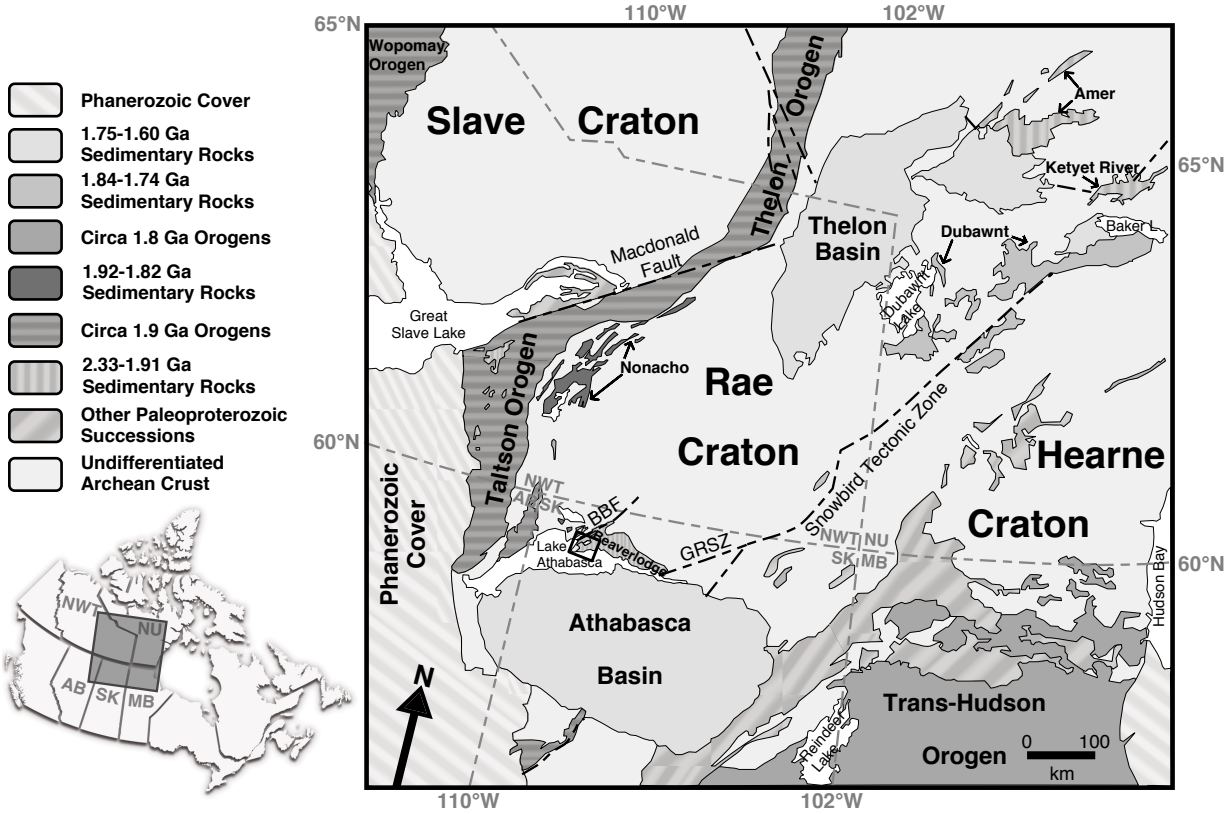

Figure 2.1 Currently exposed geology of southern Rae and surrounding cratons after Ashton et al. (2013). BBF = Black Bay Fault, GRSZ = Grease River Shear Zone; black rectangle highlights study area. Canadian provinces are labeled in gray as follows: NWT—Northwest Territories, NU—Nunavut, AB—Alberta, SK—Saskatchewan, MB—Manitoba.

the position of surrounding cratons, if unique sediment sources can be identified. Post-depositional deformation and metamorphism of these sedimentary basins can obscure primary

sedimentary structures, presenting an additional challenge, though provenance studies integrating geochronology and isotopic analysis of detrital zircon, stratigraphy, geochemistry, and structural and metamorphic data have been successful in identifying sediment provenance (e.g., Gehrels et al., 1990; Thomas et al., 2004; Weislogel et al., 2006; Horton et al., 2008; Collo et al., 2009). This approach requires robust datasets containing isotopic data from detrital zircon — common in siliciclastic sedimentary rocks — as well as a robust database of U-Pb crustal ages from a diverse suite of cratons with which to compare detrital zircon age spectra. We approach this provenance study by utilizing the DateView database (Eglington, 2004; Eglington et al., 2013), which consists of a global compilation of over 27,000 U-Pb zircon crystallization and metamorphic ages. The database also contains more than 35,000 individual detrital zircon analyses. We present new U-Pb detrital zircon data from the Murmac Bay Group on the Rae craton, integrated with available published U-Pb detrital zircon ages and compare the dominant age populations with crystallization ages recorded in DateView to discover potential sediment sources. Provenance analysis using detrital zircon geochronology can provide important insight into surrounding source terranes, and thus can be used to constrain the tectonic setting of sedimentary basins. This technique presents an opportunity, in particular, to study polydeformed or higher metamorphic grade sedimentary successions since zircon is highly refractory and resistant to isotopic resetting (Corfu et al., 2003; Finch and Hanchar, 2003; Hoskin and Schaltegger, 2003).

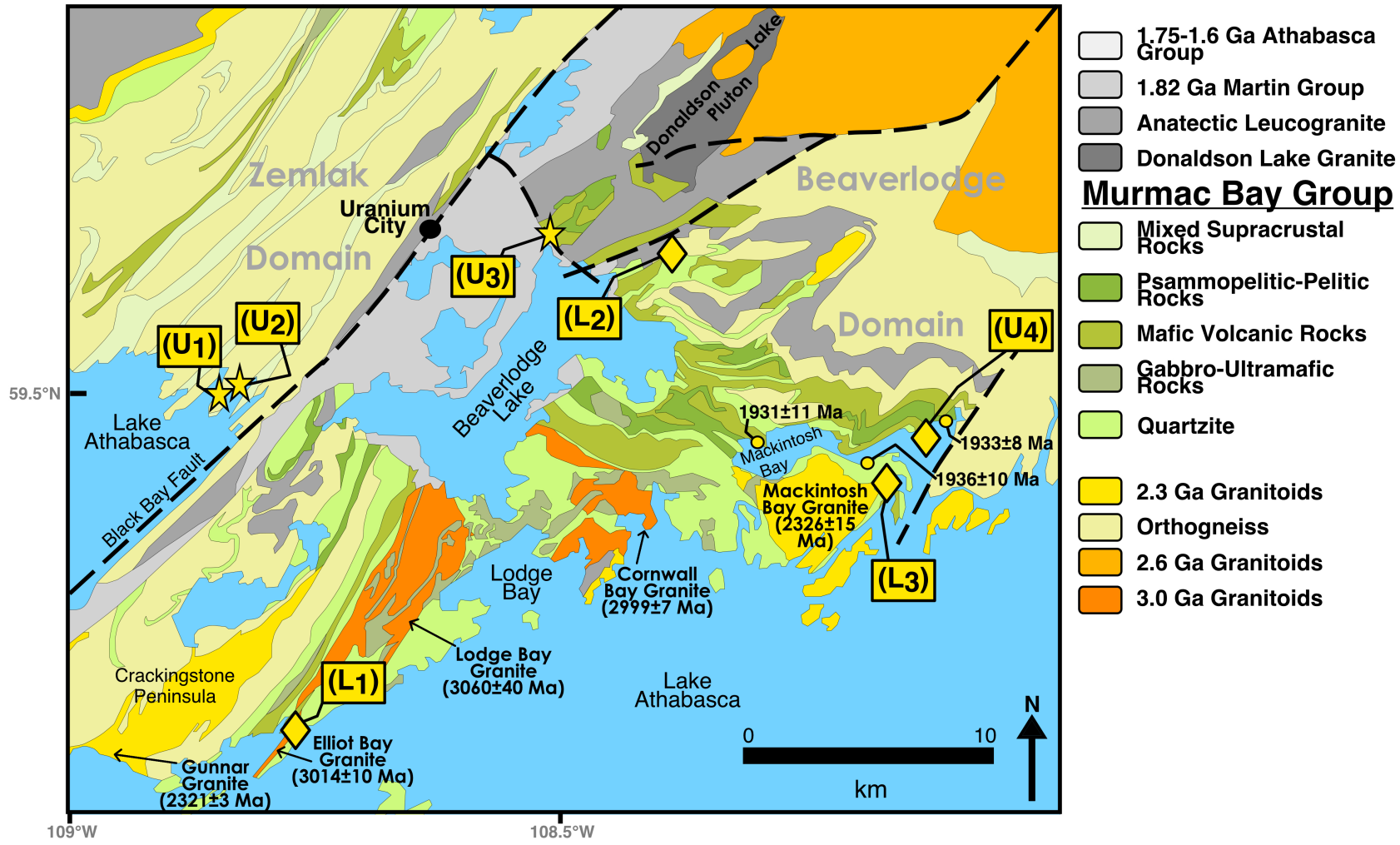

Figure 2.2 Sample locations in the Murmac Bay Group and simplified geology of the Uranium City area after Ashton et al. (2013). Diamonds are locations from previously published data (Hartlaub et al., 2006, Ashton et al., 2013); stars denote new samples collected for this study. L=Lower MBG samples, U=Upper MBG samples.

Recent detrital zircon U-Pb geochronological datasets from Paleoproterozoic sedimentary successions on the Rae and Hearne cratons have highlighted important similarities and differences between their provenances. Approaches combining geochronology with other available tools, such as radiogenic and tracer isotopic analysis, geochemical data, and stratigraphy, have been effectively applied in determining sedimentary provenance, correlating sedimentary basins, and inferring tectonic setting (e.g., Tran et al., 2008; Rainbird et al., 2010; Bethune et al., 2010, 2013; Ashton et al., 2013; Partin et al., 2014b; Wodicka et al., 2014). In particular, Rainbird et al. (2010) present a compilation of stratigraphy and detrital zircon U-Pb geochronology, comparing Paleoproterozoic sedimentary successions on the Rae craton with the broadly coeval Hurwitz group on the Hearne craton. The detrital zircon age spectra from these sedimentary successions reveal an important change in provenance in the upper stratigraphy, suggesting that the ~1.92 to 1.90 Ga units are correlative across the Rae-Hearne boundary, marking the oldest definitive trans-Churchill overlap succession (Rainbird et al., 2010). Previous tectonic models inferred the relative positions of the Rae and Hearne cratons prior to the Trans-Hudson orogeny (~1.90 Ga) differently (Hoffman, 1988; Hanmer et al., 1995a, 1995b; Berman et al., 2007; Corrigan et al., 2009), highlighting the need for robust and extensive datasets of geochronological and isotopic data to facilitate rigorous provenance and paleotectonic analysis.

Our study focuses on the Paleoproterozoic Murmac Bay Group (MBG), situated in the Beaverlodge domain, on the boundary of the Zemlak domain, on the southwestern Rae craton in northern Saskatchewan, Canada (Figure 2.2). The MBG is ideally located for provenance and paleotectonic analysis since it is adjacent to the Taltson orogeny at the Rae-Slave boundary as well as to the Snowbird tectonic zone at the boundary between the Rae and Hearne cratons. We expand on traditional approaches to determining provenance by making use of a large database of geochronological data to include candidates from more distal sources, including neighboring cratons. We determine the provenance of the MBG by comparing the U-Pb age of crustal rocks from the Rae and neighboring cratons stored in the DateView database (Eglington et al., 2013). Using these data, we test the hypothesis that the Hearne, Slave, or other nearby cratons could have provided sediment to the Murmac Bay paleo-basin, thereby providing a constraint as to their relative cratonic configuration in the early Paleoproterozoic Era, prior to the formation of Laurentia (Hoffman, 1988).

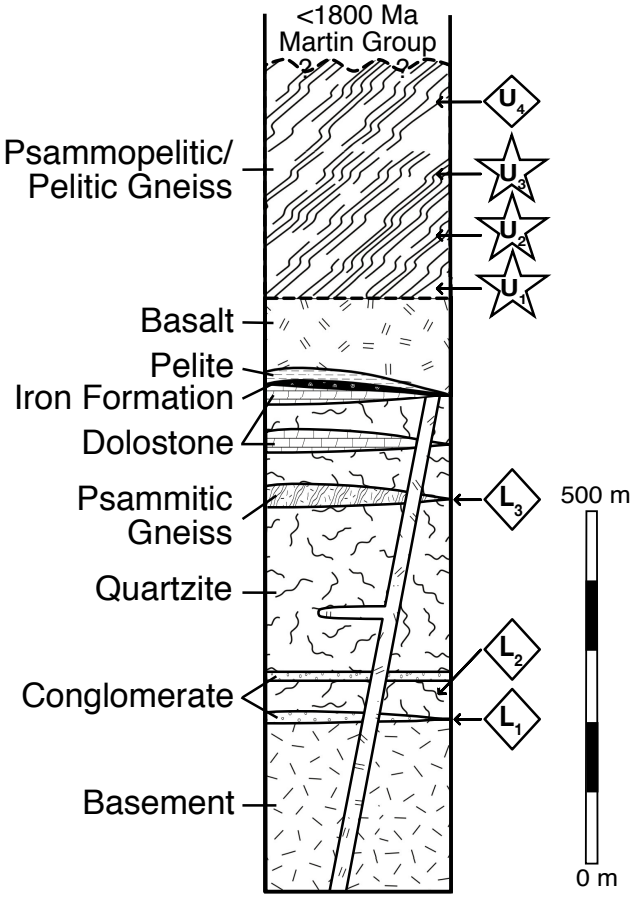

Figure 2.3 Simplified tectonostratigraphy of the MBG modified from Ashton et al. (2013) showing relative stratigraphic positions of samples. Stratigraphic order in the upper MBG (U_1, through U_4) is inferred, as primary sedimentary structures have been largely erased by multiple episodes of deformation in the upper succession.

2.2 GEOLOGICAL SETTING

The MBG is a key component of the Beaverlodge domain, one of the several lithotectonic domains within the exposed portion of the southern Rae craton in the Athabasca region of Saskatchewan, Canada. The Beaverlodge domain is bounded by the Black Bay fault to the west, the Grease River shear zone to the east (Figure 2.1), and the Oldman-Bulyea shear zone to the north. The best exposure of the MBG in its type locality is in the vicinity of Uranium City, Saskatchewan (Figure 2.2), where the metamorphic grade is lowest (greenschist to lower amphibolite facies). Thus, the MBG around Uranium City is the primary focus of this study. The <2.33 to >1.94 Ga MBG (Ashton et al., 2013) broadly consists of a lower and upper succession unconformably deposited on Mesoarchean granitic basement. Previous mapping efforts (e.g., Hartlaub et al., 2004; Ashton et al., 2007; Ashton et al., 2013) provide a tectonostratigraphic framework, summarized below.

2.2.1 Lower Murmac Bay Group

In the vicinity of Uranium City, the lower MBG was deposited unconformably on the Mesoarchean granitic basement, represented by ~3.06 to 2.99 Ga granites (Persons, 1988; Hartlaub et al., 2004). The North Shore plutons, a ~2.33 to 2.29 Ga felsic plutonic suite intrude the granitic basement, and also underlie the lower MBG along the Crackingstone peninsula (Figure 2.2). These plutons have been interpreted to be a product of syn- to post-collisional

extension following the ~2.50 to 2.30 Ga Arrowsmith orogeny (Hartlaub et al., 2007; Ashton et al., 2009, 2013). In the Elliot Bay region (Figure 2.2) the granitic basement is locally overlain by the basal polymictic conglomerate of the MBG that, where present, grades into a mature grey quartzite, which represents the basal unit for most of the MBG (Figure 2.3; Hartlaub et al., 2004; Ashton et al., 2013). The quartzite is intercalated with metamorphosed psammite, oligomictic conglomerate and dolostone, which is, in turn, interlayered with silicate and oxide facies iron formation toward the top of the unit (Hartlaub et al., 2004). Mafic volcanic rocks sit stratigraphically above the basal quartzite (Hartlaub et al., 2004; Ashton et al., 2013), representing the top of the lower MBG (Figure 2.3).

The lower MBG, and possibly the lowermost upper MBG, are intruded by ultramafic rocks and coarse-grained black gabbro dykes and sills, the age of which has not been determined, but which have been interpreted as feeder dykes to MBG volcanism (Hartlaub et al., 2004).

2.2.2 Upper Murmac Bay Group

The upper MBG is composed of laterally extensive quartzofeldspathic pelitic to psammopelitic rocks that are locally migmatitic at higher metamorphic grades. At the base of the upper MBG, the pelitic to psammopelitic rocks are locally interlayered with lower MBG volcanic rocks (Hartlaub et al., 2004). The lack of preserved sedimentary structures makes it difficult to determine the cause of this interlayering, which could be a result of deformation. It has been suggested that an intraformational unconformity exists, which separates the upper and lower units of the MBG (Ashton et al., 2013; Bethune et al., 2013).

2.2.3 Metamorphism and Deformation

The MBG has experienced at least two episodes of metamorphism, as indicated by monazite growth in deformation fabrics at ~1.93 Ga (Figure 2.2) and at ~1.91 Ga (Bethune et al., 2013). The earliest metamorphism is attributed to the terminal collision of the Rae and Slave cratons, or alternatively, the collision between the already amalgamated Slave and Rae cratons with the Buffalo Head terrane during the ~1.99 to 1.93 Ga Thelon and Taltson orogenic events (Hoffman, 1988; Card et al., 2010, 2014). The younger ~1.91 Ga metamorphism is attributed to the development of the Snowbird tectonic zone during the Snowbird orogeny (Berman et al., 2007; Bethune et al., 2013).

Metamorphic grade in the MBG is lowest (greenschist facies) just east of the Black Bay fault, which marks the boundary between the Beaverlodge and the Zemlak domain to the west (Figure 2.2), increasing eastward in grade to upper amphibolite and local granulite facies in the central Beaverlodge domain (Hartlaub et al., 2007; Ashton et al., 2009; Bethune et al., 2013). The Black Bay fault is a long-lived discontinuity interpreted to have experienced dextral and normal displacement, causing the eastern block to be downthrown (Ashton et al., 2009) prior to ~1.90 Ga (Bethune et al., 2013). Rocks of the upthrown west block are of higher metamorphic grade, some intensely ductily deformed (Hartlaub et al., 2004). Immediately west of the Black Bay fault, exposed upper amphibolite facies paragneisses have been interpreted as belonging to the MBG based on lithological association (Ashton et al., 2013).

2.2.4 Age and Tectonic Setting of the Murmac Bay Group: Previous Work

The MBG was originally interpreted to be Archean (~2.70 Ga) based on thermal ionization mass spectrometry (TIMS) U-Pb geochronology of detrital zircon from two samples of lower MBG rocks and two granites (~2.60 Ga Donaldson Lake and Dead Man) interpreted to intrude the lower MBG (Hartlaub et al., 2004). Further study in this region resulted in the discovery of ~2.30 Ga volcaniclastic rocks in the lower MBG, pointing to an early Paleoproterozoic maximum depositional age rather than Archean (Hartlaub et al., 2006, 2007).

Further mapping and analytical work re-evaluated previously reported intrusive relationships between plutons and the MBG; for instance, the migmatitic pelite intruded by the Dead Man granite has been re-interpreted to be part of a structurally deeper basement complex distinct from the MBG, based on ~2.34 Ga metamorphic monazite (Ashton et al., 2013; Bethune et al., 2013). Several samples included in previous studies from the MBG and the Donaldson Lake pluton (Hartlaub et al., 2004) were re-analyzed using laser ablation inductively-coupled plasma mass spectrometry (LA-ICPMS) techniques to obtain a more robust dataset along with newly collected samples from the lower MBG and one from the upper MBG, and an intrusive quartz-feldspar porphyry dyke (Ashton et al., 2013; Hartlaub et al., 2006). The Donaldson Lake granite intrudes the entire MBG and analysis of zircon from this unit originally yielded a poorly constrained crystallization age of 2634 ± 55 Ma (TIMS) from four of 5 moderately discordant (5-7%) analyses (Hartlaub et al., 2004). Based on composition, style of emplacement, and re-analysis, Ashton et al. (2013) re-interpreted this unit as a crustal melt derived from regional

metamorphism containing abundant inherited grains, with a U-Pb crystallization age of 1930 ± 19 Ma (LA-ICPMS) based on 2 of 3 concordant analyses out of 12 total in this age range. Considering the constraints provided by metamorphic monazite (above) and the new age of the crosscutting Donaldson Lake granite, the deposition of the upper MBG must have ceased by ~1.93 Ga, thereby providing a minimum age constraint for the MBG. Conglomerates and arkoses of the ~1.82 Ga Martin Group unconformably overlie the MBG over much of the Beaverlodge domain (Hartlaub et al., 2004; Morelli et al., 2009).

A Paleoproterozoic maximum depositional age for the lower MBG was corroborated by a youngest detrital zircon (YDZ) of 2323 ± 2.3 Ma in the basal conglomerate unit (Ashton et al., 2013). The quartzite unit detrital zircon ages range from 3.95 to 3.40 Ga (Hartlaub et al., 2006), and detrital zircon grains from a metamorphosed psammite from within the quartzite unit range in age from 3.8 to 2.3 Ga, with the weighted mean of the four YDZ at 2329 ± 8.6 Ma (Figure 2.4; Ashton *et al.,* 2013).

A psammopelitic gneiss associated with minor quartzite from the southeastern Beaverlodge domain, near Fond-du-Lac, Saskatchewan, yielded a YDZ age of 2030 ± 16 Ma (Ashton et al., 2007; Knox, 2011) which is thought to represent the upper part of the MBG (Knox et al., 2008). Its stratigraphic position relative to upper MBG in the Uranium City area is difficult to determine, due to access limitations between these localities. The YDZ reported from the upper MBG pelite sample in the vicinity of Mackintosh Bay was 2171 ± 31 Ma (Figure 2.4), which has been considered to be the maximum depositional age constraint for the upper succession (Ashton et al., 2013; Bethune et al., 2013). paucity of Archean-aged grains in the upper MBG sample suggests a shift in sediment source for the upper pelitic to psammopelitic succession, as previously suggested by Ashton et al. (2013).

Deposition of the lower MBG is inferred to have occurred shortly after the emplacement of the North Shore plutons, based on similar ages of these plutons and the YDZ in the lower MBG, following ~2.30 Ga metamorphism of the basement rocks during the Arrowsmith orogeny (Bethune et al., 2013). While local sources (e.g., North Shore plutons) exist for the dominant ~2.33 Ga detrital zircon populations in the lower MBG, the abundance of 3.95 to 3.40 Ga detrital zircon in the basal quartzite suggests a distal source, since no source rocks of this age are known proximally (Ashton et al., 2013). Isolated dolostone layers near the top of the lower MBG suggest a shallow marine depositional environment during this time (Hartlaub et al., 2004;

Ashton et al., 2013). Recent discovery of ^{13}C-enriched carbon isotope values suggest that deposition of the dolostone occurred sometime during the ~2.20 to 2.06 Ga Lomagundi Event (McDonald and Partin, 2016), which agrees with the detrital zircon U-Pb age constraints described above.

Primary sedimentary structures are preserved only locally in the quartzite unit of the lower MBG, consisting of planar and trough crossbedding, ripple marks, and scour channels, all of which are moderately deformed (Hartlaub et al., 2004), while the upper MBG lacks sedimentary structures altogether, making the determination of stratigraphic relationships, thickness estimates, paleocurrent measurements, and depositional paleoenvironment difficult (Hartlaub et al., 2004). Thus, there are no paleocurrent data to guide our provenance study.

The basin tectonic setting of the MBG during the early and late stages of formation is still poorly defined, but could represent a rift (lower MBG) to passive margin succession (upper MBG), an intracratonic basin for the entire MBG, a foreland basin setting (upper MBG) (Hartlaub et al., 2004; Bethune et al., 2013; Ashton et al., 2013), or a combination of these. Interbedding of the basal conglomerates and quartzites may be due to episodic faulting consistent with an extensional tectonic setting (Ashton et al., 2013), possibly in a rift or an intracratonic basin setting for the lower MBG (Hartlaub et al., 2004; Bethune et al., 2013). The rift basin interpretation is also supported by the presence of basal conglomerates and mafic volcanic rocks in the lower MBG, which suggest extension (Hartlaub et al., 2004). Evidence for the foreland interpretation includes metamorphism coincident with the Taltson orogen (Bethune et al., 2013). Thus, the upper MBG could have been deposited in a passive margin, intracratonic, or foreland basin setting according to previous hypotheses. Here, we test the foreland basin hypothesis for the upper MBG by provenance. If the sediment sources can be confidently attributed to either the Slave craton or Buffalo Head-Chinchaga domain, this provides evidence in favor of deposition of the upper MBG in the foreland of the Taltson orogen, with the collision of the respective craton.

2.3 METHODS

The upper MBG is dominantly composed of finer-grained rocks (pelites to psammopelites) compared to the lower succession, making mineral separation and subsequent analysis of small zircon grains from these samples challenging. In order to further constrain the depositional age and to investigate the provenance of the upper MBG, detrital zircon grains were

handpicked from the three samples collected for this study, a pelite from the type section of the upper MBG near Uranium City, and two psammopelitic samples from upper amphibolite facies rocks just west of the Black Bay fault (sample locations are shown in Figure 2.2 and Table 2.1) interpreted to belong to the upper MBG. New samples from the upper MBG in this study are: 14KA-095 (U_1), 14KA-098 (U_2), and 14CAP0911-5 (U_3). For simplicity, our new results and results from published detrital zircon data are referred to according to relative stratigraphic order (Figures 2.3 and 2.4), with samples from the lower MBG (L_1, L_2, L_3) below those from the upper MBG (U_1, U_2, U_3, U_4).

To decrease bias, grains were picked to include a representative sample with respect to grain size, color, and morphology. Zircon grains were mounted at the Canadian Centre for Isotopic Microanalysis, University of Alberta in a 25mm epoxy mount along with zircon standards for U-Pb calibration (Temora2 and MudTank), and polished using diamond grits to expose the midsections of the crystals. In order to characterize internal zircon structures (e.g., zoning) and alteration, imaging was carried out using a Zeiss EVO MA15 scanning electron microscope equipped with a high-sensitivity, broadband cathodoluminescence (CL) detector and a backscattered electron (BSE) detector. These images revealed that most zircon grains in this study exhibited zoning in the centers of the grains characteristic of igneous growth, as well as numerous fractures and common inclusions. The majority of grains also have unzoned overgrowth rims that appear dark under CL imaging, while several grains also show signs of recrystallization, some zoned and some unzoned (see Figure B.1 in Appendix B).

U and Pb isotope ratios were determined at the Geological Survey of Canada in Ottawa using an O_2-primary beam on the Sensitive High Resolution Ion Microprobe (SHRIMP) following the procedures of Stern (1997) (Table A.1). Imaging guided selection of the target areas for analyses, dominantly within the centers of the grains unless otherwise noted in Table A.1. Grains were targeted to avoid fractures and inclusions, where possible. In order to obtain the igneous crystallization age of zircon grains, target spots were chosen in the interior of grains where igneous growth zoning could be identified in BSE and CL images. Most grains in this study exhibited this characteristic growth zoning in their centers, and care was taken to avoid any areas of grains where this growth-zoning pattern appeared mottled, recrystallized, or otherwise altered. Full U-Pb analysis results are included in Table A.1 in Appendix A.

The crystallization age data used for comparison in this study were compiled from relevant literature into the DateView (Eglington, 2004) and StratDB databases (Eglington et al., 2013). DateView contains more than 100,000 published and public-domain isotope geochemical records, which are tied to lithostratigraphy, metamorphism, tectonism, ore deposits, large igneous provinces, and full references via StratDB (Eglington et al., 2013). We added records for published zircon U-Pb geochronology on the MBG (Table 2.1), as well as igneous and metasedimentary rocks on the southern Rae and proximal cratons from zircon, including U-Pb geochronological data obtained by TIMS, LA-ICPMS, and SHRIMP methods (Hartlaub et al., 2004, 2006; Tran et al., 2008; Rainbird et al., 2010; Ashton et al., 2013; Mumford, 2013), to provide a comprehensive dataset from which to explore potential provenance locations.

Probability density function curves and histograms were calculated using FitPDF software (Eglington, 2013), screening data for ±10% discordance; maximum probabilities were normalized to 100% for ease in comparison of datasets (Figure 2.4). Primary and secondary age modes were identified qualitatively from peaks in the probability density function, and a list of potential source candidates with isotopic ages matching these peaks was compiled using StratDB. These potential candidates were also filtered to include only those records with ±10% discordance, and which were interpreted to be either igneous crystallization or inherited ages in their publication. A total of 2556 records matched these criteria within Canada, the ages of which were spatially referenced using ArcMap to determine their geographic relationships to the source locations (Figures 2.5 to 2.7). Provenance candidates matching the most dominant detrital zircon age populations were then further investigated to determine their suitability as sources for upper MBG sediments.

2.4 SAMPLE DESCRIPTION AND RESULTS

2.4.1 Sample 14KA-095 (U_1)

The two samples collected just west of the Black Bay fault (Figure 2.2) for this study (14KA-095; U_1 and 14KA-098; U_2) are upper amphibolite-facies paragneisses attributed to the upper MBG based on their lithological association (quartzite-mafic volcanic-psammopelitic gneiss; Ashton et al., 2013). Since these samples were obtained from the upthrown west block of the Black Bay fault, they are inferred to be from a lower stratigraphic level than the sample collected east of the fault (14CAP0911-5; U_3), though precise stratigraphic relationships are

difficult to determine in the upper succession due a lack of preserved sedimentary structures and a history of multiple deformation events.

Sample 14KA-095 (U_1) is an upper-amphibolite facies, grey-brown, quartzofeldspathic, psammopelitic gneiss with anastomosing penetrative foliation. It contains 30 to 40 % quartz (up to 1 cm), ~25% feldspar (up to 1.5 cm), 15 to 20% biotite, ~10% muscovite, ~10% chlorite after biotite, and minor titanite, zircon, and sulfides. Sixty-seven analyses were performed on a total of 65 grains from this sample. Detrital zircon grains in this sample are euhedral to subhedral, cloudy to translucent brown, with an average length of 190 μm and an average length to width ratio of 1.9. Grain morphology ranges from rounded to equant to elongate, most non-rounded grains are doubly terminated. Analyses were targeted to avoid fractures and inclusions present in most grains. The centers of these grains typically (88%) showed oscillatory growth zoning, though in about half of the grains this zoning was altered or convoluted. One zircon grain analyzed has a featureless interior in images. Overgrowths that appear dark in CL images are present in all zircon grains in this sample, averaging 35 μm in thickness (Figure B.1 in Appendix B). Two analysis spots were targeted in metamorphic domains where they were large enough to accommodate the spot size; one on an overgrowth rim that was dark in CL images (s3177-067.2), and one on an interpreted recrystallized zone that embayed a zone exhibiting igneous growth zoning (s3177-071.1). The Th/U ratio ranges from 0.004 to 1.05 and all grains in this sample with Th/U ≤ 0.47 exhibit evidence of alteration of original igneous growth zoning (e.g., mottling) in CL images.

The $^{207}Pb/^{206}Pb$ ages in sample U_1 range from 2.54 to 1.91 Ga. The largest population (n=17) of zircon ages is centered on 2.31 Ga, with minor populations at 2.12 Ga (n=13), 2.08 Ga (n=10), and 1.93 Ga (n=9; Figure 2.4). The youngest grain that does not exhibit evidence of alteration of igneous zoning in images in this sample is 2005 ± 18 Ma (S3177.001.1; 4.8% discordance, Th/U=0.52) and thus is interpreted as the YDZ in this sample. This grain is prismatic in shape with a metamorphic overgrowth around the rim too narrow for analysis, thus the analysis was targeted in the interior of the grain in an igneous domain exhibiting both sector and igneous growth zoning. Only two grains in this sample yielded ages ≥2.50 Ga (Figure 2.4). The analyses collected from metamorphic overgrowths on two grains described above yielded $^{207}Pb/^{206}Pb$ ages of 1917 ± 15 Ma (s3177-067.2) and 1931 ± 11 Ma (s3177-071.1) and Th/U values

of 0.06 and 0.01, respectively, corresponding to the timing of known metamorphic events in this region (Bethune et al., 2013).

2.4.2 Sample 14KA-098 (U_2)

This sample from the west of the Black Bay fault (Figure 2.2) is similar in appearance and character to sample 14KA-095 (U_1), but is coarser grained. It consists of ~40% quartz, ~20% feldspar, ~20% biotite, ~10% muscovite, with minor cordierite, garnet, sillimanite, apatite, and zircon.

A total of 64 analyses were performed on 60 detrital zircon grains taken from sample 14KA-098 (U_2). Grains in this sample are mainly transparent to cloudy to translucent brown, with an average length of 170 μm, and an average length to width ratio of 1.6, grain morphology is also similar to that seen in sample U_1. Most grains (79%) showed oscillatory growth zoning at their centers, two-thirds of the grains showed evidence of alteration fronts extending into their centers. All zircon grains in this sample also showed overgrowth rims that appeared dark under CL, with an average thickness of 32 μm (Figure B.1). One grain in this sample has a metamorphic zone that was thick enough to accommodate the U-Pb spot, which was thus targeted for analysis, in a featureless, recrystallized outer rim (s3178-068.1). The Th/U ratio in this sample ranged from 0.17 to 0.89, and all grains with Th/U ≤0.40 show evidence of alteration of the igneous growth zoning in CL images. The range of $^{207}Pb/^{206}Pb$ ages in this sample is from 2.41 to 1.85 Ga with the dominant population (n=25) of detrital zircon ages centered around 2.31 Ga. Secondary populations can be seen at 2.26 Ga (n=7) 2.17 Ga (n=6), and 2.07 Ga (n=9), and there are no Archean zircon in this sample (Figure 2.4). The YDZ that does not show any evidence of alteration of igneous zoning or recrystallization in this sample is dated at 2056 ± 14 Ma (S3178.121.1), a prismatic grain that shows evidence of alteration around the rim, but was targeted for analysis in an interior domain that showed characteristic igneous growth zoning in BSE and CL images. The analysis performed on the recrystallized rim yielded an age of 1999±9 Ma (s3178-068.1), with Th/U of 0.20 (Figure 2.4), as the age of this metamorphic rim is older than the interpreted crystallization age of the Donaldson Lake pluton which intrudes the MBG (~1.93 Ga; Ashton et al., 2013), this metamorphism may have occurred prior to transportation and deposition of this grain, making this the youngest detrital age from sample U_2.

2.4.3 Sample 14CAP0911-5 (U_3)

A greenschist-facies pelitic schist was collected from the upper MBG in the vicinity of Uranium City (Figure 2.2). This sample is very fine-grained with planar foliation, ~50% micas (biotite and chlorite), 20 to 25% quartz, ~5% ~5% rutile and feldspar, and with minor chlorite, quartz, and carbonate occurring as either veins or along cleavage planes. This sample did not yield abundant detrital zircon grains; a total of 38 grains were selected for U-Pb analysis, facilitating 40 analyses. The zircon grains in this sample are cloudy to medium translucent brown, with an average length of 85 μm, and the average length to width aspect ratio of 1.5. The zircon grains in this sample are mostly equant to rounded and several of these grains are broken fragments.

Analysis spots were chosen to avoid fractures within the grains, most (90%) of which exhibit oscillatory growth zoning though a few grains are clear and featureless. The majority (75%) of grains in this sample also have thin (≤15 μm) overgrowth rims, which are dark in CL images (Figure B.1). The Th/U ratio ranges from 0.07-1.01, with the lowest values (≤0.36) occurring on grains that exhibit evidence of alteration in CL images. The $^{207}Pb/^{206}Pb$ ages for this sample range from 3.05 to 1.99 Ga. Most analyses plot between 2.33 and 2.00 Ga, with the highest population (n=7) plotting at 2.17 Ga and secondary populations at 2.33 Ga (n=5) and 2.10 Ga (n=4; Figure 2.4). The YDZ in sample U_3 is 1989 ± 29 Ma (S3179.046.1; -2% discordance, Th/U=0.48), a small broken grain with apparent igneous growth zoning (Figure 2.4). The next youngest grain (with a smaller error) is 2014 ± 11 Ma. The probability density plot shows that most of the analyzed grains have Paleoproterozoic crystallization ages, whereas only five grains exhibit Archean crystallization ages (Figure 2.4).

2.4.4 Detrital Zircon Age Probability Density Plots and Histograms

Zircon U-Pb age data are displayed in probability density plots and histograms keyed to stratigraphic position, where known, in Figure 2.4. Ashton et al. (2013) reported the age of the youngest detrital zircon grain in the lower succession as 2329 ± 8.6 Ma from the psammitic gneiss (L_3) sample near the stratigraphic top of the lower MBG; this together with zircon analyses from the basal conglomerate (L_1), defining a single peak ~2.30 Ga, establishes a maximum depositional age for the lower MBG ~2.30 Ga, while the quartzite (L_2) contains only Archean (>3412 ± 11 Ma) grains (Hartlaub et al., 2006). The psammopelitic gneiss (L_3) also

contains zircon grains of both late Archean and early Paleoproterozoic ages, implying that the sediments comprising L_3 had a more diverse provenance than that of the quartzite (Ashton et al., 2013). Both L_2 and L_3 have dominant zircon populations with ages between 3.90 and 3.60 Ga. Overall, the lower MBG (L_1, L_2, L_3) contains a greater abundance of Archean grains than samples from the upper MBG.

In contrast, the upper MBG samples exhibit a paucity of Archean zircon grains, reinforcing the idea of a shift in sediment source between deposition of the lower and upper MBG. The samples (U_3 and U_4) collected east of the Black Bay fault (Figure 2.2) contain minor amounts of Neoarchean grains, the latter (U_4; Ashton *et al.,* 2013) with a secondary peak near 2.60 Ga. In both of these samples, the dominant population is ~2.17 Ga. The two gneissic samples (U_1 and U_2) collected for this study from the west side of the Black Bay fault (Figure 2.2) have dominant populations centered around 2.30 Ga and secondary peaks around 2.10 Ga. These samples both contain a similar range of zircon ages (2540 - 1850 Ma).

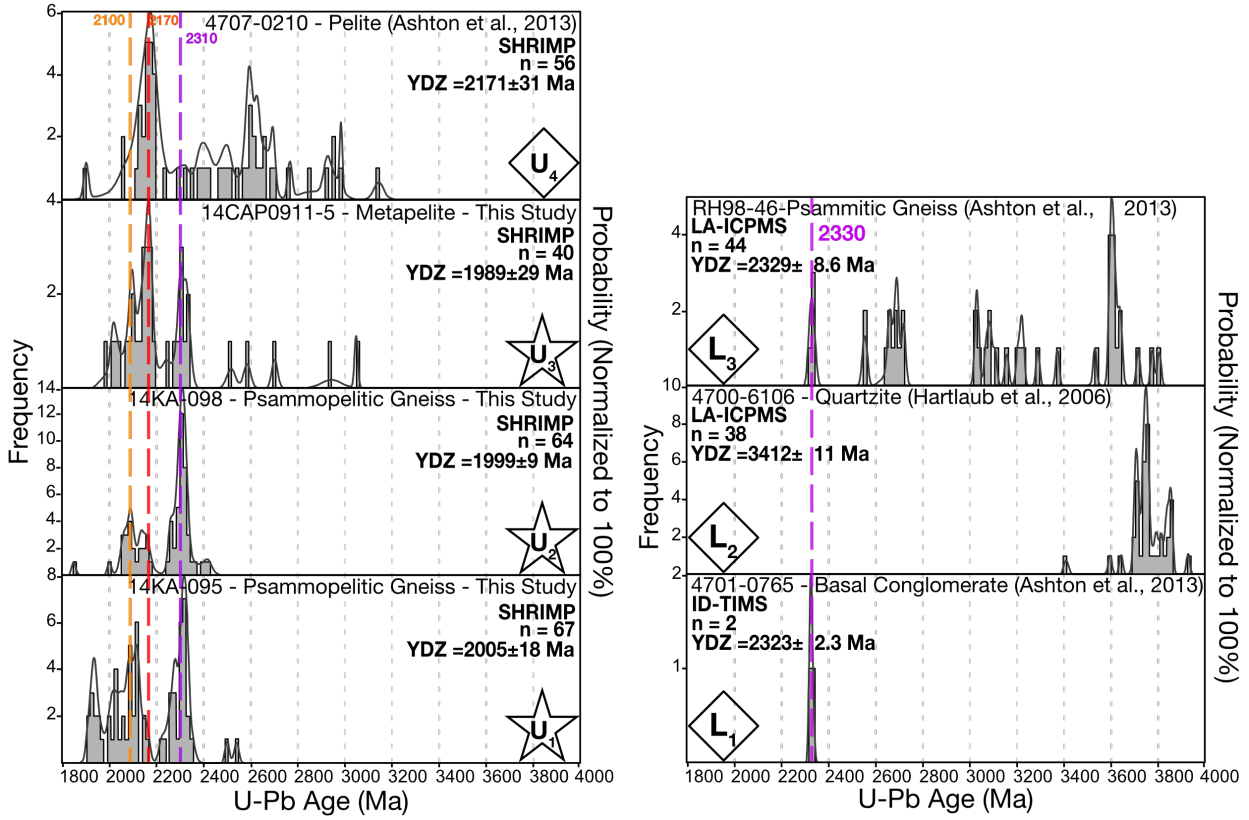

Figure 2.4 U-Pb age data for the MBG compiled and plotted using FitPDF. Probability curves shown in light grey and histograms outlined in black. Probability is normalized to 100%. YDZ=youngest detrital zircon.

2.5 DISCUSSION

2.5.1 Assessing Metamorphic vs. Igneous Origin of Zircons

Care was taken to interpret the youngest detrital zircon in each sample by choosing grains that did not show significant alteration textures or that might indicate metamorphic zircon growth by Th/U ratios. The Th/U ratio is considered to be characteristic of the crystallization environment of the zircon, with Th/U>0.2 indicating crystallization from a melt and Th/U<0.07 associated with metamorphic zircon

Table 2.1 Summary of U-Pb detrital zircon geochronology for the MBG. YDZ = youngest detrital zircon. In our study, we assessed the YDZ to reflect the zircon with the youngest age that did not show textural evidence of alteration and had unambiguous Th/U ratios consistent with an igneous rather than a metamorphic origin. Younger ages were obtained in our analysis, but are unlikely to provide a robust indication of maximum depositional age. The YDZ from literature data is cited from the source. Full U-Pb data for samples collected for this study provided in Table A.1.

TABLE 2.1. DETRITAL ZIRCON GEOCHRONOLOGY DATA

Sample ID	Field Sample ID	Rock Type	Sample Locations*		Age Range (Ga)	Primary Age Peak (Ga)	Secondary Age Peaks (Ga)	YDZ (Ga)	Technique	Reference
			Latitude (°N)	Longitude (°E)						
U4	4707-0210	Pelite	59.4841	-108.2695	3.14 - 1.90	2.17	2.60, 2.13	2.17	SHRIMP	(Ashton et al., 2013)
U3	14CAP0911-5	Metapelite	59.5634	-108.5276	3.05 - 1.99	2.17	2.33, 2.10	1.99	SHRIMP	This paper
U2	14KA-098	Psammopelitic gneiss	59.5132	-108.7520	2.41 - 1.85	2.33	2.09	2.00	SHRIMP	This paper
U1	14KA-095	Psammopelitic gneiss	59.5044	-108.7695	2.54 - 1.91	2.33	2.12, 2.08, 1.94	2.01	SHRIMP	This paper
L3	RH98-46	Psammopelitic gneiss	59.4668	-108.2929	3.80 - 2.33	3.60	3.05, 2.72, 2.33	2.33	LA-ICPMS	(Ashton et al., 2013)
L2	4700-6106	Quartzite	59.5561	-108.4400	3.95 - 3.41	3.75	3.86, 3.71	3.41	LA-ICPMS	(Hartlaub et al., 2006)
L1	4701-0765	Conglomerate	59.3876	-108.7233	2.33	2.33	N.A.†	2.32	TIMS	(Ashton et al., 2013)

*sample locations provided in WGS84
†N.A.=not applicable

(Rubatto, 2002; Hoskin and Schaltegger, 2003). Th/U ratios similar to or greater than magmatic values have been recorded, however, in metamorphic zircon (Möller et al., 2003; Timms et al., 2006). Möller et al. (2003) suggest that low Th/U may be an indicator of metamorphic zircon growthonly in a system where other phases such as monazite and allanite compete for Th. The Th/U ratio may also be affected during metamorphism by a grain boundary fluid phase with a high Th/U, or an enrichment in Th relative to U in response to deformation due to differential element mobility (Timms et al., 2006). Thus, Th/U may not always be in itself a robust indicator of metamorphic zircon growth, and must be combined with observations from imaging as well. Only four zircon analyses in our study yielded Th/U ratios less than 0.07, two of which were obtained from rims in sample U_1 (Figure A.1).

Visual analysis was an important factor in distinguishing whether the targeted analysis spots came from metamorphic or igneous sectors of the zircon grains. Zircon grains picked for this study exhibited a pitted surface texture characteristic of detrital zircon. Most zircon grains in the three samples had overgrowth rims that were very dark in CL images; one such rim was wide enough to accommodate the beam size, and was targeted for analysis to investigate the timing of this overgrowth, yielding an age of 1917 ± 15 Ma (Th/U=0.06). Another analysis targeted in an area that appeared to be recrystallized, where zircon of a different texture was "embayed" into the regular growth-zoned texture, to further investigate the timing of metamorphism, which yielded an age of 1931 ± 11 Ma (Th/U=0.01). These correspond to the previously reported ages of metamorphic monazite growth in the MBG (Bethune et al., 2013). Considering that most zircon grains in this study, from many different ages, exhibit overgrowth rims, we interpret that these rims formed during post-depositional metamorphic events.

2.5.2 Age of the Upper Murmac Bay Group

U-Pb ages younger than ~2.00 Ga were obtained either from overgrowth rims, or from zircon grains which exhibited evidence of alteration of the original oscillatory growth banding in CL and/or BSE images, such as convoluted zones propagating through fractures (Corfu et al., 2003; Hoskin and Schaltegger, 2003), recrystallization or metamorphism (Figure B.1), which might have occurred prior to transport and deposition, or may represent mixed ages. The interpreted youngest detrital zircon grains in our samples were dated at 2005 ± 18 Ma (U_1), 1999 ± 9 Ma (U_2), and 1989 ± 29 Ma (U_3), giving a weighted mean of 1999 ± 13 Ma. The dominant population in zircon aged younger than this is centered around 1.93 Ga, which corresponds to the aforementioned ~1.93 Ga crosscutting Donaldson Lake pluton and ~1.93 to ~1.91 Ga metamorphic monazite ages (Bethune et al., 2013). Although a single ~1.97 Ga grain is not within error of known metamorphic events or our youngest detrital zircon age, a second spot in the same domain of this grain yielded a younger age of ~1.91 Ga, suggesting the U-Pb age of this grain could represent a mixed age. We interpret zircon grains from our samples with ages ≲2.00 Ga as having been metamorphosed or otherwise altered after deposition. The three grains aged between 1.93 Ga and 1.98 Ga all are within error of either known metamorphism at ~1.93 Ga or our interpreted maximum depositional age. These as well as other grains that exhibit alteration textures might also have been affected by Pb-loss either before or after deposition, resulting in

erroneously young ages. Therefore, we interpret the YDZ age in our samples to be 1999±13 Ma (weighted mean), representing a new maximum depositional age constraint for the upper MBG in its type locality.

2.5.3 Identifying Potential Sources

Provenance candidates were determined by matching dominant age peaks in the MBG detrital zircon spectra to published igneous crystallization ages stored within the DateView database (Eglington, 2004; Eglington et al., 2013). The least common crystallization ages from the database, which matched detrital zircon age peaks in our data were identified and investigated further as potentially unique sediment sources. This approach does present limitations in that only published isotope data is being considered, hence any undated, undiscovered, eroded, or buried potential source rocks cannot be assessed in our study. Much of the Canadian Shield has only as of yet been mapped and dated at a reconnaissance level, and the Precambrian geologic record itself is inherently incomplete, however, as more data becomes available over time, this method will benefit from an increasingly robust dataset.

Approximately 2800 spatially referenced potential source rocks are identified for zircon grains in these samples within the Canadian Shield (Figure 2.5), as identified from igneous crystallization ages recorded in the DateView database. Rae and neighboring cratons are highlighted in green (Figure 2.5). Potential sources for dominant populations of 3.90 to 3.60 Ga in the lower MBG samples L_2 and L_3 were found solely on the neighboring Slave craton, though there are a number of potential source locations for the 2.70 to 2.30 Ga populations from samples L_1 and L_3 proximal to the study area on the Rae craton, as well as on neighboring cratons.

To narrow the search for sources for the upper MBG, only Paleoproterozoic (2.50 to 1.90 Ga) potential source locations are plotted in Figure 2.6, and it can be seen that there are a great number of candidates for the dominant populations ~2.30 Ga in samples U_1, U_2 and U_3. A close-up view of the study area highlights the lack of ~2.17 Ga source candidates for the dominant populations from samples U_3 and U_4 locally on the Rae craton (Figure 2.7). Potential sources for this ~2.17 Ga age mode can be found, however, on the neighboring Slave and Buffalo Head cratons, the ages of which are identified in Figure 2.7.

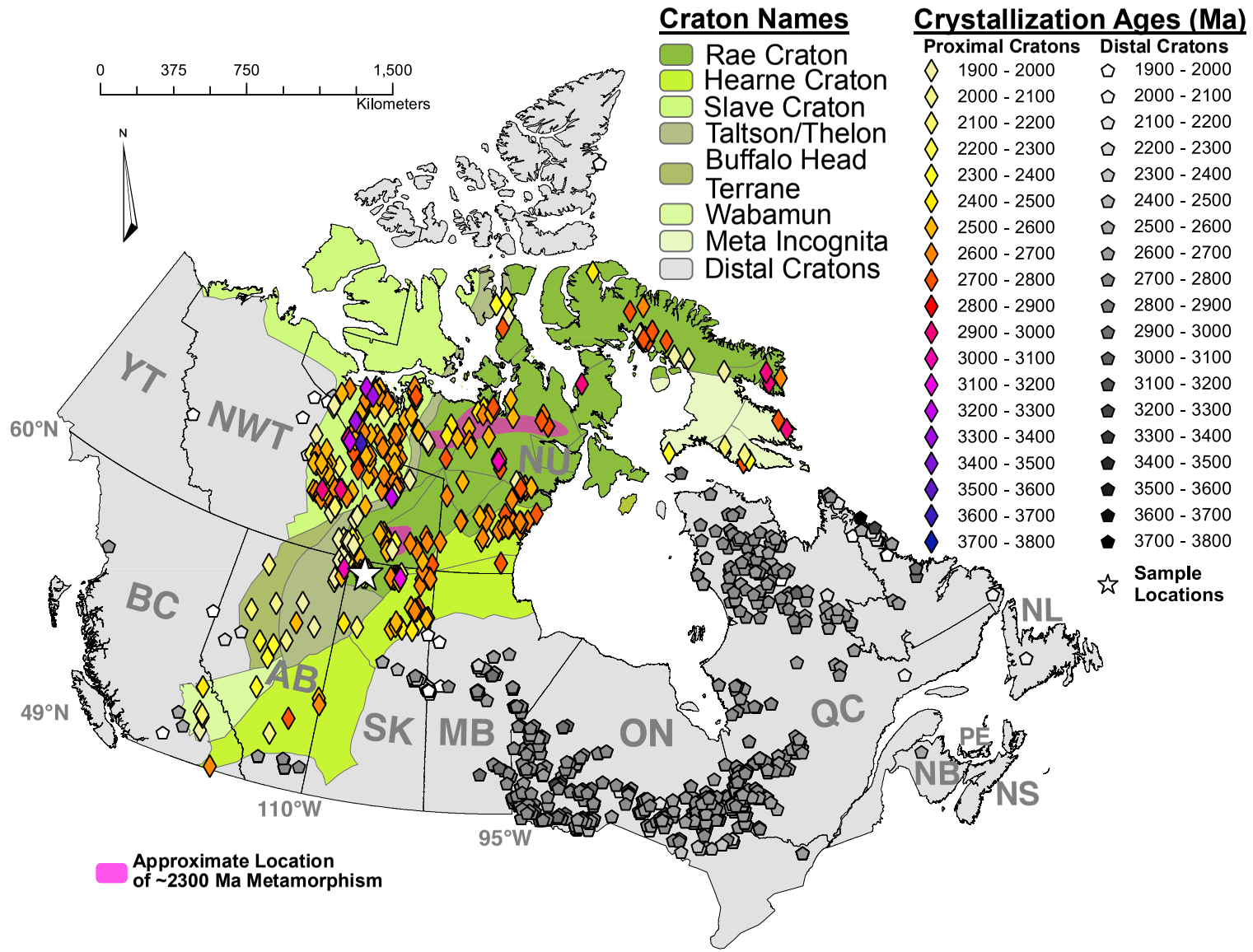

Figure 2.5 Potential provenance locations for MBG detrital zircon age peaks within Canada derived from the DateView database. Candidate source locations on proximal cratons are shown in color, distal cratons in grey scale.

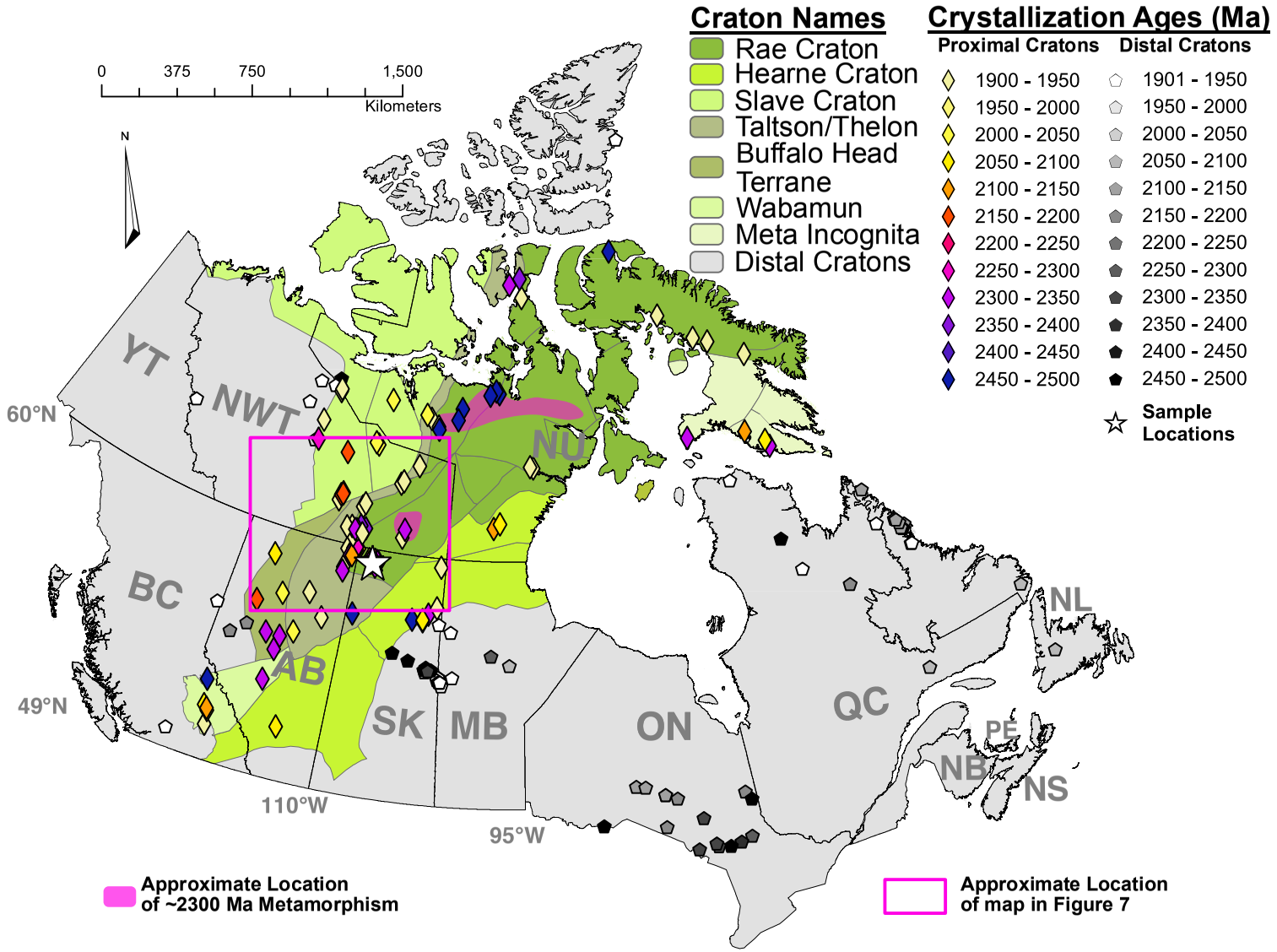

Figure 2.6 Potential provenance locations for MBG detrital zircon age peaks of Paleoproterozoic age derived from the DateView database.

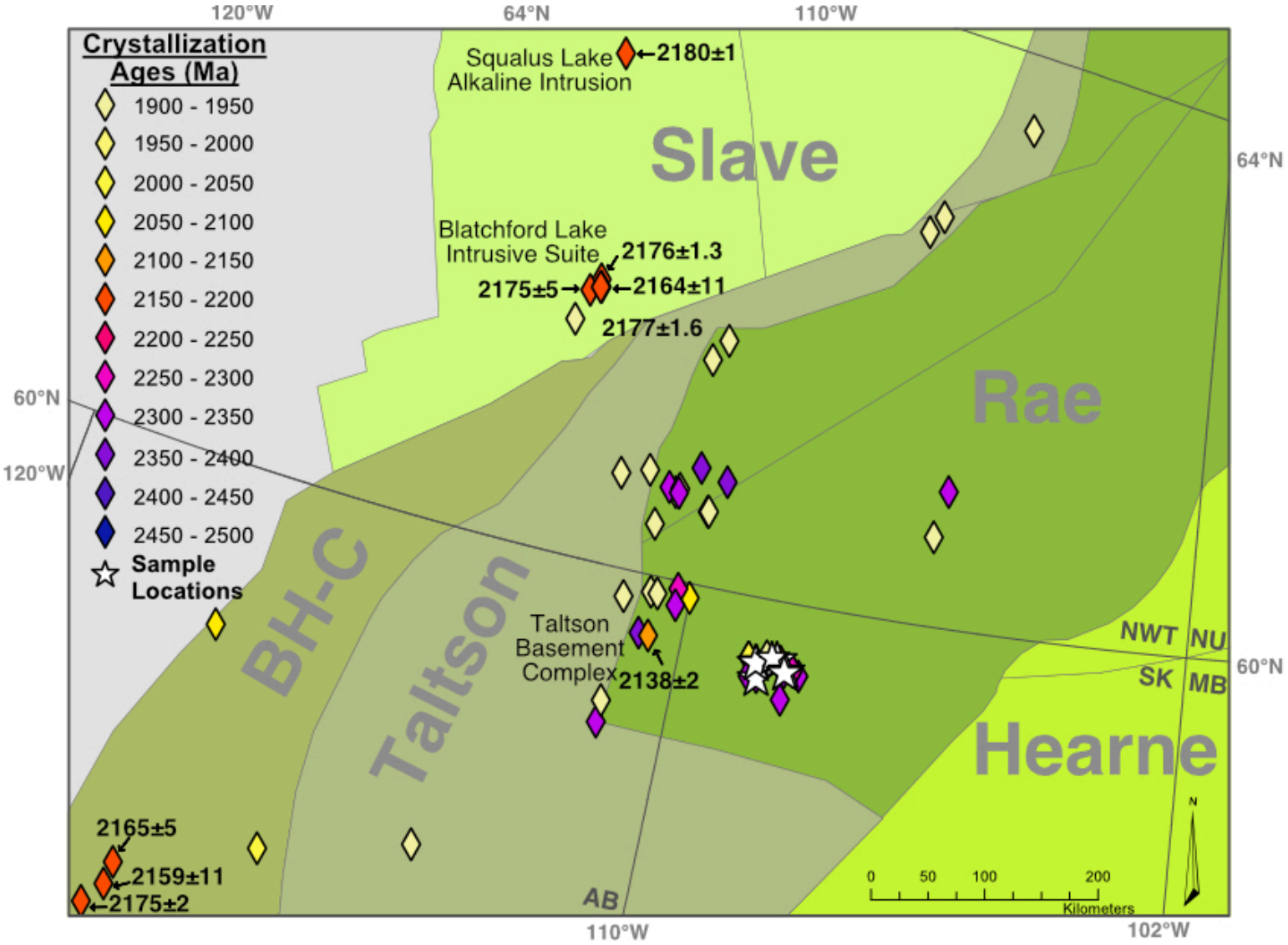

Figure 2.7 Closeup view of study area showing potential provenance locations proximal to study area. Candidate sources for the dominant ~2.17 Ga detrital zircon age population are annotated with their interpreted crystallization ages. Reference data for these ages appears in Table 2.2. BH-C = Buffalo Head – Chinchaga domain.

2.5.4 Provenance of the Lower Murmac Bay Group

The maturity of the quartzite in the lower MBG indicates a long period of weathering, erosion, and transportation that could support an interpretation of far-traveled sediment sources. The only 3.90 to 3.60 Ga provenance locations identified from this study are located in the Acasta Gneiss complex on the Slave craton (Figure 2.5); rocks of this age are globally quite rare. Ages for the Acasta Gneiss complex include tonalitic gneisses dated at 3611 ± 11 Ma (Bowring and Williams, 1999) and 3661 ± 47 Ma (Iizuka et al., 2007), corresponding to dominant age modes from samples L_2 and L_3 (Figure 2.4). Also, a granitic and a quartz dioritic gneiss from the Acasta region were interpreted to have crystallized at 3941 ± 43 Ma and 3931 ± 34 Ma, both with overgrowths suggesting an anatexis or recrystallization event at 3689 ± 61 Ma and 3677 ± 49 Ma, respectively (Iizuka et al., 2007). Yamashita et al. (2000) examined a series of clastic sedimentary rocks proximal to the Acasta Gneiss complex with depositional ages ranging from ~3.13 Ga to ~2.58 Ga, and reported T_{DM} ages between 3.70 and 2.90 Ga, including three zircon grains with U-Pb ages >3.40 Ga The authors suggest that the disagreement between U-Pb and T_{DM} ages may be due to Pb-loss shifting the apparent U-Pb age younger than the actual crystallization, as the rocks described were interpreted to have undergone extensive crustal reworking and recycling. Although limited Eoarchean crustal preservation might be a contributing factor to a lack of other identified sources for zircon grains of this age, the Acasta Gneiss complex is still permissible as a sediment source for the lower MBG, though other as of yet unidentified sources might exist.

Many potential source locations were identified for zircon in sample L_3 with a dominant age mode of 2.65 to 2.75 Ga, both proximally on the Rae craton (Ashton et al., 2013), and on the neighboring Hearne and Slave cratons (Figure 2.5) as 2.70 Ga granite-greenstone belts. Rae craton potential sources include plutonic rocks in the Snowbird Lake region near the boundary between the Rae and Hearne cratons (Martel et al., 2008). The Thluicho Lake Group, a metasedimentary succession deposited <1.92 to 1.82 Ga in the neighboring Zemlak domain, also has a minor population of detrital zircon that fall within this age range, and are interpreted to have been locally derived (Bethune et al., 2010). If the sediment transport was directed from the Acasta Gneiss complex to the MBG, there exist several potential sources for this age mode

between these locations in the current craton configuration. Thus, ~2.70 Ga is not a unique age population from which to distinguish sediment source.

Likewise, the 2.30 to 2.38 Ga dominant populations seen in samples from both upper and lower MBG are centered around ~2.33 Ga and correspond with several proximal potential source locations (e.g., North Shore plutons; Hartlaub *et al.*, 2007), as well as more distal locations from the neighboring Taltson, Buffalo Head-Chinchaga domain, Wabamun, and Slave craton (Figure 2.6). Thus, the ~2.33 Ga age mode is also not a unique age mode for determining provenance via the methods of this study. The maturity of the quartzite in the lower MBG is consistent with a distal source for these sediments, hence the proximal ~2.30 Ga plutonic rocks (Hartlaub et al., 2007) might not be the most likely source. However, ~2.50 to 2.30 Ga rocks of the Arrowsmith orogeny along the western and northern margin of the Rae craton (Berman et al., 2013, 2005) could permissibly be a source of detritus of this age recorded in the psammopelitic to pelitic rocks of the upper MBG (U_1, U_2, and U_3). Th/U ratios less than 0.1 were also found in a few grains aged 2.33 to 2.35 Ga (Figure A.1) in the upper MBG samples, which can be attributed to Arrowsmith orogenesis. The neighboring Thluicho Lake Group also contains abundant detrital zircon of Arrowsmith age (2.47 to 2.25 Ga; Bethune et al., 2010).

While there is a dominant age population at ~2.33 Ga in both the upper and lower MBG, the upper MBG shows several dominant age populations that are younger than this. If ~2.33 Ga represents the maximum depositional age of the lower unit and ~2.17 Ga that of the upper unit (Ashton et al., 2013), then a hiatus of at least 160 million years between deposition of the upper and lower MBG is possible. Therefore, it is permissible that the boundary between the upper and lower MBG represents a significant unconformity, consistent with previous work asserting this possibility (Ashton et al., 2013; Bethune et al., 2013). Our contribution widens this gap by another ~160 million years, which would allow for up to a ~320 million year unconformity between the lower and upper MBG.

2.5.5 Provenance of the Upper Murmac Bay Group

The paucity of Archean grains in the upper MBG samples, along with the abundance of grains aged <2.33 Ga is consistent with a shift in sediment source between deposition of the upper and lower successions. The hiatus between deposition of the upper and lower MBG could

permissibly have been up to ~320 million years. Only one sample (U_4) from the upper MBG has a dominant Archean population ~2.60 Ga. Detrital zircon from the nearby Thluicho Lake Group also exhibit dominant populations of this age, which were attributed to proximal widespread felsic plutonism in the Rae craton ~2.64 to 2.58 Ga (Bethune et al., 2010; Skulski and Villeneuve, 1999).

The 2.15 to 2.19 Ga dominant age modes present in samples U_3 and U_4 correspond to only a few potential sources identified on the Slave craton and Buffalo Head-Chinchaga domain (Table 2.2), therefore, it is an ideal detrital zircon age population with which to investigate provenance. Figure 2.7 highlights these potential sources for these zircon populations that are centered around ~2.17 Ga, the most proximal being in the Blatchford Lake intrusive suite on the Slave craton, which intrudes the ~2.68 Ga Burwash formation turbidites (Bleeker et al., 2004). Interpreted crystallization ages for possible sources within the Blatchford Lake intrusive suite include: the Nechalacho layered suite at 2164 ± 11 Ma (LA-ICPMS; Mumford, 2013), the Hearne Channel granite at 2175 ± 5 Ma (TIMS; Bowring et al., 1984), the Grace Lake granite at 2176 ± 1 Ma (TIMS; Sinclair et al., 1994), and the Thor Lake syenite at 2177 ± 2 Ma (TIMS; Mumford, 2013). A more distal potential source candidate on the Slave craton is the Squalus Lake alkaline intrusion to the north of the Blatchford Lake intrusive suite, with an interpreted crystallization age at 2180 ± 1 Ma (TIMS; Villeneuve and van Breemen, 1994). Three samples from core in the Buffalo Head-Chinchaga domain, which is currently buried beneath Phanerozoic cover, were interpreted to have crystallized at 2159 ± 11 Ma, 2165 ± 5 Ma, and 2175 ± 2 Ma (TIMS; Villeneuve et al., 1993), respectively.

The upper MBG samples also contain a large number of grains ranging in age from 2.00 to 2.14 Ga. The nearby 2.13 to 2.09 Ga Rutledge River metasedimentary succession (Taltson), contains a population of 2.17 to 2.13 Ga detrital zircon, and records metamorphic zircon and monazite growth at ~2.09 to 2.06 Ga (Bostock and van Breemen, 1994). A few grains from this study exhibit Th/U ratios, which may be indicative of metamorphic origin (<0.2) within the same age range as the Rutledge River metamorphic zircon (Figure B.1). Gneisses in the subsurface from the Buffalo Head-Chinchaga domain also record crystallization ages between ~2.09 Ga to 2.07 Ga and 2.19 Ga to 2.16 Ga (Villeneuve et al., 1993). A syenogranite gneiss from the Taltson basement complex has been dated at ~2.14 Ga, though majority of the metaplutonic gneisses in this complex have ages ~2.40 - 2.30 Ga (McNicoll et al., 2000). These potential sources from the

Taltson basement complex lie geographically between the ~2.17 Ga provenance candidate locations and the MBG (Fig. 6). This suggests that sediment transport could have been directed from either the Slave or Buffalo Head during the time of deposition of the upper MBG.

2.5.6 Provenance Summary

The detrital zircon U-Pb age data from our samples highlight the relative lack of Archean grains in the upper MBG. As noted in Ashton et al. (2013), detrital zircon in the upper MBG are primarily younger than 2.33 Ga, whereas, detrital zircon in the lower unit are all ≥2.32 Ga, which demonstrates a shift in sediment source between the upper and lower MBG. This shift could be the result of burial or denudation of previous source rocks, exhumation of new sources associated with tectonic activity (Ashton et al., 2013), or evolution of drainage pathways. We consider the possibility of a potentially long-lived unconformity (Ashton et al., 2013; Bethune et al., 2013) to be plausible, based on the time gap indicated by our new age constraints. Since sediment was most likely sourced from the direction of the Blatchford Lake intrusive suite of the Slave craton or the subsurface granites of the Buffalo Head-Chinchaga domains, then the ~2.30 Ga zircon grains are most reasonably sourced either locally, or from the Taltson basement complex. The depositional age constraints of the upper MBG (<2.00 Ga to >1.93 Ga) suggest a connection with the Taltson orogen. The likelihood of sediment sources from the Slave craton and/or Buffalo Head domain support the hypothesis that the upper MBG was deposited in the foreland of the Taltson orogen.

Table 2.2 Summary of potential provenance candidates for the ~2.17 Ga dominant detrital zircon age population from the upper MBG.

TABLE 2.2. DETAILS OF POTENTIAL SOURCE ROCKS

Sample ID	Crystallization Age (Ma)	Technique	Description	Reference
Slave Craton				
79-13	2175 ± 5	TIMS	Hearne Channel Granite – Blatchford Lake Intrusive Suite	(Bowring et al., 1984)
90TL-16	2176 ± 1.3	TIMS	Grace Lake Granite – Blatchford Lake Intrusive Suite	(Sinclair et al., 1994)
600A	2164 ± 11	LA-ICPMS	Nechalacho Layered Suite – Blatchford Lake Intrusive Suite	(Mumford, 2013)
1201A	2177 ± 1.6	TIMS	Thor Lake Syenite – Blatchford Lake Intrusive Suite	(Mumford, 2013)
VN-92-XX	2180 ± 1	TIMS	Squalus Lake Alkaline Intrusion	(Villeneuve and van Breemen, 1994)
Buffalo Head-Chinchaga Domain				
Chevron Irving Cadotte	2165 ± 5	TIMS	Core from Buffalo Head Terrane	(Villeneuve et al., 1993)
Chevron et al Sheldon	2159 ± 11	TIMS	Core taken from Chinchaga Low	(Villeneuve et al., 1993)
Pan Am A-1 Bald Mt	2175 ± 2	TIMS	Core taken from Chinchaga Low	(Villeneuve et al., 1993)

2.6 CONCLUSIONS

New detrital zircon geochronological data from the upper MBG constrain the maximum depositional age of this succession at 1999 ± 13 Ma, which represents the weighted mean of the three youngest detrital zircon ages. By comparing our new data with previously published geochronological data for the MBG (Figure 2.4 and Table 2.1), we assess the differences in age populations between the upper and lower units of the MBG. While the lower unit contains only early Paleoproterozoic and Archean detrital zircon grains (3.95 to 2.33 Ga), the upper unit is dominated by <2.33 Ga zircon grains and exhibits a relative lack of zircon grains older than 2.33 Ga. Our findings reinforce the idea of a long-lived hiatus in deposition between the upper and lower MBG based on this difference in dominant age populations and disparity in inferred depositional ages, during which time there was a change in sediment source to the MBG basin (Ashton et al., 2013; Bethune et al., 2013). Additionally, U-Pb results of zircon overgrowth rims of 1931 ± 11 Ma and 1917 ± 15 Ma in our study agree with metamorphic monazite ages (Bethune et al., 2013).

The dominant age peaks in the lower MBG point to the Acasta Gneiss complex as a possible provenance location, as these are the only known exposed rocks within the database with crystallization ages matching the 3.90 to 3.60 Ga peaks seen in samples L_2 and L_3. Provenance candidates matching younger peaks in lower MBG samples (2.70 Ga and 2.33 Ga) are located both locally, and geographically between the Acasta Gneiss complex and the MBG, confirming it as a potential source for sediments in the lower MBG, though other as yet undiscovered potential sources might exist.

Based on available datasets, the ~2.17 Ga dominant age population in the upper MBG samples has two possible provenance locations, the most proximal being the Blatchford Lake intrusive suite located on the Slave craton, and the other from within the Buffalo Head-Chinchaga domain in Alberta, the latter currently buried under Phanerozoic cover. Geographically between the Blatchford Lake intrusive suite and the MBG there are several potential source rocks that could provide the source for the ~2.33 Ga dominant age peaks seen in the upper MBG, along with several proximal sources, however, there are fewer candidates for zircon aged between 2.00 and 2.14 Ga, dominantly ~2.13 Ga, which are located geographically between the Blatchford Lake intrusive suite and the MBG in the Taltson basement complex. We thus conclude that the most likely provenance source from currently known potential sources contained within the database for the ~2.17 Ga detrital zircon is the Blatchford Lake intrusive suite and the Buffalo Head-Chinchaga domains. Consequently, the ~2.33 Ga contributions to the MBG are likely to have been sourced locally or from the Taltson basement complex. Evidence from proximity, overlap in timing, and now provenance support the interpretation that the upper MBG was deposited in the foreland of the Taltson orogenic belt.

The most probable identified potential sources of both the 3.90 to 3.60 Ga and 2.17 Ga detrital zircon are located on the Slave craton, indicating that the Slave and Rae cratons would have been proximal during the time of MBG deposition in order for the Slave craton to have contributed to MBG sediments. The youngest detrital zircon grains in the lower MBG place timing of initial deposition in the Murmac Bay basin after 2.33 Ga. Thus, the Rae and Slave cratons would have to be proximal sometime after 2.33 Ga in order for the Slave craton to be a sediment source for the lower MBG sediments, if sediments in the lower unit were indeed sourced from the Acasta Gneiss complex. The two cratons would have remained in proximity during the deposition of the upper MBG. The upper MBG shows a distinct shift in sediment

source, possibly due to new tectonic activity resulting from amalgamation of the Slave and Rae cratons, or from accretion of the Buffalo Head-Chinchaga domain to the already sutured Rae and Slave cratons (Card et al., 2014).

With our interpreted sediment transport into the MBG basin being directed from the present-day north and west, we see no unambiguous contribution from the Hearne craton in these MBG sediments, and thus are unable to determine its position relative to the Rae craton in this study.

Determining sedimentary provenance in polydeformed terranes faces numerous challenges, particularly if primary sedimentary structures are altered or erased by deformation. Tracer isotopic analysis (e.g., Hf) can serve as a next step to further elucidate sediment provenance and tectonic setting. The methods presented in this paper are a first step in identifying potential sediment sources and highlight a practical application for integrating large geochronological databases into provenance analysis.

CHAPTER 3: AN INTEGRATED U-PB, HF, AND O ISOTOPIC PROVENANCE ANALYSIS OF THE PALEOPROTEROZOIC MURMAC BAY GROUP, NORTHERN SASKATCHEWAN, CANADA†

3.1 INTRODUCTION

Paleoproterozoic sedimentary successions were deposited during a time in history when Earth underwent major tectonic events as well as geochemical changes in the atmosphere-ocean system (e.g., Hoffman, 1988; Lyons et al., 2014). The Canadian Shield is host to a number of Paleoproterozoic sedimentary sequences, many of which have been studied using geochronology integrated with other available tools such as radiogenic and tracer isotopic analysis, geochemical data, and stratigraphy, to determine sedimentary provenance, correlate sedimentary basins, and infer tectonic setting (e.g., Tran et al., 2008; Rainbird et al., 2010; Ashton et al., 2013; Partin et al., 2014a; Wodicka et al., 2014; Shiels et al., 2016). Difficulties often arise in determining depositional environment, stratigraphic thickness, and basin tectonic setting in older sedimentary successions, as they have often been subject to one or more episodes of deformation or metamorphism, which can obscure or completely erase primary sedimentary structures. In the absence of primary sedimentary structures, coupled geochronological and isotopic investigations can reveal a substantial amount of information about sediment provenance, tectonic setting, and crustal growth.

Such is the case in the Paleoproterozoic Murmac Bay Group (MBG), which is situated on the southern Rae craton in the Canadian Shield, proximal to the Taltson orogeny, the eastern margin of the Slave craton, and the northern margin of the Buffalo Head-Chinchaga domains (Figure 3.1). The MBG, which is broadly divided into an upper and lower succession, has undergone at least two episodes of metamorphism (Bethune et al., 2013), and consequently primary sedimentary structures are only locally preserved in lower MBG quartzite, while they are absent in upper succession (Hartlaub et al., 2004). A provenance study using detrital zircon U-Pb geochronology (Shiels et al., 2016) identified three major age populations in the upper

† Shiels, C., Partin, C.A., Stern, R.A., 2017. An integrated U-Pb, Hf, and O isotopic provenance analysis of the Paleoproterozoic Murmac Bay Group, northern Saskatchewan, Canada. Precambrian Research. *In Review*.

MBG: one at ~2.31 Ga, representing the late-stage Arrowsmith orogeny, and two subdominant populations at ~2.17 Ga and ~2.10 Ga. Two potential sources for the subdominant peaks were identified on the neighboring Slave craton and Buffalo Head-Chinchaga domains, which may have important implications for the timing of amalgamation of the cratons that make up the western Canadian Shield. Accurately defining the age, provenance, and basin tectonic setting of the MBG allows for a fuller tectonic picture of the Rae craton and its surrounding environment during its depositional interval.

Here we focus on the ~2.00 to 1.93 Ga upper MBG, for which we present new zircon Hf and O isotopic data in concert with previously acquired U-Pb ages from the same grains (Shiels et al., 2016) to constrain the tectonic setting of the upper MBG basin and to characterize crustal growth in the southwestern Rae craton and surrounding cratons that now make up the western Canadian Shield.

3.1.1 Detrital zircon as an archive of geological events

The crystal structure of zircon preserves the magmatic isotopic composition and provides a reliable record of U-Pb, Lu-Hf, and O isotopic ratios at the time of crystallization (Hanchar and Hoskin, 2003). Zircon is able to crystallize from a wide range of melt compositions; it is a strongly refractory mineral that is highly resistant to isotopic resetting and alteration by physical, hydrothermal, and metamorphic processes. As such, zircon is a prevalent accessory mineral in igneous, metamorphic, and sedimentary rocks of the upper crust. Detrital zircon grains contained in sediments and sedimentary rocks have the potential to retain primary isotopic composition of the original igneous and metamorphic source rocks even through several episodes of sedimentary recycling.

Technological advancements in analytical techniques have allowed for precise U-Pb geochronology (e.g., Gehrels, 2011), Lu-Hf, and O isotopic analyses within the same zone of a single zircon grain (Hawkesworth and Kemp, 2006; Kemp et al., 2006). The combination of geochronological and isotopic data from detrital zircon provides insight into sediment provenance and tectonic setting (Cawood et al., 2012; Gehrels, 2014) and generation, evolution, and growth rate of continental crust (Belousova et al., 2010; Dhuime et al., 2012; Hawkesworth et al., 2010; Hawkesworth and Kemp, 2006).

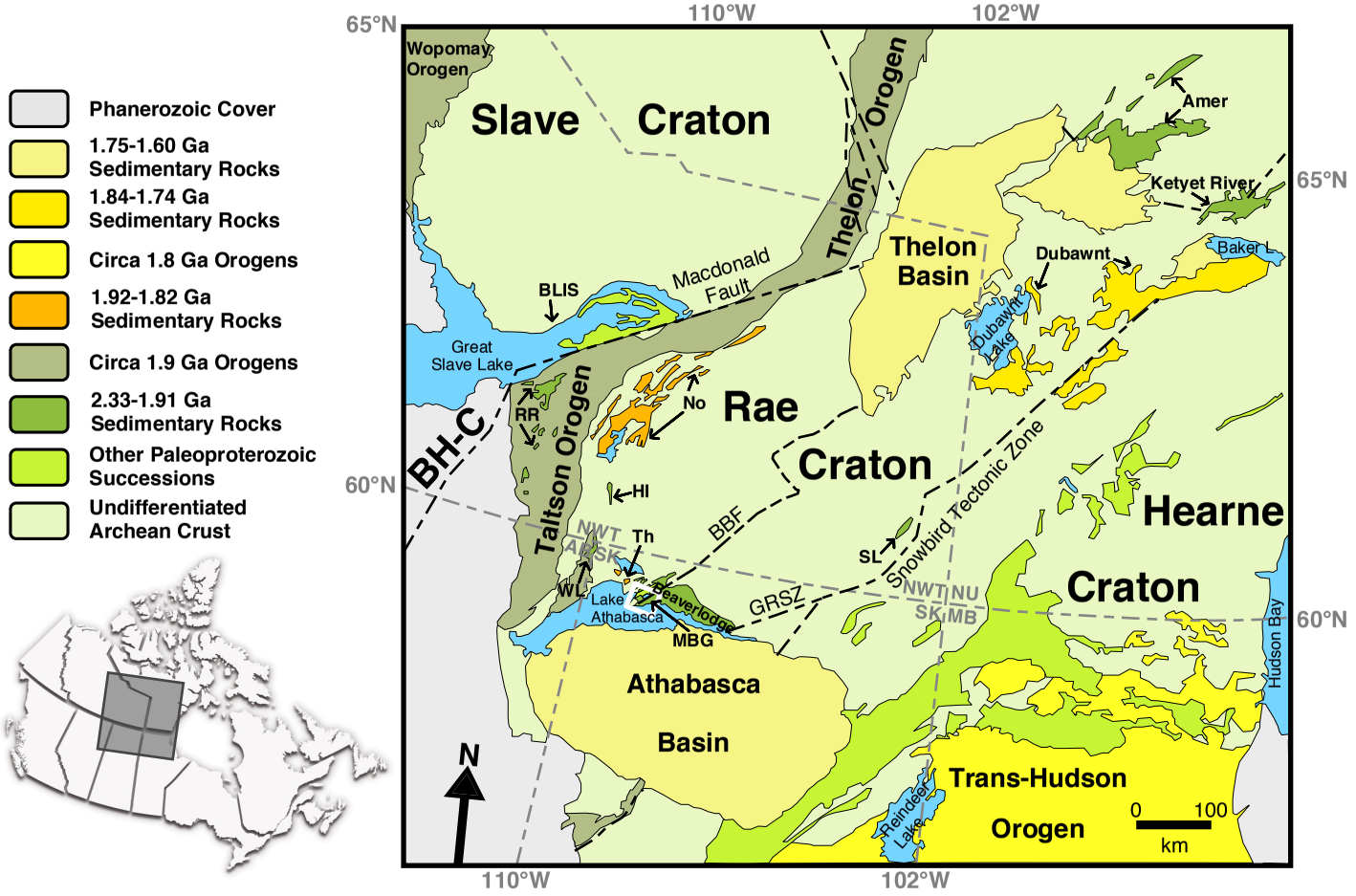

Figure 3.1 Currently exposed generalized geology of southern Rae and surrounding cratons in the Canadian Shield after Ashton et al. (2013). BBF = Black Bay Fault, BH-C = Buffalo Head-Chinchaga domains, BLIS = Blatchford Lake intrusive suite, GRSZ = Grease River Shear Zone, HI = Hill Island Lake metasedimentary rocks, No = Nonacho Group, RR = Rutledge River basin, SL= Snowbird Lake Group, Th = Thluicho Lake Group, WL = Waugh Lake Group; white rectangle highlights study area. Grey dashed lines are provincial boundaries, black dashed lines represent faults.

3.1.2 Zircon crystallization and crust formation

Analysis of the U-Pb isotopic system provides high precision ages of zircon crystallization, typically the age of crustal melting, and less commonly the age of high-grade metamorphism. Zircon preserves close to the $^{176}Hf/^{177}Hf$ of the melt from which it crystallizes, even through weathering and deformation (Hawkesworth and Kemp, 2006). Two stages of crust formation, described by Campbell and Hill (1988), are required for the formation of zircon: i) extraction of juvenile basaltic crust from the mantle, such as at mid-ocean ridges, which would exhibit the radiogenic composition of the mantle source and ii) remelting of this primitive crust and possible incorporation of sediments to form more felsic magma, which would inherit the isotopic composition of both the juvenile and reworked parental components, such as in island and continental arc settings (Iizuka et al., 2010; Wang et al., 2011, 2009). Isotopic analysis of zircon has the potential to reveal the timing of each of these stages. Since zircon $^{176}Hf/^{177}Hf$ is close to that of the melt from which it crystallized, a Hf model age can be calculated that estimates the timing of mantle extraction of the juvenile crustal source magma in the first stage, while zircon U-Pb ages represent the crystallization age from the more felsic, parental magma in the second stage. The difference between these two ages has been termed crustal residence time (Iizuka et al., 2010). The calculated Hf model age (T_{NC}) assumes that the parental magma lacked a mixed crustal or sedimentary component (Arndt and Goldstein, 1987). If this is not the case, then the T_{NC} age represents a hybrid age of the multiple source components (Iizuka et al., 2010; Roberts and Spencer, 2015), which were likely extracted from the mantle at different times. In this case, the T_{NC} age reflects only the minimum age of extraction of reworked crust with a mixed component (Nebel et al., 2007).

Oxygen isotopes fractionate only during low-temperature surficial processes in fluids or authigenic materials, such as evaporation, and formation of clays and ice sheets. The ratio of $^{18}O/^{16}O$ typical of magma derived from a homogeneous mantle ($\delta^{18}O_{VSMOW}$ = 5.3 ± 0.6‰; Valley, 2003) becomes elevated in rocks that have experienced sedimentary recycling or sea-floor hydrothermal alteration (Hawkesworth and Kemp, 2006; Valley, 2003). Zircon preserves the $\delta^{18}O$ of magma at the time of crystallization; oxygen diffusion in zircon is slow enough that the magmatic $\delta^{18}O$ is preserved even through high- temperature metamorphic and diagenetic processes (King et al., 1998; Peck et al., 2003), although some alteration of the $\delta^{18}O$ value can occur in metamict crystals (Roberts and Spencer, 2015). Thus, oxygen isotope analysis can serve

to distinguish between zircons that crystallized from juvenile, mantle-derived parental magmas and those whose parental magma contained mixed juvenile and sedimentary components, which would record a hybrid T_{NC} age (Hawkesworth et al., 2010).

3.2 STUDY AREA AND SAMPLES

3.2.1 Geological setting

The >2.33 to <1.93 Ga MBG is a greenschist- to upper amphibolite- and locally granulite-facies metasedimentary succession deposited in the Beaverlodge domain, near the southern margin of the Rae craton in the Canadian Shield (Figures 3.1 and 3.2). It is broadly divided into an upper and lower succession, which lie unconformably above the Mesoarchean granitic basement (Figure 3.2). The lower MBG consists of local basal polymictic conglomerate that grades into mature grey quartzite, which is in turn intercalated with metamorphosed psammite, oligomictic conglomerate, dolostone, and silicate and oxide facies iron formation toward the top of the unit, beneath mafic volcanic rocks (Ashton et al., 2013; Hartlaub et al., 2004). The lower succession, and possibly the lowermost upper MBG, are intruded by ultramafic rocks and coarse-grained black gabbro dykes and sills, which have not been dated, but are interpreted as feeder dykes to MBG volcanism (Hartlaub et al., 2004). The weighted mean of the four youngest detrital zircon grains in the lower MBG yield a maximum depositional age of 2329 ± 8.6 Ma (Ashton et al., 2013). Deposition of the lower succession is inferred to have taken place shortly after emplacement of the proximal 2.33 to 2.29 Ga North Shore plutons, following ~2.34 to 2.30 metamorphism (Hartlaub et al., 2004) of basement rocks during the Arrowsmith orogeny (Figure 3.3; Bethune et al., 2013). A recent $\delta^{13}C$ isotope study suggests deposition of part of the lower MBG during the ~2.20 to 2.06 Ga Lomagundi Event (McDonald and Partin, 2016) in a shallow marine environment (Ashton et al., 2013; Hartlaub et al., 2004).

The upper succession is laterally extensive, and composed of quartzofeldspathic pelitic to psammopelitic rocks that are locally migmatitic at higher metamorphic grades. The base of this unit is locally interlayered with lower MBG mafic volcanic rocks (Hartlaub et al., 2004); the cause of this interlayering is difficult to determine due to a lack of preserved sedimentary structures in the upper MBG. A maximum depositional age of 1999 ± 13 Ma was determined from the weighted mean of the youngest detrital zircon grains in three samples from the upper MBG (Shiels et al., 2016), narrowing the depositional age range from the previously published

maximum depositional age of 2.17 Ga (Ashton et al., 2013; Bethune et al., 2013). A minimum age constraint for deposition is provided by the crosscutting relationship with the ~1.93 Ga Donaldson Lake granite (Ashton et al., 2013), and monazite growth in deformation fabrics at ~1.93 and ~1.91 Ga (Bethune et al., 2013). The ~1.82 Ga Martin Group unconformably overlies the MBG over much of the Beaverlodge domain (Hartlaub et al., 2004; Morelli et al., 2009).

3.2.2 Provenance and tectonic setting

Provenance of MBG sediments was investigated by Shiels et al. (2016) using DateView (Eglington, 2004; Eglington et al., 2013), a large database of more than 100,000 published and public-domain isotope geochemical records to find potential source rocks by matching crystallization ages with peaks in the MBG U-Pb age spectra. The upper MBG U-Pb age spectrum displays three dominant populations at 2.31 Ga, 2.17 Ga, and 2.10 Ga and exhibits a paucity of Archean grains (Shiels et al., 2016). Proximal potential sources for the 2.31 Ga population include the 2.33 to 2.29 Ga North Shore plutons in the Beaverlodge domain (Hartlaub et al., 2007), and more distally, ~2.40 to 2.30 Ma metaplutonic rocks of the Taltson Basement Complex (McNicoll et al., 2000).

The tectonic settings of the upper and lower MBG successions are not as yet well defined. Interbedding of the basal conglomerates and quartzites may be due to episodic faulting consistent with an extensional tectonic setting (Ashton et al., 2013), possibly in a rift or intracratonic basin for the lower succession (Bethune et al., 2013; Hartlaub et al., 2004); the rift basin interpretation is supported by the presence of basal conglomerate and mafic volcanics in the lower MBG, suggesting an extensional setting (Hartlaub et al., 2004). The upper succession is contemporaneous with the neighboring 1.99 to 1.93 Ga Taltson orogeny, which represents a subduction-related magmatic arc emplaced into older rocks of the Taltson basement complex resulting from either the amalgamation of the Slave and previously accreted Buffalo Head terrane and Rae cratons, or accretion of the Buffalo Head terrane to an already sutured Slave and Rae (Card et al., 2014). The upper MBG sediments are likely, at least in part, sourced from the neighboring Slave craton or Buffalo Head-Chinchaga domains (Shiels et al., 2016). This along with metamorphism coeval with the Taltson orogen (Bethune et al., 2013) suggests that deposition occurred in the foreland of the Taltson orogen.

3.2.3 Sample description

Three samples were collected for this study from the upper MBG: a fine-grained, greenschist-facies pelitic schist from the type section of the upper MBG near Uranium City, Saskatchewan, and two quartzofeldspathic, upper amphibolite-facies paragneisses located west of the Black Bay fault (Figure 3.2). Precise stratigraphic relationships between the three samples are difficult to determine, however, since the west block of the Black Bay fault is the upthrown block, the two samples collected there are inferred to be from a lower stratigraphic level than the sample collected from the east, downthrown block. Full sample descriptions are presented in Shiels et al. (2016).

3.3 METHODS

Detrital zircon grains were separated from crushed samples using conventional separation techniques for U-Pb analysis as in Shiels et al. (2016). In order to reduce sampling bias, I handpicked zircon grains from mineral separates to include a representative sample with regard to color, morphology, and size, with the smallest grains analyzed being necessarily large enough to accommodate the largest beam size (40-49 μm for Hf isotope analysis). I then mounted selected zircon grains in a 25 mm epoxy mount alongside Temora2 and Mudtank zircon primary reference material for calibration in all subsequent analyses and then polished to expose the midsections of the grains. Cathodoluminescence (CL) and backscattered electron (BSE) images revealed that the majority of grains analyzed exhibited igneous oscillatory- or sector-zoning patterns in their interiors, as well as distinctive unzoned overgrowths that appeared dark in CL images (Figure B.1). I targeted analyses largely within the igneous zoned regions, as they are likely to preserve the magmatic chemistry at the time of crystallization. A few analyses were performed in unzoned overgrowth rims that were wide enough to accommodate the beam size.

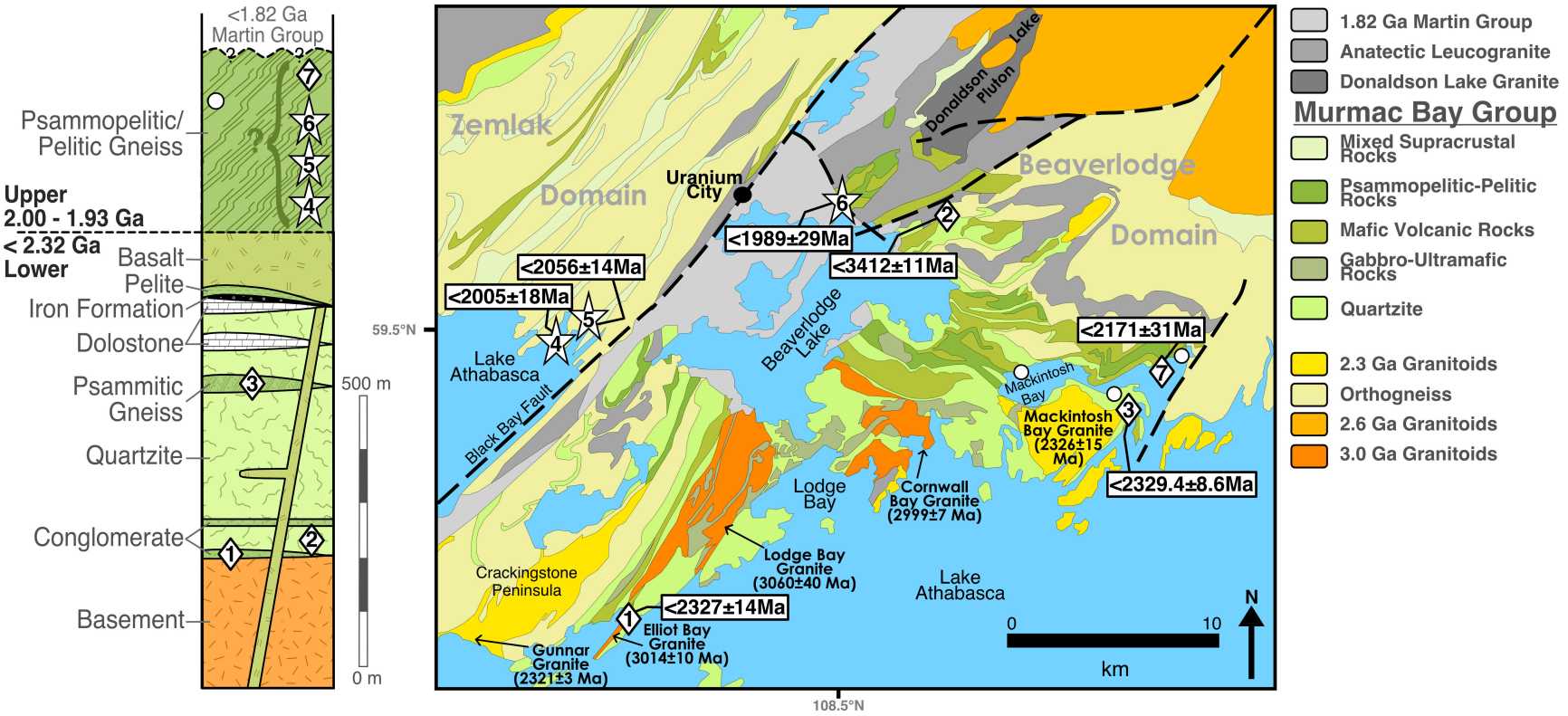

Figure 3.2 Simplified geology and lithostratigraphy of the western Beaverlodge domain after Ashton et al. (2013) and Shiels et al. (2016). Sample locations labeled as follows: diamonds are U-Pb detrital zircon ages from previously published data, except number one, which is a TIMS age thought to be controlled by felsite clasts (Ashton et al., 2013; Hartlaub et al., 2006), stars denote new samples collected for this study, circles indicate metamorphic ages as indicated by monazite growth (Bethune et al., 2013). Stratigraphic order in the upper MBG is inferred, as primary sedimentary structures have been largely erased by multiple episodes of deformation in the upper succession.

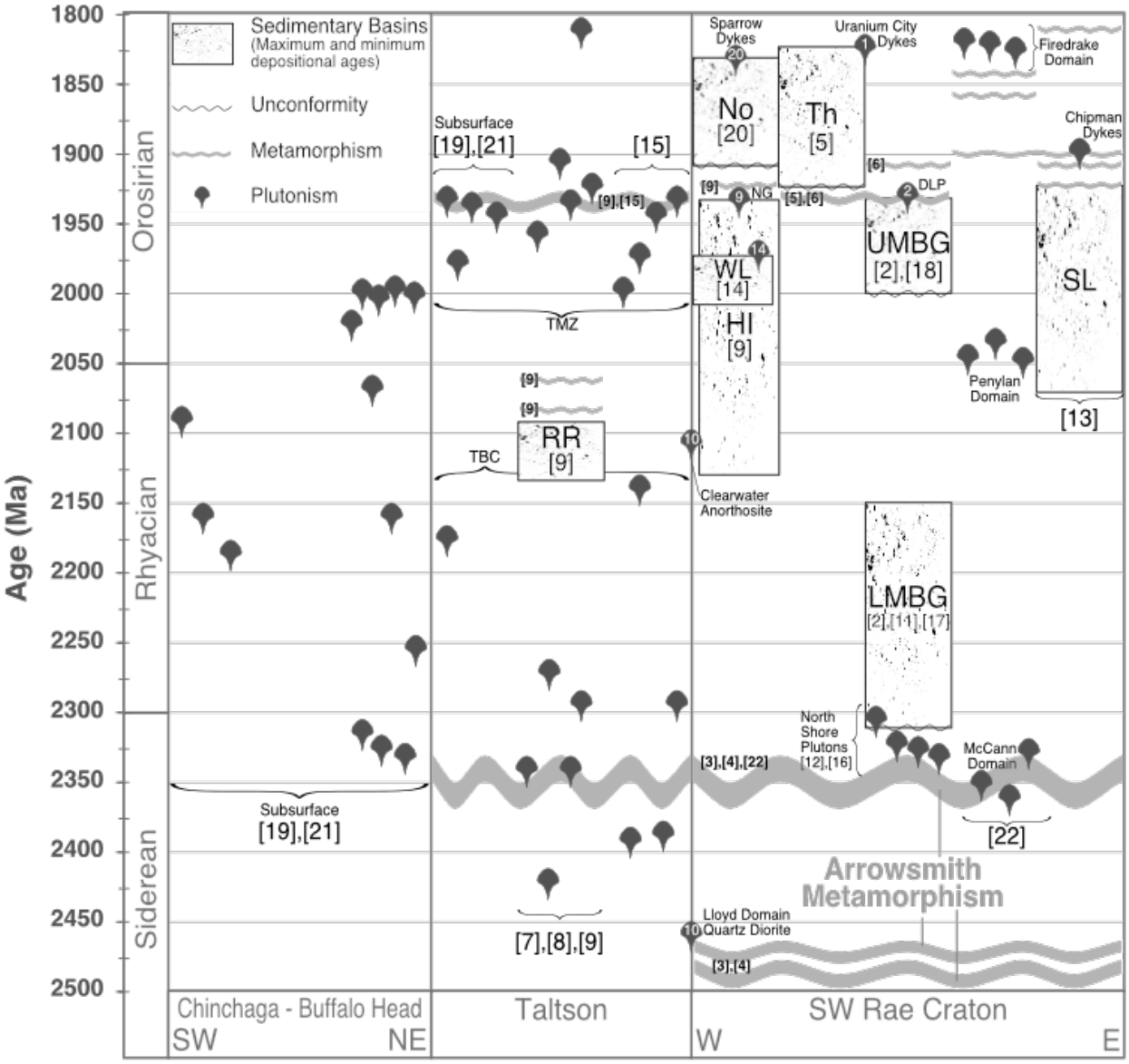

Figure 3.3 Time-space diagram depicting timing of sedimentary deposition, metamorphism and plutonism from the Buffalo Head-Chinchaga domains, Taltson and southwestern Rae craton. References cited: Ashton et al., 2009[1], 2013[2]; Berman et al., 2005[3], 2013[4]; Bethune et al., 2010[5], 2013[6]; Bostock and Loveridge, 1988[7]; Bostock et al., 1991[8]; Bostock and van Breemen, 1994[9]; Card et al., 2014[10]; Hartlaub et al., 2006[11], 2007[12]; Martel et al., 2008[13]; McDonough and McNicoll, 1997[14]; McNicoll et al., 2000[15]; Partin et al., 2014[16]; Partin and Sylvester, 2016[17]; Shiels et al., 2016[18]; Thériault and Ross, 1991[19]; Van Breemen and Aspler, 1994[20]; Villeneuve et al., 1993[21]; Davis et al., 2015[22]. DLP = Donaldson Lake pluton, NG = Natael granite, TBC = Taltson basement complex, TMZ = Taltson magmatic zone, LMBG = lower Murmac Bay Group, UMBG = upper Murmac Bay Group, remaining abbreviations as in Figure 3.1.

.

3.3.1 Oxygen isotope analysis

Analysis of oxygen isotopes ($^{18}O/^{16}O$) by Secondary Ion Mass Spectrometry (SIMS) was conducted at the Canadian Centre for Isotopic Microanalysis using a Cameca IMS 1280 multicollector ion microprobe. Full methodology is reported in Partin et al. (2014b). Briefly, a $^{133}Cs^{+}$ primary beam was operated with impact energy of 20 keV and beam current of ~ 2.0 nA. The ~10 μm diameter probe was rastered (18 x 18 μm) for 75 s prior to acquisition, and then 5 x 5 μm during acquisition resulting in a spot size of ~13 x 15 μm across and ~2 μm in depth. The normal incidence electron gun was utilized for charge compensation. The mass/charge separated oxygen ions were detected simultaneously in Faraday cups L'2 ($^{16}O^{-}$) and H1 ($^{18}O^{-}$) at mass resolutions (m/Δm at 10%) of 1900 and 2250, respectively. Secondary ion count rates for ^{16}O and ^{18}O were typically ~2 x 10^9 and 4 x 10^6 counts/s utilizing 10^{10} Ω and 10^{11} Ω amplifier circuits, respectively. Instrumental mass fractionation (IMF) was monitored by repeated analysis of reference material (Temora2: $\delta^{18}O_{VSMOW}$ = +8.2 ‰; Mudtank: $\delta^{18}O_{VSMOW}$ = +4.87).

$$\delta^{18}O_{VSMOW} = \left(\frac{\left(\frac{^{18}O}{^{16}O}\right)_{sample}}{\left(\frac{^{18}O}{^{16}O}\right)_{VSMOW}} - 1 \right) 1000(‰) \qquad \text{(Eq. 1)}$$

$\delta^{18}O$ was determined using Equation 1 (Faure, 1977), relative to Vienna standard mean ocean water (VSMOW). Oxygen and hafnium data are reported in Table C.1.

3.3.2 U-Pb geochronology

U-Pb isotopes were measured using an O_2-primary beam on the Sensitive High Resolution Ion Microprobe (SHRIMP II) at the Geological Survey of Canada in Ottawa following the procedures of Stern (1997), with 20 μm spots targeted directly on top of, or immediately next to and within, the same zone as previous O-isotope analysis spots as determined by CL and BSE images. Full analytical methods and data are reported in Shiels et al. (2016).

3.3.3 Hf isotope analysis

Hafnium isotopes were measured at Memorial University by laser ablation multi-collector inductively-coupled plasma mass-spectrometry (LA-MC-ICP-MS) as described by Souders et al. (2013). I acquired analyses by ablating a spot directly on top of U-Pb analysis

spots to allow for analysis of the same zone, using a 10 Hz pulse over a sixty-second ablation period, with power density at 5 J/cm^2. Most analysis spots were 49 μm in diameter, but a 40 μm spot was used for some smaller sized grains in order to avoid overlap in zircon domains. Chondritic values of $^{176}Lu/^{177}Hf = 0.0336$ and $^{176}Hf/^{177}Hf = 0.282785$ (Bouvier et al., 2008) were used to calculate εHf, with errors ranging from 0.5 to 2.4 εHf units. Full data for all analyzed zircon grains are listed in Table C.1.

3.4 RESULTS

3.4.1 U-Pb geochronology

All detrital zircon ages of the upper MBG with <10% discordance are displayed as a combined frequency histogram and probability density curve in Figure 3.4a, ranging from 3.14 to 1.85 Ga. A major U-Pb age peak at 2.31 Ga corresponds to the late stages of the Arrowsmith orogeny (2.5 to 2.3 Ga; Berman et al., 2005, 2013; Hartlaub et al., 2007), with secondary peaks at 2.17 and 2.10 Ga. The weighted mean age of the three youngest detrital zircon grains that were not recrystallized or otherwise altered after deposition is 1999 ± 13 Ma, representing the maximum depositional age for the upper MBG; the few grains younger than this age were interpreted to have formed during metamorphism (Shiels et al., 2016).

3.4.2 Oxygen isotopes

Oxygen isotope data (n=138) are plotted against U-Pb ages and T_{DM} in Figure 3.5. All analyses are below $\delta^{18}O_{VSMOW} = 10.65‰$, with three analyses falling below the accepted value for mantle-derived magma ($\delta^{18}O_{VSMOW} = 5.3 \pm 0.6‰$; Valley, 2003) suggesting alteration of their source rocks by hydrothermal or meteoric fluids (Valley, 2003; Valley et al., 2005; Roberts and Spencer, 2015). There is a noticeable step-wise increase in $\delta^{18}O$ from ~6.5‰ at 2.50 Ga to >9.0‰ at 2.33 Ga, which coincides with the timing of the Great Oxidation Event (e.g., Lyons et al., 2014). More than half of the grains analyzed record mantle-like $\delta^{18}O$ values, which are defined as $\delta^{18}O < 6.5‰$, taking into account analytical precision and that small amounts of sediment and subducting slabs are likely incorporated into the mantle, but would have a minimal effect on smearing of the Hf model ages (Hawkesworth et al., 2010; Hawkesworth and Kemp, 2006; Roberts and Spencer, 2015; Wang et al., 2011, 2009). Zircons with $\delta^{18}O > 6.5‰$ are therefore interpreted to have crystallized from magmas with a mixed supracrustal component.

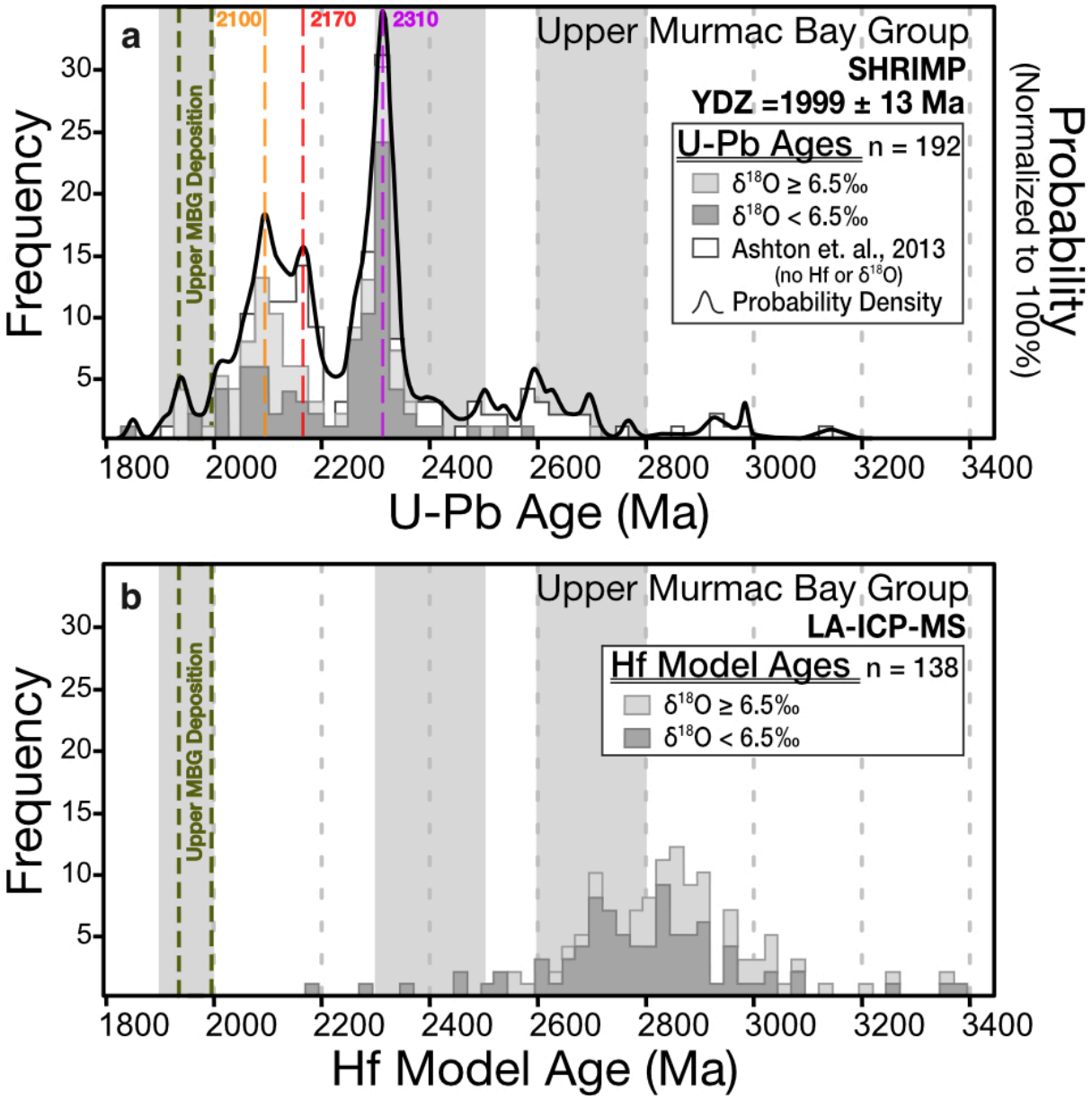

Figure 3.4 Frequency and probability of a) U-Pb ages for the upper Murmac Bay Group: dark grey histogram indicates $\delta^{18}O < 6.5‰$, and light grey is $\delta^{18}O > 6.5‰$, from Shiels et al. (2016); white is from Ashton et al. (2013), which were not analyzed for Hf or O isotopes, YDZ = youngest detrital zircon, and b) frequency of calculated Hf model ages. Grey bars indicate timing of regional tectonic events: 2.0-1.9 Ga Taltson orogeny, 2.5-2.3 Ga Arrowsmith orogeny, and 2.8-2.6 Ga assembly of Sclavia. SHRIMP = sensitive high-resolution ion microprobe, LA-ICP-MS = laser ablation inductively-coupled plasma mass spectrometry.

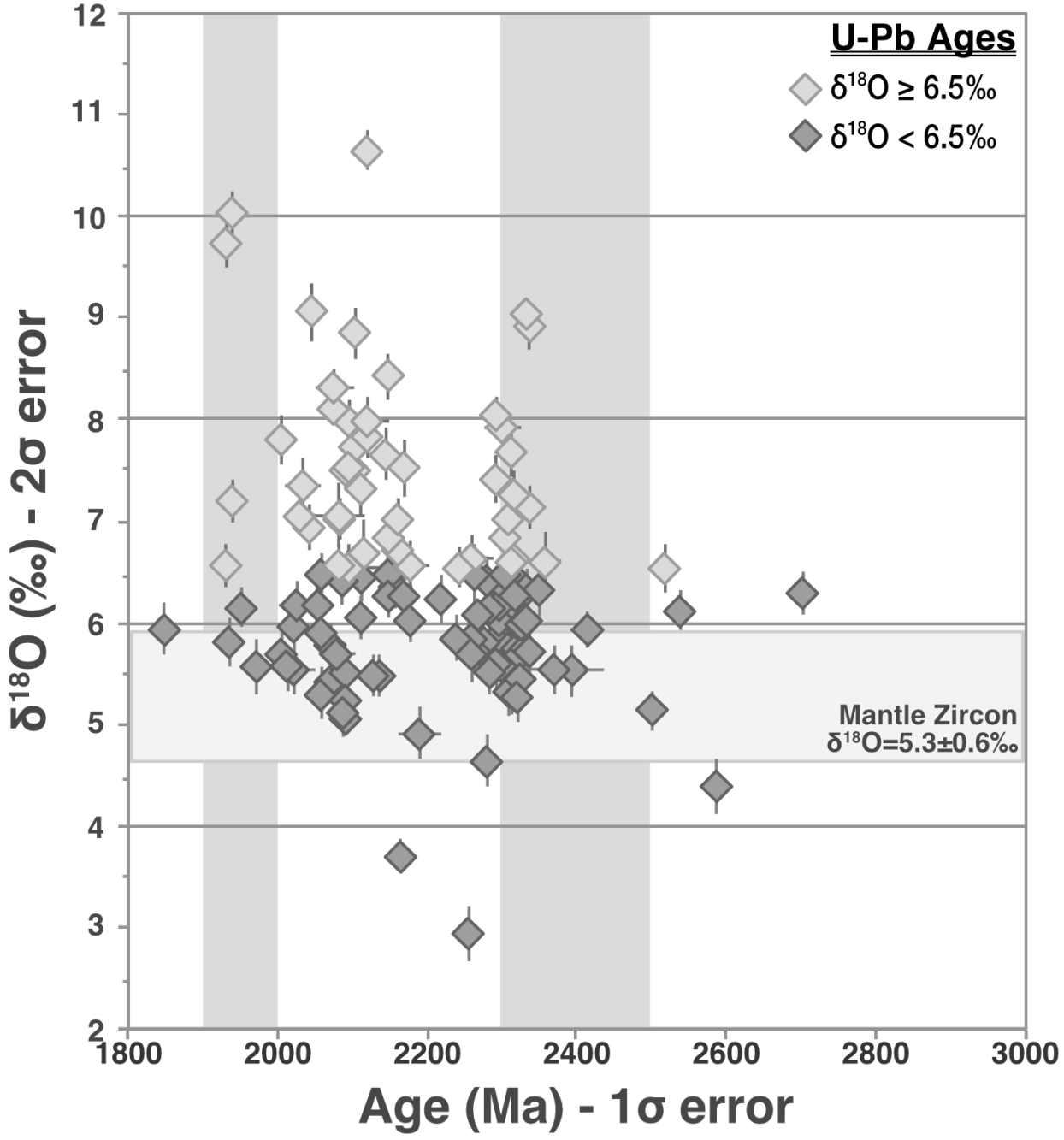

Figure 3.5 Detrital zircon $\delta^{18}O$ data from the upper Murmac Bay Group plotted against U-Pb crystallization age. Dark grey indicates $\delta^{18}O < 6.5‰$, light grey is $\delta^{18}O > 6.5‰$. Grey bars indicate timing of regional tectonic events: 2.0-1.9 Ga Taltson orogeny, and 2.5-2.3 Ga Arrowsmith orogeny.

3.4.3 Lu-Hf isotopes

Epsilon Hf is plotted against U-Pb crystallization age in Figure 3.6. The depleted mantle growth line (DM) is modeled using $^{176}Lu/^{177}Hf = 0.0388$, present day $^{176}Hf/^{177}Hf = 0.28325$

(Andersen et al., 2009; Griffin et al., 2000), and a ^{176}Lu decay constant of $1.867x10^{-11}yr^{-1}$ (Söderlund et al., 2004). The DM model age is based on the $^{176}Hf/^{177}Hf$ ratio of mid-ocean ridge basalts, however, since new continental crust is primarily generated at subduction zones, it has been suggested that the $^{176}Hf/^{177}Hf$ ratio of island arc volcanic rocks would be a more appropriate value for calculating a Hf model age. Figure 3.6 also shows a "new crust" (NC) line with present day εHf = +13.2 (Dhuime et al., 2011), based on the mean value for island arc volcanic rocks, which is similar to the present day average εHf value of +13.4 for mid-ocean ridge basalts from Chauvel et al. (2008). A mean present day εHf =+13.3 was also calculated by Iizuka et al. (2013) using primary Hf isotopic data from modern island arcs and excluding samples containing contaminated and anomalous mantle. Epsilon Hf values for the upper MBG samples range from -7.6 to +5.7, nearly half (48%) of which are positive values, indicating a more juvenile source magma. Most (82%) that plot between the CHUR and DM lines also exhibit mantle-like $\delta^{18}O$ values (Fig. 6).

Zircon Hf model ages were calculated using the U-Pb ages and Hf isotopic compositions. This calculation projects the εHf value back to the new crust growth line by assuming a $^{176}Lu/^{177}Hf$ ratio for the source of the melt from which the zircon crystallized. The initial $^{176}Lu/^{177}Hf$ used in this calculation has a high degree of influence on the results, and since there are observable differences in this ratio within the crust, we assign an appropriate $^{176}Lu/^{177}Hf$ ratio to each analyzed detrital zircon, based on whether the $\delta^{18}O$ of that zircon indicates crystallization in a more mafic or mantle-derived melt ($\delta^{18}O < 6.5‰$), or from a more mixed, crustal melt with a significant sedimentary component ($\delta^{18}O > 6.5‰$). The $^{176}Lu/^{177}Hf$ ratio is represented by the slope of a line intersecting the depleted mantle curve on a plot of εHf against U-Pb crystallization age (Figure 3.6; Kemp et al., 2006), such that zircon from source magmas with different ages, but the same mantle extraction age and composition, will fall along the same line (Pietranik et al., 2008), assuming that no mixing of magmas or incorporation of crustal materials has occurred between crystallizations. T_{DM} ages for this study were calculated with $^{176}Lu/^{177}Hf$ = 0.022 for zircons with $\delta^{18}O < 6.5‰$, and $^{176}Lu/^{177}Hf$ = 0.010 for those with $\delta^{18}O > 6.5‰$ after Pietranik et al. (2008).

As zircons with high $\delta^{18}O$ values are interpreted to have crystallized from melt with a significant sedimentary component or altered mafic crust, the T_{DM} calculated for these grains represents a mixed or hybrid age, and can only be considered as a minimum age of extraction

from the mantle. Thus, the T_{DM} of zircons that record more primitive, mantle-like $\delta^{18}O$ values are considered the best measure of the timing of crustal generation (Hawkesworth et al., 2010; Hawkesworth and Kemp, 2006). The T_{DM} ages are shown as a frequency histogram (Figure 3.4b), where it can be seen that the Hf model ages of mantle-like zircon grains define two peaks centered around 2.83 Ga and 2.70 Ga.

3.5 DISCUSSION

3.5.1 Tectonic basin setting

Detrital zircon U-Pb age spectra can elucidate the tectonic setting of their depositional basins (Cawood et al., 2012). The peaks and troughs in U-Pb age spectra have been associated with collisional events during supercontinent assembly (e.g., Spencer et al., 2015). Applying these interpretations to the MBG dataset, the spectra of U-Pb ages for the lower MBG are consistent with deposition in an extensional basin, as less than 5% of analyzed grains are dated within 150 million yr of deposition (Cawood et al., 2012). The U-Pb age spectrum of the upper MBG (Figure 3.4a) is most consistent with syn-orogenic deposition (Spencer et al., 2015) during the 1.99 Ga to 1.93 Ga Taltson orogeny in a foreland basin setting, illustrated by the dearth of detrital zircon ages contemporary with deposition, but a significant proportion of ages (42%) within 150 million yr of the depositional age (Cawood et al., 2012).

3.5.2 Crustal residence and crustal growth

The difference between Hf model age and U-Pb age is illustrated in Figure 3.5. Zircon grains with $\delta^{18}O > 6.5‰$ all have T_{NC} ages less than 2.87 Ga and all but two have a crustal residence time less than 600 million yr. In contrast, zircon with juvenile, mantle-like $\delta^{18}O$ signatures exhibit a wider range in both T_{NC} ages and crustal residence time, which may indicate that zircons from a parent magma with a mixed supracrustal component crystallized relatively quickly after extraction from the mantle in the source region. Likewise, zircons with the longest crustal residence times tend to have positive εHf values and mantle-like $\delta^{18}O$ signatures, suggesting that a long period of crustal residence can occur without incorporation of supracrustal material, though these observations could be a consequence of the $^{176}Lu/^{177}Hf$ values chosen for calculation of T_{NC}. Frequency of T_{NC} ages for zircons with mantle-like $\delta^{18}O$ peak at 2.83 Ga and 2.70 Ga (Figure 3.4b), representing periods of crustal growth in this region, which correlate well

with peaks in Sm-Nd model ages for the western Churchill province (Peterson et al., 2010). These may represent important periods of crustal growth on the Rae and surrounding cratons.

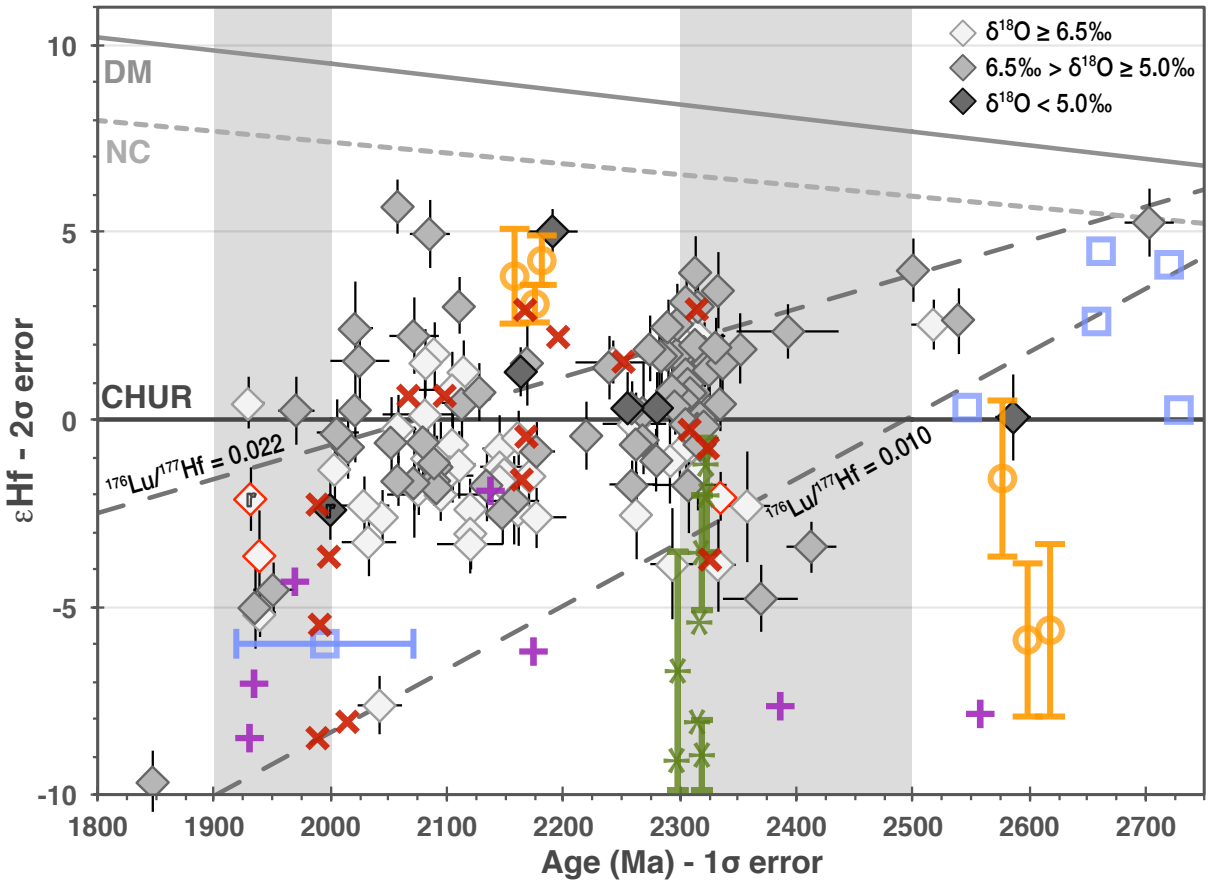

Figure 3.6 Detrital zircon εHf plotted against U-Pb crystallization ages for the upper Murmac Bay Group. Dark grey indicates $\delta^{18}O < 6.5‰$, light grey is $\delta^{18}O > 6.5‰$, zircons with $\delta^{18}O < 5.0‰$ have a black outline. Red outline indicates Th/U ≤ 0.1, indicating a metamorphic origin, and "r" indicates the analysis was targeted in an overgrowth rim. CHUR = chondritic uniform reservoir, DM = depleted mantle, NC = new crust. Diamonds are εHf values from this study, all other marks indicate converted εNd values (Vervoort et al., 2011) from potential sediment sources: asterisks (*) = North Shore plutons (Hartlaub et al., 2007, 2005); crosses (+) = Taltson Basement Complex and magmatic zone (McNicoll et al., 2000; Thériault and Ross, 1991); circles= Blatchford Lake intrusive suite and surrounding country rock (Bowring et al., 1984; Mumford, 2013; Sinclair et al., 1994; Yamashita et al., 1999; Yamashita and Creaser, 1999); x's (x) = subsurface core samples from the Buffalo Head-Chinchaga domains (Thériault and Ross, 1991; Villeneuve et al., 1993); squares (□) = Snowbird Lake area rocks (Martel et al., 2008).

3.5.3 Comparison to proximal Paleoproterozoic sedimentary successions

The Amer and Ketyet River groups that lie to the northeast of the MBG on the Rae craton (Figures 3.1 and 3.3) show stratigraphic similarities to the MBG. Their lower assemblages share similarities in detrital zircon U-Pb ages with the lower MBG and their maximum depositional

ages are poorly constrained at ~2.30 Ga (Rainbird et al., 2010; Ashton et al., 2013). The upper assemblages of these supracrustal successions share U-Pb age peaks at ~2.30 Ga, similar to the upper MBG, however, both exhibit major peaks in the 2.60 to 2.40 Ga range (Rainbird et al., 2010), which are not well-represented in our upper MBG samples. The Amer and Ketyet River groups also lack the major ~2.17 Ga and ~2.10 Ga U-Pb age populations seen in the upper MBG.

Metasedimentary rocks in the Snowbird Lake area near the eastern margin of the Rae craton, along the Snowbird tectonic zone (Figures 3.1 and 3.3), were deposited between ~2.07 Ga and 1.92 Ga bracketed by their youngest detrital zircon and the oldest age of metamorphism (Martel et al., 2008). These metasedimentary rocks contain a population of U-Pb ages in the 2.70 Ga to 1.93 Ga range, with less than half of them aged between 2.31 Ga and 2.10 Ga. They also exhibit a negative εNd value (Martel et al., 2008).

The Thluicho Lake Group near the northern shore of Lake Athabasca in the neighboring Zemlak domain (Figures 3.1 and 3.3) is constrained in depositional age between 1.92 Ga and 1.82 Ga (Bethune et al., 2010). The U-Pb detrital zircon age spectrum of Thluicho Lake Group shows a majority of ages between 2.60 Ga and 2.30 Ga, with major peaks at 2.60 Ga, 2.40 Ga, and 2.30 Ga, they contain few ages in the 2.30 Ga to 2.10 Ga range (Bethune et al., 2010), suggesting a different source than that of upper MBG sediments. There is a possible correlation between the Thluicho Lake Group and the 2.06 Ga to 1.83 Ga Nonacho Group (Van Breemen and Aspler, 1994) to the north near the Rae–Taltson boundary (Figures 3.1 and 3.3), based on tectonostratigraphic similarities and a correlation of a major population of 2.48 Ga to 2.31 Ga U-Pb ages, though the Thluicho Lake Group lacks representation for principal 3.30 to 3.05 Ga, 2.48 to 2.31 Ga, and 2.13 to 2.06 Ga age groups noted in the Nonacho Group (Bethune et al., 2010; Van Breemen and Aspler, 1994).

The 2.01 to 1.97 Ga Waugh Lake supracrustal gneisses lie to the northwest, near the border of Saskatchewan, Alberta, and the Northwest Territories (Figures 3.1 and 3.3), and are thought to have been deposited in a Taltson aged back-arc basin (McDonough et al., 2000). The Waugh Lake Group is lithologically similar to the MBG (Ashton et al., 2013). Of ten detrital zircon grains analysed for U-Pb ages, nine were in the 2.33 to 2.00 Ga range, with one grain at 2.74 Ga (McDonough and McNicoll, 1997).

Geographically between Waugh Lake and the Nonacho Group is the ~2.13 to 1.93 Ga Hill Island Lake Group (Figures 3.1 and 3.3); of the nine zircon grains analyzed in a greywacke

sample, two are dated at 2.17 Ga, one at 2.13 Ga, and the remaining six are <1.92 Ga (Bostock and van Breemen, 1994). The Hill Island Lake Assemblage has been correlated with rocks of the Rutledge River Basin in the Taltson Magmatic Zone (Figures 3.1 and 3.3), which were deposited in a rift setting prior to the Taltson orogeny (Bostock and van Breemen, 1994). The ~2.13 to 1.93 Ga Rutledge River Group has detrital zircon age populations matching the ~2.10, ~2.17, and ~2.31 Ga age peaks seen in the upper MBG, and contain few Archean detrital zircons (Bostock and van Breemen, 1994), suggesting a similar source and the possibility of correlation between the Rutledge River Basin rocks and the upper MBG. Modern detrital zircon studies of these sediments, including Hf and O isotopic investigations, are needed to further characterize and correlate Paleoproterozoic Rae craton sedimentary successions.

3.5.4 Provenance of the upper Murmac Bay Group

A number of potential sources have been identified for upper MBG sediments based on correlation of peaks in the U-Pb age spectrum, both locally on the Rae craton and on neighboring cratons. Very few of these rocks have been analyzed for the Lu-Hf isotope system or O isotope ratios; however, published εNd data exists for several potential source rocks. Using the present day Terrestrial Array (Vervoort et al., 2011) we have converted available εNd values for potential source rocks to εHf, which is plotted against U-Pb crystallization age along with published εHf values from potential source rocks and from this study (Figure 3.6). Values that have been converted are reported in Table C.2, and marked with an asterisk in the following text.

The most proximal potential sources are the 2.33 to 2.29 Ga North Shore plutons (Hartlaub et al., 2007), which have an εHf range of -0.5 to -12.8 (Hartlaub et al., 2007; Partin et al., 2014). The majority of zircons aged ~2.31 Ga from this study exhibit positive εHf values and mantle-like $\delta^{18}O$, suggesting a juvenile, mantle-sourced parental magma. Thus, the North Shore plutons are not a likely source for the majority of similarly aged upper MBG detrital zircon grains. Other juvenile ~2.31 Ga magmatism has been identified in the detrital zircon record of Paleoproterozoic successions on the northeastern Rae craton (Partin et al., 2014), but their source remains elusive. The nearby Taltson Basement Complex has only a few analyses within the age range of upper MBG deposition that all exhibit negative εHf* values, with all but two samples falling well below the range of the upper MBG. A local source for the positive εHf values has yet to be identified, as no known juvenile crustal ~2.31 Ga rocks have been identified on the Rae

craton, with the exception of one on the Meta Incognita microcontinent on northeastern Rae craton (Partin et al., 2014a).

The 2.17 and 2.10 Ga age peaks in the U-Pb spectrum have no discovered potential local sources in the Beaverlodge domain of the southwestern Rae craton (Shiels et al., 2016). The closest potential source rock falls between these two age peaks at ~2.14 in the Taltson basement complex, with an εHf* value of -1.58 (McNicoll et al., 2000), falling within range of upper MBG sediments of similar age. The most proximal potential sources for the ~2.17 zircon are i) the ~2.17 Ga A-type granites of the Blatchford Lake intrusive suite (BLIS) on the southern margin of the neighboring Slave craton (Bowring et al., 1984; Möller and Williams-Jones, 2013; Mumford, 2013; Sinclair et al., 1994), and ii) three ~2.17 Ga gneisses from the subsurface of the neighboring Buffalo Head-Chinchaga domains (Villeneuve et al., 1993), and one dated at 2088 ± 22 Ma (Thériault and Ross, 1991). A-type granites in the BLIS have εHf* values that range from +2.8 to +5.1 (Mumford, 2013; Sinclair et al., 1994), indicating a juvenile mantle source that falls within the εHf range of samples in this study. The BLIS intrudes the 2.62 Ga Defeat granodiorite suite (εHf=-3.3 to -8.0; Yamashita et al., 1999), the 2.59 Ga Morose granite (εHf=-3.4 to +0.8; Mumford, 2013), and the ~2.60 Ga metasedimentary Burwash Formation (εHf=+3.7 to +8.1; Yamashita and Creaser, 1999; Mumford, 2013). If upper MBG sediments were sourced from the BLIS, it is reasonable to predict that these surrounding country rocks should also be represented in upper MBG sediments. While there are only a few Archean detrital zircon grains identified in this study, one grain is reasonably within the range of the Morose granite. An upper MBG sample analyzed for U-Pb ages by Ashton et al. (2013) contained a slightly larger percentage of Archean grains, especially aged ~2.60 Ga, though this sample was not analyzed for Lu-Hf or O isotopes. The paucity of Archean grains in this study makes it difficult to determine a representative range of εHf values for these ages, further isotopic analyses of upper MBG samples could elucidate this matter.

The ~2.17 and 2.1 Ga samples from the Buffalo Head-Chinchaga domains have εHf* values range from -1.6 to +2.1 (Thériault and Ross, 1991; Villeneuve et al., 1993), which are well within the range of contemporaneous upper MBG values. Several other 1.98 to 2.33 Ga subsurface samples taken proximally in the Buffalo Head-Chinchaga domains in the same studies have positive εHf* values. Crystallization ages and εHf* values of these subsurface rocks

most closely match the εHf signature of the upper MBG, although there are no known rocks older than 2.33 Ga in the Buffalo Head-Chinchaga domain.

The BLIS provides a potential source for only the 2.17 Ga age peak and exhibits positive εHf values. If upper MBG sediments were sourced from the Slave craton, the most proximal potential sources for the ~2.10 Ga U-Pb age peak are the 2.11 Ga Indin dykes and the 2.03 Ga Booth river complex near the boundary of the Slave craton and the Wopmay orogen (Bleeker et al., 2008; Davis and Bleeker, 2007). Potential local sources for this age peak are the ~2.04 Ga igneous rocks recently identified in the Penylan domain of the Rae craton (Davis et al., 2015).

If upper MBG sediments were sourced from the Buffalo Head-Chinchaga domains, the three major 2.31 Ga, 2.17 Ga, and 2.10 Ga age peaks in the detrital zircon U-Pb spectrum are all represented by potential source rocks currently located in the subsurface of northern Alberta, based on crystallization age and εHf* values. There are no discovered potential sources in the same domain, however, for the minor population of Archean grains. The minor Archean input to the upper MBG detrital zircon U-Pb spectrum was most likely regionally sourced from the Rae craton, where Archean rocks are ubiquitous. Thus, provenance of upper MBG sediments from the Buffalo Head-Chinchaga domains is the most likely scenario, based on available data and the coincidence in timing of the Taltson orogeny.

3.6 CONCLUSIONS

Integrated studies of detrital zircon U-Pb geochronology and Lu-Hf and O isotope data from the upper Murmac Bay Group provide insight into sedimentary provenance, the tectonic setting of the depositional basin, and regional crustal growth events. Our major findings are summarized as follows:

i) The combined U-Pb age spectrum for the upper MBG supports the interpretation of deposition in a syn-orogenic foreland basin during the 2.00 to 1.90 Ga Taltson orogeny.

ii) Two periods of crustal growth are identified in the detrital zircon Hf model age spectrum with mantle-like $\delta^{18}O$ at 2.83 and 2.70 Ga, corresponding to peaks noted in Sm-Nd model ages from western Churchill province (cf. Peterson et al., 2010), which supports these as periods of regional crustal growth suggesting that Rae craton crustal rocks in part comprise a source for upper MBG sediments. There are no Hf model ages in these upper MBG samples that

correspond to periods of crustal growth identified on the neighboring Slave craton at 3.80 and 3.40 Ga (Pietranik et al., 2008).

iii) While Hf and O isotopes do not uniquely identify the provenance for upper MBG sediments, they offer insight into the two potential sources identified in Shiels et al. (2016). 2.10 Ga to 2.33 Ga granites from the subsurface of the Buffalo Head-Chinchaga domains that are contemporaneous with upper MBG detrital zircon crystallization ages also have similar εHf* signatures; crystallization ages of these granites are also correlative to the three most prominent peaks in the upper MBG U-Pb age spectrum. The Buffalo Head-Chinchaga domain does not contain any potential sources for the minor amount of Archean grains present in upper MBG samples, however these may be undiscovered, or have been sourced from the surrounding Rae craton.

iv) A lack of correlation between the εHf*signatures of ~2.30 Ga upper MBG detrital zircon and local granites of the North Shore plutons supports the interpretation that not all provenance is locally derived from proximal Rae craton crustal rocks.

A-type granites from the Blatchford Lake intrusive suite on the eastern margin of the Slave craton have εHf* signatures within range of coeval ~2.17 Ga upper MBG detrital zircon grains, although the εHf* values of the surrounding Archean country rock tends to be lower than that of the few similarly aged upper MBG detrital zircons. The most proximal source for the 2.10 Ga peak in the upper MBG U-Pb age spectrum on the Slave craton is located near the Wopmay orogen boundary. The samples from this study contained very few Archean grains, making it difficult to recognize a representative εHf range for the Archean. Thus, the Slave craton is likely not a unique source for upper MBG sediments, based on available isotopic data.

The Buffalo Head-Chinchaga domains are a possible sediment source based on available geochronological and isotopic data, as their subsurface igneous rocks correspond to both upper MBG sediments U-Pb crystallization age peaks and positive εHf* values. Thus, the most probable source of upper MBG is the Buffalo Head-Chinchaga domains, though the Slave craton may have also contributed to the sediments. Since the Buffalo Head domain would have to be proximal to the upper MBG paleobasin during deposition, the Taltson orogen is likely the result of collision between the Buffalo Head and the southwest Rae margin, and the Slave craton would have likely been either already amalgamated with Rae or with Buffalo Head during this time as proposed in Card et al. (2014).

CHAPTER 4: CONCLUSIONS

The focus of this thesis is to elucidate the tectonic setting of the upper Murmac Bay Group paleobasin and to provide insight into the relative proximity of the cratonic neighbors to the southwest Rae craton during upper Murmac Bay Group deposition thus providing narrower constraints on the timing of their amalgamation. The specific objectives were to i) further constrain the depositional period of the upper succession of the Murmac Bay Group and ii) investigate provenance of upper Murmac Bay Group sediments to determine if sediments were sourced locally, or from neighboring cratons by detrital zircon provenance analysis. Isotopic analysis was conducted on detrital zircon contained in three samples of the upper Murmac Bay Group from its type locality near Uranium City, Saskatchewan in order to achieve these goals.

In chapter two, U-Pb geochronology was conducted on upper Murmac Bay Group detrital zircons, and a new maximum depositional age of 1999 ± 13 Ma was determined from the three youngest detrital zircons contained within the study samples. This new age narrows the time period in which deposition could have occurred from the previously reported from 240 million years to ~70 million years, and widens the gap between deposition of lower and upper successions by up to ~320 million years, supporting the interpretation of a significant unconformity within the Murmac Bay Group (Ashton et al., 2013; Bethune et al., 2013). A depositional age of <2.00 Ga to >1.93 Ga also supports deposition of upper Murmac Bay Group sediments during the ~1.99 Ga to 1.93 Ga Taltson orogeny (Hoffman, 1988; Card et al., 2010, 2014).

As outlined in chapter two, the U-Pb crystallization ages of upper Murmac Bay Group detrital zircons were then compared with published and geo-referenced crystallization ages from the Canadian Shield, which are stored in the DateView database, to narrow down possible sources for the sediments. While several possible sources exist proximally on the Rae craton and in the Taltson magmatic zone, two prominent age populations in the upper Murmac Bay Group detrital zircon age spectrum, at ~2.17 Ga and 2.10 Ga, were identified. With the exception of a ~2.14 Ga syenogranite gneiss in the Taltson basement complex, no local sources for these ages have as yet been discovered. The most proximal probable source for ~2.17 Ga, the Blatchford Lake intrusive suite, is situated on the eastern margin of the Slave craton. Other possible source rocks are granites that are currently buried beneath Phanerozoic sediments on the Buffalo Head-

Chinchaga domains of northern Alberta, which have dates corresponding to both the ~2.17 Ga and the ~2.10 Ga age peaks. The craton from which the upper Murmac Bay Group sediments originated must have necessarily been proximal to, or possibly amalgamated with, the southwest Rae craton during deposition (<2.00 Ga to >1.94 Ga).

Chapter three further constrains provenance by analysing the same detrital zircon grains for Hf and O isotopes, to compare their isotopic signatures to those of potential source rocks. The εHf signature of upper Murmac Bay detrital zircons shows largely positive values, especially in the most prominent age peak (~2.31 Ga). The paucity of Archean detrital zircons in the upper Murmac Bay Group samples, along with a dearth of published isotopic data for Archean rocks of the proximal Canadian Shield, makes these ages less than ideal for provenance determination. While most potential source rocks have not previously been evaluated for Hf and/or O isotopes, some have been analyzed for εNd, which can be converted to εHf values using the equation for the Terrestrial Array (Vervoort et al., 2011). Comparing these converted values with upper Murmac Bay Group εHf values (Figure 3.6), it can be seen that North Shore plutons and Taltson magmatic zone rocks, the most proximal potential sources for the ~2.31 Ga zircons, tend to have far lower, negative εHf* values, pointing to a more distal or undiscovered source for these ages.

The ~2.17 Ga rocks of the Blatchford Lake intrusive suite have positive values within the range of upper Murmac Bay Group εHf values, however, potential source rocks with ages matching the prominent ~2.31 Ga and ~2.10 Ga detrital zircon age peaks have not been discovered on the proximal Slave craton margin. Thus, while the Blatchford Lake intrusive suite is a permissible sediment source, there must be another source for these ages. Granites of the Buffalo Head-Chinchaga domains most closely match the εHf values of the upper Murmac Bay Group for ages from ~2.33 Ga to 2.00 Ga, making this the most probable source based on isotopic analyses of detrital zircons.

Conclusions based on the first stage of this research, as presented in chapter two, suggested that both the Slave craton and Buffalo Head domain represent likely sediment sources for the upper MBG. With only U-Pb data available, a local source was assumed as permissible for the ~2.3 Ga zircon population, as represented by the North Shore plutons. Conclusions based on the final stage of this research, as presented in chapter three, support the original conclusions that either the Slave craton and Buffalo Head domain represent permissible sediment sources for

the upper MBG. The Buffalo Head domain is considered more probable, since Eoarchean detritus (similar in age to Slave crustal rocks) is not found in the upper MBG. However, the Hf data shows that the ~2.3 Ga detrital zircon cannot be locally derived, since it their εHf signatures are incompatible with those of the North Shore plutons of the Beaverlodge domain. The reader is encouraged to obtain the most recent version of chapter three, which is expected to be published in *Precambrian Research* later in 2017 following peer-review.

The combined U-Pb age spectra of the upper Murmac Bay Group (Figure 3.4a) suggest syn-orogenic deposition (Spencer et al., 2015) during the 1.99 Ga to 1.93 Ga Taltson orogeny in a foreland basin setting, illustrated by the significant proportion of ages within 150 million years of the depositional age, and a lack of ages contemporaneous with deposition (Cawood et al., 2012). Based on these conclusions, it is probable that upper Murmac Bay Group sediments were sourced from the Buffalo Head-Chinchaga domains as they were amalgamated to the southwest Rae craton during the Taltson orogeny. It is permissible that the Slave craton was amalgamated either to the Rae craton or to the Buffalo Head-Chinchaga domains during this time.

CHAPTER 5: FUTURE CONSIDERATIONS

The results presented in this study are limited by the deficiency of published isotopic analyses for rocks of the Canadian Shield. Further exploration, mapping, sampling and analysis using modern isotopic techniques would serve to expand the knowledge base of Canadian Shield tectonics, and allow databases of isotopic data, such as DateView, to become ever more comprehensive, and thus paleogeographic reconstructions to become better constrained. There is always the possibility that the sources of sediments may be currently buried, undiscovered, or undated, or they may have simply eroded away. The matter of preservation bias should not be discounted, as this results in a more complete record of supercontinent assembly than that of extensional and rifting events in Earth's history.

Additional isotopic analysis of other Rae craton Paleoproterozoic sedimentary successions could also aid in their correlation, and further elucidate depositional settings, provenance, and timing of tectonic events. Acquisition and publication of reliable paleomagnetic data would also aid in resolving some of the current questions regarding the timing of amalgamation of the cratons that form the Canadian Shield.

REFERENCES

Andersen, T., Andersson, U.B., Graham, S., Åberg, G., Simonsen, S.L., 2009. Granitic magmatism by melting of juvenile continental crust: new constraints on the source of Palaeoproterozoic granitoids in Fennoscandia from Hf isotopes in zircon. J. Geol. Soc. 166, 233–247. doi:10.1144/0016-76492007-166

Arndt, N.T., Goldstein, S.L., 1987. Use and abuse of crust-formation ages. Geology 15, 893–895.

Ashton, K.E., Hartlaub, R.P., Bethune, K.M., Heaman, L.M., Rayner, N., Niebergall, G.R., 2013. New depositional age constraints for the Murmac Bay group of the southern Rae craton, Canada. Precambrian Res., Paleoproterozoic tectonic assembly of the western Canadian shield: new findings and implications for the reconstruction of Laurentia/Nuna 232, 70–88. doi:10.1016/j.precamres.2012.05.008

Ashton, K.E., Hartlaub, R.P., Heaman, L.M., Morelli, R.M., Card, C.D., Bethune, K., Hunter, R.C., 2009. Post-Taltson sedimentary and intrusive history of the southern Rae Province along the northern margin of the Athabasca Basin, Western Canadian Shield. Precambrian Res. 175, 16–34. doi:10.1016/j.precamres.2009.09.004

Ashton, K.E., Knox, B., Bethune, K.M., Rayner, N., 2007. Geochronological update and basement geology along the northern margin of the Athabasca Basin east of Fond-du-Lac (NTS 74O/06 and/07), southeastern Beaverlodge-southwestern Tantato domains, Rae Province (Misc. Rep. No. 2007-4.2), Summary of Investigations. Saskatchewan Ministry of Energy and Resources, Saskatchewan Geological Survey.

Aspler, L.B., Chiarenzelli, J.R., 1998. Two Neoarchean supercontinents? Evidence from the Paleoproterozoic. Sediment. Geol. 120, 75–104. doi:10.1016/S0037-0738(98)00028-1

Belousova, E.A., Kostitsyn, Y.A., Griffin, W.L., Begg, G.C., O'Reilly, S.Y., Pearson, N.J., 2010. The growth of the continental crust: Constraints from zircon Hf-isotope data. Lithos 119, 457–466. doi:10.1016/j.lithos.2010.07.024

Berman, R.G., Davis, W.J., Pehrsson, S., 2007. Collisional Snowbird tectonic zone resurrected: Growth of Laurentia during the 1.9 Ga accretionary phase of the Hudsonian orogeny. Geology 35, 911–914. doi:10.1130/G23771A.1

Berman, R.G., Pehrsson, S., Davis, W.J., Ryan, J.J., Qui, H., Ashton, K.E., 2013. The Arrowsmith orogeny: Geochronological and thermobarometric constraints on its extent and tectonic setting in the Rae craton, with implications for pre-Nuna supercontinent reconstruction. Precambrian Res., Paleoproterozoic tectonic assembly of the western Canadian shield: new findings and implications for the reconstruction of Laurentia/Nuna 232, 44–69. doi:10.1016/j.precamres.2012.10.015

Berman, R.G., Sanborn-Barrie, M., Stern, R.A., Carson, C.J., 2005. Tectonometamorphism at ca. 2.35 and 1.85 Ga in the Rae domain, western Churchill province, Nunavut, Canada: Insights from structural, metamorphic and in situ geochronological analysis of the southwestern Committee Bay belt. Can. Mineral. 43, 409–442. doi:10.2113/gscanmin.43.1.409

Bethune, K.M., Berman, R.G., Rayner, N., Ashton, K.E., 2013. Structural, petrological and U–Pb SHRIMP geochronological study of the western Beaverlodge domain: Implications for crustal architecture, multi-stage orogenesis and the extent of the Taltson orogen in the SW Rae craton, Canadian Shield. Precambrian Res., Paleoproterozoic tectonic assembly

of the western Canadian shield: new findings and implications for the reconstruction of Laurentia/Nuna 232, 89–118. doi:10.1016/j.precamres.2013.01.001
Bethune, K.M., Hunter, R.C., Ashton, K.E., 2010. Age and provenance of the Paleoproterozoic Thluicho Lake Group based on detrital zircon U–Pb SHRIMP geochronology: new insights into the protracted tectonic evolution of the southwestern Rae Province, Canadian Shield. Precambrian Res. 182, 83–100. doi:10.1016/j.precamres.2010.07.003
Bleeker, W., Hamilton, M., Söderlund, U., 2008. Towards a Complete Event Barcode for the Slave Craton, II: The ca. 1884 Ma Ghost Swarm, in: Geological Association of Canada/Mineralogical Association of Canada, Abstracts. Presented at the Geological Association of Canada/Mineralogical Association of Canada, Abstracts, p. 23.
Bleeker, W., Ketchum, J., Davis, B., Sircombe, K., Stern, R., Waldron, J., 2004. The Slave Craton from on top: the crustal view [abs.], in: The Lithoprobe Celebratory Conference: From Parameters to Processes - Revealing the Evolution of a Continent. Presented at the From Parameters to Processes - Revealing the Evolution of a Continent, Toronto, ON.
Bostock, H.H., Loveridge, W.D., 1988. Geochronology of the Taltson magmatic zone and its eastern cratonic margin, District of Mackenzie. Radiogenic Age Isot. Stud. Report 2, 59–65.
Bostock, H.H., van Breemen, O., 1994. Ages of detrital and metamorphic zircons and monazites from a pre-Taltson magmatic zone basin at the western margin of Rae Province. Can. J. Earth Sci. 31, 1353–1364.
Bostock, H.H., van Breemen, O., Loveridge, W.D., 1991. Further geochronology of plutonic rocks in northern Taltson magmatic zone, District of Mackenzie, NWT. Radiogenic Age Isot. Stud. Report 4, 67–78.
Bouvier, A., Vervoort, J.D., Patchett, P.J., 2008. The Lu–Hf and Sm–Nd isotopic composition of CHUR: Constraints from unequilibrated chondrites and implications for the bulk composition of terrestrial planets. Earth Planet. Sci. Lett. 273, 48–57. doi:10.1016/j.epsl.2008.06.010
Bowring, S.A., Van Schmus, W.R., Hoffman, P.F., 1984. U–Pb zircon ages from Athapuscow aulacogen, East Arm of Great Slave Lake, N.W.T., Canada. Can. J. Earth Sci. 21, 1315–1324. doi:10.1139/e84-136
Bowring, S.A., Williams, I.S., 1999. Priscoan (4.00–4.03 Ga) orthogneisses from northwestern Canada. Contrib. Mineral. Petrol. 134, 3–16.
Campbell, I.H., Allen, C.M., 2008. Formation of supercontinents linked to increases in atmospheric oxygen. Nat. Geosci. 1, 554–558.
Campbell, I.H., Hill, R.I., 1988. A two-stage model for the formation of the granite-greenstone terrains of the Kalgoorlie-Norseman area, Western Australia. Earth Planet. Sci. Lett. 90, 11–25.
Card, C.D., Ashton, K.E., Bethune, K.M., 2010. The case for separate Taltson and Thelon orogenies: Evidence from the Shield in western Saskatchewan [abs.], in: Proceedings, GeoCanada 2010. Presented at the GeoCanada 2010 - Working With the Earth, Calgary, AB, Canada.
Card, C.D., Bethune, K.M., Davis, W.J., Rayner, N., Ashton, K.E., 2014. The case for a distinct Taltson orogeny: Evidence from northwest Saskatchewan, Canada. Precambrian Res. 255, Part 1, 245–265. doi:10.1016/j.precamres.2014.09.022
Cawood, P.A., Hawkesworth, C.J., Dhuime, B., 2012. Detrital zircon record and tectonic setting. Geology 40, 875–878.

Chacko, T., De, S.K., Creaser, R.A., Muehlenbachs, K., 2000. Tectonic setting of the Taltson magmatic zone at 1.9-2.0 Ga: a granitoid-based perspective. Can. J. Earth Sci. 37, 1597–1609. doi:10.1139/e00-029

Chauvel, C., Lewin, E., Carpentier, M., Arndt, N.T., Marini, J.-C., 2008. Role of recycled oceanic basalt and sediment in generating the Hf–Nd mantle array. Nat. Geosci. 1, 64–67. doi:10.1038/ngeo.2007.51

Collo, G., Astini, R.A., Cawood, P.A., Buchan, C., Pimentel, M., 2009. U–Pb detrital zircon ages and Sm–Nd isotopic features in low-grade metasedimentary rocks of the Famatina belt: implications for late Neoproterozoic–early Palaeozoic evolution of the proto-Andean margin of Gondwana. J. Geol. Soc. 166, 303–319. doi:10.1144/0016-76492008-051

Condie, K.C., 1998. Episodic continental growth and supercontinents: a mantle avalanche connection? Earth Planet. Sci. Lett. 163, 97–108.

Condie, K.C., Bickford, M.E., Aster, R.C., Belousova, E., Scholl, D.W., 2011. Episodic zircon ages, Hf isotopic composition, and the preservation rate of continental crust. Geol. Soc. Am. Bull. 123, 951–957.

Corfu, F., Hanchar, J.M., Hoskin, P.W.O., Kinny, P., 2003. Atlas of Zircon Textures. Rev. Mineral. Geochem. 53, 469–500. doi:10.2113/0530469

Corrigan, D., Pehrsson, S., Wodicka, N., de Kemp, E., 2009. The Palaeoproterozoic Trans-Hudson Orogen: a prototype of modern accretionary processes. Geol. Soc. Lond. Spec. Publ. 327, 457–479. doi:10.1144/SP327.19

Davis, W.J., Bleeker, W., 2007. New ages for Paleoproterozoic mafic intrusions in the western Slave Province and their potential relationship to tectonic events in the adjacent Wopmay orogen, in: Geological Association of Canada/Mineralogical Association of Canada, Abstracts. p. 20.

Davis, W.J., Pehrsson, S.J., Percival, J.A., 2015. Results of a U-Pb zircon geochronology transect across the southern Rae craton. NWT Geol. Surv. Can. Open File 7655, 56.

De, S.K., Chacko, T., Creaser, R.A., Muehlenbachs, K., 2000. Geochemical and Nd-Pb-O isotope systematics of granites from the Taltson Magmatic Zone, NE Alberta: implications for early Proterozoic tectonics in western Laurentia. Precambrian Res. 102, 221–249. doi:10.1016/S0301-9268(00)00068-1

Dhuime, B., Hawkesworth, C., Cawood, P., 2011. When continents formed. Science 331, 154–155.

Dhuime, B., Hawkesworth, C.J., Cawood, P.A., Storey, C.D., 2012. A Change in the Geodynamics of Continental Growth 3 Billion Years Ago. Science 335, 1334–1336. doi:10.1126/science.1216066

Eglington, B., 2013. FitPDF.

Eglington, B.M., 2004. DateView: a Windows geochronology database. Comput. Geosci. 30, 847–858. doi:10.1016/j.cageo.2004.06.002

Eglington, B.M., Pehrsson, S.J., Ansdell, K.M., Lescuyer, J.-L., Quirt, D., Milesi, J.-P., Brown, P., 2013. A domain-based digital summary of the evolution of the Palaeoproterozoic of North America and Greenland and associated unconformity-related uranium mineralization. Precambrian Res. 232, 4–26.

Faure, G., 1977. Principles of isotope geology. John Wiley and Sons, Inc.,New York, NY.

Finch, R.J., Hanchar, J.M., 2003. Structure and chemistry of zircon and zircon-group minerals. Rev. Mineral. Geochem. 53, 1–25.

Gehrels, G., 2014. Detrital Zircon U-Pb Geochronology Applied to Tectonics. Annu. Rev. Earth Planet. Sci. 42, 127–149. doi:10.1146/annurev-earth-050212-124012
Gehrels, G., 2011. Detrital Zircon U-Pb Geochronology: Current Methods and New Opportunities, in: Busby, C., Azor, A. (Eds.), Tectonics of Sedimentary Basins. John Wiley & Sons, Ltd, pp. 45–62.
Gehrels, G.E., McClelland, W.C., Samson, S.D., Patchett, P.J., Jackson, J.L., 1990. Ancient continental margin assemblage in the northern Coast Mountains, southeast Alaska and northwest Canada. Geology 18, 208–211. doi:10.1130/0091-7613(1990)018<0208:ACMAIT>2.3.CO;2
Griffin, W.L., Pearson, N.J., Belousova, E., Jackson, S.E., Van Achterbergh, E., O'Reilly, S.Y., Shee, S.R., 2000. The Hf isotope composition of cratonic mantle: LAM-MC-ICPMS analysis of zircon megacrysts in kimberlites. Geochim. Cosmochim. Acta 64, 133–147.
Hanchar, J.M., Hoskin, P.W.O., 2003. Zircon. Reviews in Mineralogy and Geochemistry, vol 53. Mineralogical Society of America/Geochemical Society, Washington, DC.
Hanmer, S., Williams, M., Kopf, C., 1995a. Modest movements, spectacular fabrics in an intracontinental deep-crustal strike-slip fault: Striding-Athabasca mylonite zone, NW Canadian Shield. J. Struct. Geol. 17, 493–507. doi:10.1016/0191-8141(94)00070-G
Hanmer, S., Williams, M., Kopf, C., 1995b. Striding-Athabasca mylonite zone: implications for the Archean and Early Proterozoic tectonics of the western Canadian Shield. Can. J. Earth Sci. 32, 178–196. doi:10.1139/e95-015
Hartlaub, R.P., Chacko, T., Heaman, L.M., Creaser, R.A., Ashton, K.E., Simonetti, A., 2005. Ancient (Meso- to Paleoarchean) crust in the Rae Province, Canada: Evidence from Sm–Nd and U–Pb constraints. Precambrian Res. 141, 137–153. doi:10.1016/j.precamres.2005.09.001
Hartlaub, R.P., Heaman, L.M., Ashton, K.E., Chacko, T., 2004. The Archean Murmac Bay Group: evidence for a giant Archean rift in the Rae Province, Canada. Precambrian Res., Archaean Tectonics, Volume 2 131, 345–372. doi:10.1016/j.precamres.2004.01.001
Hartlaub, R.P., Heaman, L.M., Chacko, T., Ashton, K.E., 2007. Circa 2.3-Ga Magmatism of the Arrowsmith Orogeny, Uranium City Region, Western Churchill Craton, Canada. J. Geol. 115, 181–195. doi:10.1086/510641
Hartlaub, R.P., Heaman, L.M., Simonetti, A., Böhm, C.O., 2006. Relicts of Earth's earliest crust: U-Pb, Lu-Hf, and morphological characteristics of >3.7 Ga detrital zircon of the western Canadian Shield. Geol. Soc. Am. Spec. Pap. 405, 75–89. doi:10.1130/2006.2405(05)
Hawkesworth, C., Cawood, P., Dhuime, B., 2013. Continental growth and the crustal record. Tectonophysics, Moho: 100 years after Andrija Mohorovicic 609, 651–660. doi:10.1016/j.tecto.2013.08.013
Hawkesworth, C., Cawood, P., Kemp, T., Storey, C., Dhuime, B., 2009. A Matter of Preservation. Science 323, 49–50. doi:10.1126/science.1168549
Hawkesworth, C.J., Dhuime, B., Pietranik, A.B., Cawood, P.A., Kemp, A.I.S., Storey, C.D., 2010. The generation and evolution of the continental crust. J. Geol. Soc. 167, 229–248.
Hawkesworth, C.J., Kemp, A.I.S., 2006. Using hafnium and oxygen isotopes in zircons to unravel the record of crustal evolution. Chem. Geol., Special Issue in Honour of R.K. O'Nions 226, 144–162. doi:10.1016/j.chemgeo.2005.09.018
Hoffman, P.F., 1988. United Plates of America, The Birth of a Craton: Early Proterozoic Assembly and Growth of Laurentia. Annu. Rev. Earth Planet. Sci. 16, 543–603. doi:10.1146/annurev.ea.16.050188.002551

Horton, B.K., Hassanzadeh, J., Stockli, D.F., Axen, G.J., Gillis, R.J., Guest, B., Amini, A., Fakhari, M.D., Zamanzadeh, S.M., Grove, M., 2008. Detrital zircon provenance of Neoproterozoic to Cenozoic deposits in Iran: Implications for chronostratigraphy and collisional tectonics. Tectonophysics, Asia out of Tethys: Geochronologic, Tectonic and Sedimentary Records 451, 97–122. doi:10.1016/j.tecto.2007.11.063

Hoskin, P.W., Schaltegger, U., 2003. The composition of zircon and igneous and metamorphic petrogenesis. Rev. Mineral. Geochem. 53, 27–62.

Iizuka, T., Campbell, I.H., Allen, C.M., Gill, J.B., Maruyama, S., Makoka, F., 2013. Evolution of the African continental crust as recorded by U–Pb, Lu–Hf and O isotopes in detrital zircons from modern rivers. Geochim. Cosmochim. Acta 107, 96–120. doi:10.1016/j.gca.2012.12.028

Iizuka, T., Komiya, T., Rino, S., Maruyama, S., Hirata, T., 2010. Detrital zircon evidence for Hf isotopic evolution of granitoid crust and continental growth. Geochim. Cosmochim. Acta 74, 2450–2472.

Iizuka, T., Komiya, T., Ueno, Y., Katayama, I., Uehara, Y., Maruyama, S., Hirata, T., Johnson, S.P., Dunkley, D.J., 2007. Geology and zircon geochronology of the Acasta Gneiss Complex, northwestern Canada: New constraints on its tectonothermal history. Precambrian Res. 153, 179–208. doi:10.1016/j.precamres.2006.11.017

Kemp, A.I.S., Hawkesworth, C.J., Paterson, B.A., Kinny, P.D., 2006. Episodic growth of the Gondwana supercontinent from hafnium and oxygen isotopes in zircon. Nature 439, 580–583. doi:10.1038/nature04505

King, E.M., Valley, J.W., Davis, D.W., Edwards, G.R., 1998. Oxygen isotope ratios of Archean plutonic zircons from granite–greenstone belts of the Superior Province: indicator of magmatic source. Precambrian Res. 92, 365–387.

Knox, B., Bethune, K.M., Ashton, K.E., Williams, M.L., Rayner, N., 2008. U-Pb SHRIMP and chemical monazite geochronology of rocks in the central Beaverlodge Domain, Saskatchewan: Constraints on ages of rock units and implications for the tectonic evolution of the SW Rae province [abs.], in: Mineralogical Association of Canada, Abstract. Presented at the GAC-MAC-CSEG-SGA Joint Annual Meeting, Québec City, Québec, p. 86.

Knox, B.R., 2011. A geological investigation of the South-central Beaverlodge Domain, Southern Rae Province: with emphasis on the nature and timing of deformation and associated metamorphism (MSc Thesis). University of Regina, Regina, SK.

Lancaster, P.J., Storey, C.D., Hawkesworth, C.J., Dhuime, B., 2011. Understanding the roles of crustal growth and preservation in the detrital zircon record. Earth Planet. Sci. Lett. 305, 405–412. doi:10.1016/j.epsl.2011.03.022

Lyons, T.W., Reinhard, C.T., Planavsky, N.J., 2014. The rise of oxygen in Earth/'s early ocean and atmosphere. Nature 506, 307–315.

Martel, E., van Breemen, O., Berman, R.G., Pehrsson, S., 2008. Geochronology and tectonometamorphic history of the Snowbird Lake area, Northwest Territories, Canada: New insights into the architecture and significance of the Snowbird tectonic zone. Precambrian Res. 161, 201–230.

McDonald, B., Partin, C.A., 2016. Is the Lomagundi Event present on the Rae craton? A case study from the Murmac Bay Group. Can. J. Earth Sci. 53, 457–465.

McDonough, M.R., McNicoll, V.J., 1997. U–Pb age constraints on the timing of deposition of the Waugh Lake and Burntwood (Athabasca) groups, southern Taltson magmatic zone, northeastern Alberta. Radiogenic Age Isot. Stud. Rep. 10, 101–111.
McDonough, M.R., McNicoll, V.J., Schetselaar, E.M., Grover, T.W., 2000. Geochronological and kinematic constraints on crustal shortening and escape in a two-sided oblique-slip collisional and magmatic orogen, Paleoproterozoic Taltson magmatic zone, northeastern Alberta. Can. J. Earth Sci. 37, 1549–1573. doi:10.1139/e00-089
McNicoll, V.J., Thériault, R.J., McDonough, M.R., 2000. Taltson basement gneissic rocks: U-Pb and Nd isotopic constraints on the basement to the Paleoproterozoic Taltson magmatic zone, northeastern Alberta. Can. J. Earth Sci. 37, 1575–1596. doi:10.1139/e00-034
Möller, A., O'Brien, P.J., Kennedy, A., Kröner, A., 2003. Linking growth episodes of zircon and metamorphic textures to zircon chemistry: an example from the ultrahigh-temperature granulites of Rogaland (SW Norway). Geol. Soc. Lond. Spec. Publ., Geochronology: Linking the Isotopic Record with Petrology and Textures 220, 65–81. doi:10.1144/GSL.SP.2003.220.01.04
Möller, V., Williams-Jones, A.E., 2013. Magmatic controls on the formation of the Nechalacho rare metal deposit, Thor Lake, Northwest Territories, Canada [abs.], in: Society of Economic Geologists Annual Meeting, Whistler, British Columbia, Canada, Abstracts.
Morelli, R.M., Hartlaub, R.P., Ashton, K.E., Ansdell, K.M., 2009. Evidence for enrichment of subcontinental lithospheric mantle from Paleoproterozoic intracratonic magmas: Geochemistry and U–Pb geochronology of Martin Group igneous rocks, western Rae Craton, Canada. Precambrian Res. 175, 1–15.
Mumford, T.R., 2013. Petrology of the Blatchford Lake Intrusive Suite, Northwest Territories, Canada (PhD Thesis). Carleton University, Ottawa, Canada.
Nebel, O., Nebel-Jacobsen, Y., Mezger, K., Berndt, J., 2007. Initial Hf isotope compositions in magmatic zircon from early Proterozoic rocks from the Gawler Craton, Australia: a test for zircon model ages. Chem. Geol. 241, 23–37.
Partin, C.A., Bekker, A., Corrigan, D., Modeland, S., Francis, D., Davis, D.W., 2014a. Sedimentological and geochemical basin analysis of the Paleoproterozoic Penrhyn and Piling groups of Arctic Canada. Precambrian Res. 251, 80–101.
Partin, C.A., Bekker, A., Sylvester, P.J., Wodicka, N., Stern, R.A., Chacko, T., Heaman, L.M., 2014b. Filling in the juvenile magmatic gap: Evidence for uninterrupted Paleoproterozoic plate tectonics. Earth Planet. Sci. Lett. 388, 123–133.
Partin, C.A., Sylvester, P.J., 2016. Variations in zircon Hf isotopes support earliest Proterozoic Wilson cycle tectonics on the Canadian Shield. Precambrian Res. 280, 279–289. doi:10.1016/j.precamres.2016.05.008
Payne, J.L., McInerney, D.J., Barovich, K.M., Kirkland, C.L., Pearson, N.J., Hand, M., 2016. Strengths and limitations of zircon Lu-Hf and O isotopes in modelling crustal growth. Lithos 248–251, 175–192. doi:10.1016/j.lithos.2015.12.015
Peck, W.H., Valley, J.W., Graham, C.M., 2003. Slow oxygen diffusion rates in igneous zircons from metamorphic rocks. Am. Mineral. 88, a1003–1014.
Pehrsson, S.J., Berman, R.G., Davis, W.J., 2013. Paleoproterozoic orogenesis during Nuna aggregation: A case study of reworking of the Rae craton, Woodburn Lake, Nunavut. Precambrian Res. 232, 167–188.
Persons, S.S., 1988. U-Pb Geochronology of Precambrian Rocks in the Beaverlodge Area, Northwestern Saskatchewan. University of Kansas, Geology, Lawrence, Kansas.

Peterson, T.D., Pehrsson, S., Skulski, T., Sandeman, H., 2010. Compilation of Sm-Nd isotope analyses of igneous suites, western Churchill Province. Geol. Surv. Can. Open File 6439, 18.
Pietranik, A.B., Hawkesworth, C.J., Storey, C.D., Kemp, A.I.S., Sircombe, K.N., Whitehouse, M.J., Bleeker, W., 2008. Episodic, mafic crust formation from 4.5 to 2.8 Ga: New evidence from detrital zircons, Slave craton, Canada. Geology 36, 875–878. doi:10.1130/G24861A.1
Rainbird, R.H., Davis, W.J., Pehrsson, S.J., Wodicka, N., Rayner, N., Skulski, T., 2010. Early Paleoproterozoic supracrustal assemblages of the Rae domain, Nunavut, Canada: intracratonic basin development during supercontinent break-up and assembly. Precambrian Res. 181, 167–186.
Roberts, N.M., Spencer, C.J., 2015. The zircon archive of continent formation through time. Geol. Soc. Lond. Spec. Publ. 389, 197–225.
Rubatto, D., 2002. Zircon trace element geochemistry: partitioning with garnet and the link between U–Pb ages and metamorphism. Chem. Geol. 184, 123–138. doi:10.1016/S0009-2541(01)00355-2
Shiels, C., Partin, C.A., Eglington, B.M., 2016. Provenance approaches in polydeformed metasedimentary successions: Determining nearest neighboring cratons during the deposition of the Paleoproterozoic Murmac Bay Group. Lithosphere 8, 519–532. doi:10.1130/L537.1
Sinclair, W.D., Hunt, P.A., Birkett, T.C., 1994. U-Pb zircon and monazite ages of the Grace Lake Granite, Blatchford Lake Intrusive Suite, Slave Province, Northwest Territories (Radiogenic Age Isot. Stud No. 8). Geologic Survey of Canada.
Skulski, T., Villeneuve, M., 1999. Geochronological compilation of the Rae and Hearne provinces (No. 3706).
Söderlund, U., Patchett, P.J., Vervoort, J.D., Isachsen, C.E., 2004. The 176 Lu decay constant determined by Lu–Hf and U–Pb isotope systematics of Precambrian mafic intrusions. Earth Planet. Sci. Lett. 219, 311–324.
Souders, A.K., Sylvester, P.J., Myers, J.S., 2013. Mantle and crustal sources of Archean anorthosite: a combined in situ isotopic study of Pb–Pb in plagioclase and Lu–Hf in zircon. Contrib. Mineral. Petrol. 165, 1–24.
Spencer, C.J., Cawood, P.A., Hawkesworth, C.J., Prave, A.R., Roberts, N.M.W., Horstwood, M.S.A., Whitehouse, M.J., 2015. Generation and preservation of continental crust in the Grenville Orogeny. Geosci. Front. 6, 357–372. doi:10.1016/j.gsf.2014.12.001
Stern, R.A., 1997. The GSC Sensitive High Resolution Ion Microprobe (SHRIMP): analytical techniques of zircon U-Th-Pb age determinations and performance evaluation. Radiogenic Age Isot. Stud. Rep. 10, 1–31.
Thériault, R.J., Ross, G.M., 1991. Nd isotopic evidence for crustal recycling in the ca. 2.0 Ga subsurface of western Canada. Can. J. Earth Sci. 28, 1140–1147.
Thomas, W.A., Astini, R.A., Mueller, P.A., Gehrels, G.E., Wooden, J.L., 2004. Transfer of the Argentine Precordillera terrane from Laurentia: Constraints from detrital-zircon geochronology. Geology 32, 965–968. doi:10.1130/G20727.1
Timms, N.E., Kinny, P.D., Reddy, S.M., 2006. Enhanced diffusion of Uranium and Thorium linked to crystal plasticity in zircon. Geochem. Trans. 7, 10. doi:10.1186/1467-4866-7-10
Tran, H.T., Ansdell, K.M., Bethune, K.M., Ashton, K., Hamilton, M.A., 2008. Provenance and tectonic setting of Paleoproterozoic metasedimentary rocks along the eastern margin of

Hearne craton: Constraints from SHRIMP geochronology, Wollaston Group, Saskatchewan, Canada. Precambrian Res. 167, 171–185. doi:10.1016/j.precamres.2008.08.003
Valley, J.W., 2003. Oxygen Isotopes in Zircon. Rev. Mineral. Geochem. 53, 343–385. doi:10.2113/0530343
Valley, J.W., Lackey, J.S., Cavosie, A.J., Clechenko, C.C., Spicuzza, M.J., Basei, M. a. S., Bindeman, I.N., Ferreira, V.P., Sial, A.N., King, E.M., Peck, W.H., Sinha, A.K., Wei, C.S., 2005. 4.4 billion years of crustal maturation: oxygen isotope ratios of magmatic zircon. Contrib. Mineral. Petrol. 150, 561–580. doi:10.1007/s00410-005-0025-8
Van Breemen, O., Aspler, L.B., 1994. Detrital zircon ages from Nonacho Basin, western Rae Province, Northwest Territories. Geol Surv Can Curr Res 49–59.
Vervoort, J.D., Plank, T., Prytulak, J., 2011. The Hf–Nd isotopic composition of marine sediments. Geochim. Cosmochim. Acta 75, 5903–5926. doi:10.1016/j.gca.2011.07.046
Villeneuve, M.E., Ross, G.M., Thériault, R.J., Miles, W., Parrish, R.R., Broome, J., 1993. Tectonic subdivision and U-Pb geochronology of the crystalline basement of the Alberta Basin, western Canada (Bulletin No. 447). Geological Survey of Canada.
Villeneuve, M.E., van Breemen, O., 1994. A compilation of U-Pb age data from the Slave Province, Northwest Territories (Open File No. 2972). Geological Survey of Canada.
Wang, C.Y., Campbell, I.H., Allen, C.M., Williams, I.S., Eggins, S.M., 2009. Rate of growth of the preserved North American continental crust: evidence from Hf and O isotopes in Mississippi detrital zircons. Geochim. Cosmochim. Acta 73, 712–728.
Wang, C.Y., Campbell, I.H., Stepanov, A.S., Allen, C.M., Burtsev, I.N., 2011. Growth rate of the preserved continental crust: II. Constraints from Hf and O isotopes in detrital zircons from Greater Russian Rivers. Geochim. Cosmochim. Acta 75, 1308–1345.
Weislogel, A.L., Graham, S.A., Chang, E.Z., Wooden, J.L., Gehrels, G.E., Yang, H., 2006. Detrital zircon provenance of the Late Triassic Songpan-Ganzi complex: Sedimentary record of collision of the North and South China blocks. Geology 34, 97–100. doi:10.1130/G21929.1
Wilde, S.A., Valley, J.W., Peck, W.H., Graham, C.M., 2001. Evidence from detrital zircons for the existence of continental crust and oceans on the Earth 4.4 Gyr ago : Abstract : Nature. Nature 409, 175–178. doi:10.1038/35051550
Wodicka, N., St-Onge, M.R., Corrigan, D., Scott, D.J., Whalen, J.B., 2014. Did a proto-ocean basin form along the southeastern Rae cratonic margin? Evidence from U-Pb geochronology, geochemistry (Sm-Nd and whole-rock), and stratigraphy of the Paleoproterozoic Piling Group, northern Canada. Geol. Soc. Am. Bull. 126, 1625–1653.
Yamashita, K., Creaser, R.A., 1999. Geochemical and Nd isotopic constraints for the origin of Late Archean turbidites from the Yellowknife area, Northwest Territories, Canada. Geochim. Cosmochim. Acta 63, 2579–2598.
Yamashita, K., Creaser, R.A., Stemler, J.U., Zimaro, T.W., 1999. Geochemical and Nd-Pb isotopic systematics of late Archean granitoids, southwestern Slave Province, Canada: constraints for granitoid origin and crustal isotopic structure. Can. J. Earth Sci. 36, 1131–1147.
Yamashita, K., Creaser, R.A., Villeneuve, M.E., 2000. Integrated Nd isotopic and U–Pb detrital zircon systematics of clastic sedimentary rocks from the Slave Province, Canada: evidence for extensive crustal reworking in the early- to mid-Archean. Earth Planet. Sci. Lett. 174, 283–299. doi:10.1016/S0012-821X(99)00265-4

APPENDIX A: FULL U-PB GEOCHRONOLOGY AND TH DATA FOR MURMAC BAY GROUP DETRITAL ZIRCONS

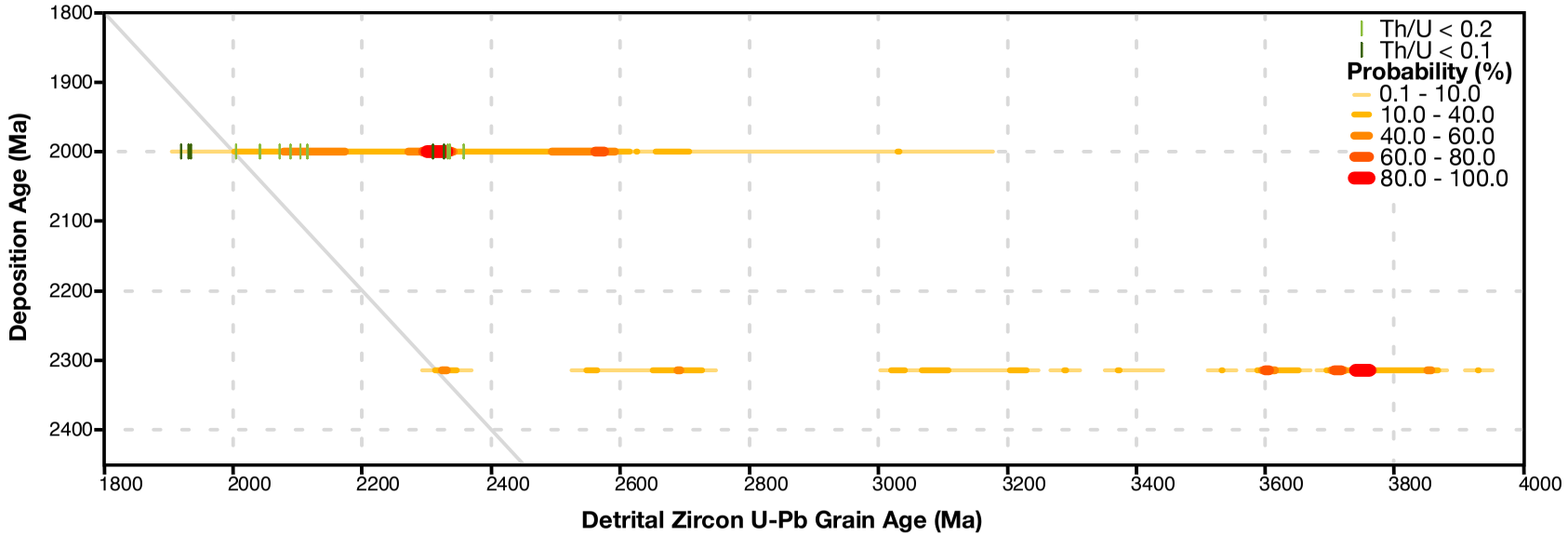

Figure A.1 Grain age presented vs. interpreted deposition age of the upper and lower MBG. Probability is represented by line weight and color. Primary zircon age peaks are represented by red and secondary peaks are represented by orange. Lower lines (~2.33 Ga) represent the lower MBG and upper lines (~1.99 Ga) represent upper MBG. Grains with Th/U < 0.2 are represented by light green dashes, and Th/U < 0.1 are in dark green.

Table A.1 U-Pb geochronological data from SHRIMP analysis of upper Murmac Bay Group

Sample Number	Spot Number	Th/U	$^{204}Pb/^{206}Pb$	$\pm^{204}Pb/^{206}Pb$ %	$^{208}Pb/^{206}Pb$	$\pm^{208}Pb/^{206}Pb$ %	$^{207}Pb^*/^{235}U$	$\pm^{207}Pb^*/^{235}U$ %	$^{206}Pb^*/^{238}U$	$\pm^{206}Pb^*/^{238}U$ %	Correlation Coefficient	$^{207}Pb^*/^{206}Pb^*$	$\pm^{207}Pb^*/^{206}Pb^*$ %	Apparent Ages (Ma) $^{206}Pb/^{238}U$	$\pm^{206}Pb/^{238}U$	$^{207}Pb/^{206}Pb$	$\pm^{207}Pb/^{206}Pb$	Discordance %
14CAP09	**s3179**																	
11-5	**-001.1**	**0.14**	**0.000204**	**28.87**	**0.04228**	**6.76**	**9.0789**	**1.60**	**0.44185**	**1.30**	**0.813**	**0.14903**	**0.93**	**2359**	**26**	**2335**	**16**	**-1.2**
	s3179																	
x	***-001.2***	***0.07***	***0.000116***	***22.36***	***0.02184***	***5.40***	***9.3013***	***1.13***	***0.45476***	***1.01***	***0.892***	***0.14834***	***0.51***	***2416***	***20***	***2327***	***9***	***-4.6***
	s3179																	
fl	**-010.1**	**0.20**	**0.000379**	**17.96**	**0.05725**	**4.90**	**6.6262**	**1.59**	**0.38118**	**1.22**	**0.767**	**0.12608**	**1.02**	**2082**	**22**	**2044**	**18**	**-2.2**
	s3179																	
*	**-013.1**	**0.61**	**0.000289**	**37.80**	**0.21015**	**8.16**	**7.5378**	**2.34**	**0.39905**	**1.67**	**0.712**	**0.13700**	**1.64**	**2165**	**31**	**2190**	**29**	**+1.3**
	s3179																	
	-015.1	1.01	0.000078	31.62	0.29886	1.71	6.6511	1.26	0.38916	1.10	0.873	0.12395	0.62	2119	20	2014	11	-6.1
	s3179																	
	-016.1	0.44	0.000341	20.42	0.11631	3.65	6.8046	1.62	0.36569	1.27	0.780	0.13495	1.01	2009	22	2163	18	+8.3
	s3179																	
	-019.1	0.71	0.000197	27.74	0.20406	2.89	12.5749	1.61	0.49173	1.41	0.877	0.18547	0.77	2578	30	2702	13	+5.6
	s3179																	
	-021.1	0.38	0.000239	22.36	0.11326	3.41	10.3765	1.62	0.45352	1.18	0.730	0.16594	1.11	2411	24	2517	19	+5.1
	s3179																	
	-024.1	0.44	0.000162	33.34	0.12478	3.97	7.5283	1.72	0.41317	1.40	0.814	0.13215	1.00	2229	26	2127	18	-5.7
	s3179																	
	-025.1	0.43	0.000122	26.73	0.12054	2.80	8.6543	1.31	0.42997	1.14	0.875	0.14598	0.63	2306	22	2299	11	-0.3
	s3179																	
	-026.1	0.38	0.000060	33.33	0.09794	2.72	17.5507	1.22	0.55464	1.14	0.934	0.22950	0.44	2844	26	3049	7	+8.3
	s3179																	+15.
	-028.1	0.50	0.000385	22.95	0.16583	3.69	7.2194	1.82	0.36073	1.39	0.762	0.14515	1.18	1986	24	2290	20	4
	s3179																	
*	**-034.1**	**0.19**	**0.000360**	**20.86**	**0.05249**	**13.49**	**7.5696**	**2.60**	**0.42681**	**2.35**	**0.903**	**0.12863**	**1.11**	**2291**	**45**	**2079**	**20**	**-12.1**
	s3179																	
	-035.1	0.37	0.000172	21.82	0.11528	2.82	7.5290	1.28	0.40417	1.09	0.853	0.13511	0.67	2188	20	2165	12	-1.2
	s3179																	
*	**-046.1**	**0.48**	**0.000529**	**21.33**	**0.15709**	**4.14**	**6.2158**	**2.19**	**0.36876**	**1.48**	**0.677**	**0.12225**	**1.61**	**2024**	**26**	**1989**	**29**	**-2.0**
	s3179																	
	-049.1	0.77	0.000835	20.01	0.23065	4.00	9.0205	2.63	0.45497	1.80	0.683	0.14380	1.92	2417	36	2273	33	-7.6
	s3179																	
	-050.1	0.54	0.000152	23.57	0.16093	2.42	7.1875	1.29	0.38344	1.10	0.856	0.13595	0.67	2092	20	2176	12	+4.5
	s3179																	
	-052.1	0.47	0.000117	30.15	0.14596	2.86	11.1379	1.92	0.54389	1.80	0.934	0.14852	0.69	2800	41	2329	12	-25.0
	s3179																	
	-053.1	0.41	0.000169	20.85	0.11901	4.29	8.6943	1.24	0.43002	1.09	0.875	0.14664	0.60	2306	21	2307	10	+0.1
	s3179																	
	-054.1	0.43	0.000261	25.82	0.14985	3.58	7.2502	1.70	0.39549	1.32	0.779	0.13296	1.06	2148	24	2137	19	-0.6
	s3179																	
fl	-059.1	0.54	0.000088	23.57	0.15474	1.93	7.0150	1.10	0.39234	0.99	0.897	0.12968	0.49	2134	18	2094	9	-2.2

	s3179																	
	-060.1	**0.27**	**0.000103**	**37.80**	**0.07817**	**4.52**	**7.6564**	**1.49**	**0.41149**	**1.23**	**0.825**	**0.13495**	**0.84**	**2222**	**23**	**2163**	**15**	**-3.2**
	s3179																	
	-061.1	0.73	0.000201	23.57	0.22141	2.42	6.1865	1.39	0.35927	1.10	0.793	0.12489	0.85	1979	19	2027	15	+2.8
	s3179																	
x	**-062.1**	**0.14**	**0.000047**	**37.80**	**0.04213**	**4.18**	**7.0072**	**1.17**	**0.38970**	**1.04**	**0.890**	**0.13041**	**0.53**	**2121**	**19**	**2103**	**9**	**-1.0**
	s3179																	
x	**-062.2**	**0.14**	**0.000072**	**30.15**	**0.04716**	**4.32**	**7.1571**	**1.18**	**0.40156**	**1.02**	**0.864**	**0.12927**	**0.60**	**2176**	**19**	**2088**	**10**	**-5.0**
	s3179																	
	-063.1	0.43	0.000113	30.15	0.14340	5.85	7.1802	1.33	0.35520	1.14	0.860	0.14661	0.68	1959	19	2307	12	+17.4
	s3179																	
fl	***-069.1***	***0.08***	***0.000207***	***23.57***	***0.02314***	***7.38***	***8.9135***	***1.42***	***0.44030***	***1.19***	***0.837***	***0.14683***	***0.78***	***2352***	***23***	***2309***	***13***	***-2.2***
	s3179																	
	-073.1	**0.15**	**0.000078**	**35.36**	**0.04220**	**5.16**	**6.4702**	**1.26**	**0.36639**	**1.06**	**0.843**	**0.12808**	**0.68**	**2012**	**18**	**2072**	**12**	**+3.3**
	s3179																	
fl	**-076.1**	**0.40**	**0.000025**	**57.74**	**0.11504**	**2.83**	**7.0047**	**1.64**	**0.38739**	**1.10**	**0.670**	**0.13114**	**1.22**	**2111**	**20**	**2113**	**21**	**+0.1**
	s3179																	
	-085.1	**0.28**	**0.000146**	**33.34**	**0.07036**	**5.04**	**8.8940**	**1.63**	**0.44364**	**1.37**	**0.843**	**0.14540**	**0.88**	**2367**	**27**	**2293**	**15**	**-3.9**
	s3179																	
	-094.1	**0.34**	**0.000392**	**21.32**	**0.10402**	**4.34**	**8.4223**	**1.75**	**0.43267**	**1.34**	**0.762**	**0.14118**	**1.14**	**2318**	**26**	**2242**	**20**	**-4.0**
	s3179																	
	-095.1	0.64	0.000181	37.80	0.18740	4.00	8.0186	1.90	0.42947	1.47	0.773	0.13541	1.20	2303	28	2169	21	-7.4
	s3179																	
	-097.1	0.55	0.000206	25.82	0.16862	2.98	9.2070	1.50	0.46537	1.24	0.823	0.14349	0.85	2463	25	2270	15	-10.3
	s3179																	
	-110.1	0.72	0.000512	21.54	0.25485	3.29	4.0402	2.00	0.23545	1.24	0.622	0.12445	1.57	1363	15	2021	28	+36.1
	s3179																	
	-111.1	**0.36**	**0.000102**	**26.73**	**0.11052**	**2.68**	**7.6383**	**1.18**	**0.40945**	**1.02**	**0.869**	**0.13530**	**0.58**	**2212**	**19**	**2168**	**10**	**-2.4**
	s3179																	
	-113.1	0.50	0.000229	27.74	0.14128	3.71	7.4150	1.72	0.40254	1.37	0.799	0.13360	1.04	2181	25	2146	18	-1.9
	s3179																	
***fl**	**-120.1**	**0.36**	**0.000892**	**25.83**	**0.12116**	**7.27**	**17.1460**	**3.59**	**0.57863**	**2.34**	**0.652**	**0.21491**	**2.72**	**2943**	**55**	**2943**	**44**	**-0.0**
	s3179																	
	-126.1	0.46	0.000049	70.71	0.13602	4.43	11.6822	1.89	0.49021	1.66	0.877	0.17284	0.91	2572	35	2585	15	+0.6
	s3179																	
	-127.1	**0.36**	**0.000289**	**24.26**	**0.10259**	**4.33**	**7.5207**	**1.74**	**0.40832**	**1.37**	**0.786**	**0.13358**	**1.08**	**2207**	**26**	**2146**	**19**	**-3.4**
	s3179																	
	-128.1	**0.27**	**0.000066**	**27.74**	**0.07367**	**2.73**	**8.9675**	**1.23**	**0.43617**	**1.01**	**0.820**	**0.14911**	**0.71**	**2333**	**20**	**2336**	**12**	**+0.1**
	s3178			**100.0**														
14KA098	**-004.1**	**0.56**	**0.000010**	**0**	**0.14816**	**2.76**	**7.9243**	**1.33**	**0.40249**	**1.15**	**0.867**	**0.14279**	**0.66**	**2181**	**21**	**2261**	**11**	**+4.2**
	s3178			**100.0**														
	-006.1	**0.61**	**0.000004**	**0**	**0.17126**	**3.16**	**8.9285**	**1.04**	**0.43725**	**0.97**	**0.926**	**0.14810**	**0.39**	**2338**	**19**	**2324**	**7**	**-0.7**
	s3178																	
	-010.1	**0.65**	**0.000201**	**35.36**	**0.18066**	**4.23**	**8.2310**	**1.87**	**0.41276**	**1.47**	**0.788**	**0.14463**	**1.15**	**2228**	**28**	**2283**	**20**	**+2.9**
	s3178																	
	-013.1	**0.64**	**0.000129**	**19.88**	**0.16912**	**1.74**	**7.6400**	**1.10**	**0.41752**	**0.99**	**0.903**	**0.13271**	**0.47**	**2249**	**19**	**2134**	**8**	**-6.4**
	s3178																	
	-014.1	0.49	0.000252	37.80	0.13003	6.22	7.2975	2.23	0.38939	1.65	0.739	0.13592	1.50	2120	30	2176	26	+3.0
	s3178																	
	-016.1	0.61	0.000237	28.87	0.19000	4.04	8.4034	1.70	0.41576	1.33	0.784	0.14659	1.05	2241	25	2307	18	+3.4

	s3178-018.1	**0.37**	**0.000025**	**70.71**	**0.11196**	**3.55**	**7.4165**	**1.38**	**0.40239**	**1.18**	**0.859**	**0.13367**	**0.71**	**2180**	**22**	**2147**	**12**	**-1.8**
	s3178-026.1	0.58	0.000184	37.80	0.16777	4.48	8.0911	1.91	0.39622	1.53	0.799	0.14811	1.15	2152	28	2324	20	+8.7
	s3178-027.1	0.60	0.000135	30.15	0.16704	3.07	8.6642	1.42	0.42617	1.21	0.848	0.14745	0.75	2288	23	2317	13	+1.4
x	**s3178-031.1**	**0.29**	**0.000021**	**50.00**	**0.08572**	**2.63**	**5.0153**	**1.11**	**0.32227**	**0.99**	**0.898**	**0.11287**	**0.49**	**1801**	**16**	**1846**	**9**	**+2.8**
	s3178-032.1	**0.36**	**0.000052**	**37.80**	**0.09928**	**2.96**	**8.2966**	**1.21**	**0.41971**	**1.09**	**0.894**	**0.14337**	**0.54**	**2259**	**21**	**2268**	**9**	**+0.5**
	s3178-039.1	**0.45**	**0.000088**	**26.73**	**0.13030**	**2.44**	**7.7707**	**1.17**	**0.39459**	**1.05**	**0.894**	**0.14283**	**0.53**	**2144**	**19**	**2262**	**9**	**+6.1**
	s3178-048.1	0.68	0.000125	20.85	0.19373	4.24	8.8238	1.14	0.43653	1.03	0.902	0.14660	0.49	2335	20	2307	8	-1.5
x	**s3178-052.1**	**0.55**	**0.000112**	**23.57**	**0.15688**	**4.22**	**8.7250**	**1.18**	**0.43525**	**1.05**	**0.894**	**0.14539**	**0.53**	**2329**	**21**	**2292**	**9**	**-1.9**
*	**s3178-053.1**	**0.32**	**0.000126**	**50.00**	**0.07745**	**7.45**	**9.0598**	**2.46**	**0.43223**	**1.60**	**0.649**	**0.15202**	**1.87**	**2316**	**31**	**2369**	**32**	**+2.7**
x	**s3178-056.1**	**0.77**	**0.000044**	**35.36**	**0.23975**	**1.61**	**7.7908**	**1.12**	**0.39727**	**1.02**	**0.910**	**0.14223**	**0.47**	**2156**	**19**	**2255**	**8**	**+5.1**
x	**s3178-058.1**	**0.89**	**0.000034**	**33.33**	**0.25424**	**1.32**	**8.8585**	**1.04**	**0.43620**	**0.97**	**0.930**	**0.14729**	**0.38**	**2334**	**19**	**2315**	**7**	**-1.0**
x	**s3178-065.2**	**0.40**	**0.000111**	**37.80**	**0.11159**	**4.30**	**7.2560**	**1.57**	**0.39328**	**1.29**	**0.824**	**0.13381**	**0.89**	**2138**	**24**	**2149**	**16**	**+0.6**
	s3178-068.1r	**0.20**	**0.000135**	**18.78**	**0.05554**	**3.45**	**6.5996**	**1.50**	**0.38948**	**1.41**	**0.943**	**0.12289**	**0.50**	**2120**	**26**	**1999**	**9**	**-7.2**
	s3178-068.2	**0.38**	**0.000105**	**31.62**	**0.10410**	**6.08**	**7.2052**	**1.30**	**0.38749**	**1.10**	**0.840**	**0.13486**	**0.71**	**2111**	**20**	**2162**	**12**	**+2.8**
	s3178-069.1	**0.39**	**0.000085**	**35.36**	**0.10262**	**3.59**	**6.7463**	**1.37**	**0.37792**	**1.16**	**0.852**	**0.12947**	**0.72**	**2067**	**21**	**2091**	**13**	**+1.4**
	s3178-074.1	**0.60**	**0.000071**	**37.80**	**0.17067**	**2.66**	**9.2490**	**1.32**	**0.45960**	**1.15**	**0.872**	**0.14595**	**0.65**	**2438**	**23**	**2299**	**11**	**-7.3**
	s3178-075.1	0.44	0.000067	44.72	0.11826	3.69	9.4674	1.45	0.46052	1.26	0.866	0.14910	0.73	2442	26	2336	12	-5.5
	s3178-076.1	0.46	0.000157	24.26	0.12538	3.11	8.2188	1.32	0.40921	1.14	0.861	0.14567	0.67	2211	21	2296	12	+4.3
	s3178-077.1	**0.24**	**0.000129**	**25.82**	**0.06474**	**4.38**	**7.8921**	**1.63**	**0.39440**	**1.51**	**0.922**	**0.14513**	**0.63**	**2143**	**27**	**2289**	**11**	**+7.5**
	s3178-079.1	**0.65**	**0.000202**	**25.00**	**0.18279**	**3.00**	**8.1297**	**1.48**	**0.40249**	**1.24**	**0.836**	**0.14649**	**0.81**	**2180**	**23**	**2305**	**14**	**+6.4**
*	**s3178-081.1**	**0.74**	**0.000860**	**24.26**	**0.18254**	**7.22**	**6.9188**	**3.32**	**0.38698**	**2.03**	**0.613**	**0.12967**	**2.62**	**2109**	**37**	**2094**	**46**	**-0.9**
	s3178-086.1	0.66	0.000062	57.74	0.17600	3.68	8.2142	1.68	0.40659	1.42	0.840	0.14652	0.91	2199	26	2306	16	+5.4
	s3178-088.1	0.56	0.000239	25.36	0.15133	3.78	8.5096	1.55	0.42513	1.25	0.804	0.14517	0.92	2284	24	2290	16	+0.3
x	**s3178-089.1**	**0.46**	**0.000143**	**21.82**	**0.13312**	**4.21**	**8.5968**	**1.18**	**0.42586**	**1.04**	**0.876**	**0.14641**	**0.57**	**2287**	**20**	**2304**	**10**	**+0.9**

	s3178-095.1	0.68	0.000068	35.36	0.19071	2.27	8.8846	1.27	0.43734	1.13	0.888	0.14734	0.58	2339	22	2315	10	-1.2
	s3178-096.1	**0.32**	**0.000170**	**33.34**	**0.09132**	**5.45**	**7.1027**	**1.72**	**0.39311**	**1.38**	**0.800**	**0.13104**	**1.03**	**2137**	**25**	**2112**	**18**	**-1.4**
	s3178-105.1	**0.39**	**0.000072**	**44.72**	**0.10335**	**4.09**	**7.0941**	**1.51**	**0.38189**	**1.28**	**0.848**	**0.13473**	**0.80**	**2085**	**23**	**2160**	**14**	**+4.1**
x	**s3178-110.2**	**0.30**	**0.000083**	**27.98**	**0.08160**	**3.17**	**7.9954**	**1.35**	**0.39413**	**1.05**	**0.778**	**0.14713**	**0.85**	**2142**	**19**	**2313**	**15**	**+8.7**
*	**s3178-117.1**	**0.61**	**0.000017**	**100.0 0**	**0.15601**	**3.49**	**9.0064**	**1.57**	**0.43998**	**1.36**	**0.866**	**0.14846**	**0.78**	**2351**	**27**	**2328**	**13**	**-1.1**
	s3178-121.1	0.64	0.000188	22.94	0.18364	2.60	6.8538	1.38	0.39151	1.14	0.829	0.12696	0.77	2130	21	2056	14	-4.2
x	**s3178-123.2**	**0.49**	**0.000065**	**35.36**	**0.12976**	**2.74**	**6.5467**	**1.24**	**0.35931**	**1.08**	**0.873**	**0.13215**	**0.60**	**1979**	**18**	**2127**	**11**	**+8.1**
	s3178-126.1	**0.32**	**0.000044**	**44.72**	**0.09597**	**3.24**	**8.9228**	**1.22**	**0.44036**	**1.07**	**0.881**	**0.14696**	**0.58**	**2352**	**21**	**2311**	**10**	**-2.1**
	s3178-127.1	**0.31**	**0.000096**	**37.80**	**0.08329**	**7.54**	**10.2495**	**1.75**	**0.47657**	**1.21**	**0.694**	**0.15598**	**1.26**	**2512**	**25**	**2413**	**21**	**-5.0**
x	**s3178-128.1**	**0.40**	**0.000095**	**24.25**	**0.11982**	**2.42**	**7.0231**	**1.14**	**0.39391**	**1.01**	**0.885**	**0.12931**	**0.53**	**2141**	**18**	**2089**	**9**	**-2.9**
	s3178-132.1r	**0.33**	**0.000142**	**17.49**	**0.09241**	**2.67**	**4.7431**	**1.06**	**0.32346**	**0.92**	**0.865**	**0.10635**	**0.53**	**1807**	**14**	**1738**	**10**	**-4.5**
	s3178-133.1	0.43	0.000142	25.00	0.11947	3.15	6.8711	1.31	0.39216	1.11	0.845	0.12708	0.70	2133	20	2058	12	-4.3
	s3178-135.1	0.42	0.000102	37.80	0.12943	3.78	6.7701	1.44	0.37983	1.17	0.807	0.12927	0.85	2075	21	2088	15	+0.7
	s3178-135.2	0.42	0.000136	35.36	0.11506	4.40	6.2240	1.62	0.35405	1.31	0.806	0.12750	0.96	1954	22	2064	17	+6.2
	s3178-139.1	**0.32**	**0.000341**	**23.57**	**0.08394**	**6.32**	**8.4288**	**1.76**	**0.42885**	**1.36**	**0.774**	**0.14254**	**1.12**	**2301**	**26**	**2258**	**19**	**-2.2**
	s3178-140.1	**0.46**	**0.000158**	**18.17**	**0.12309**	**2.18**	**7.1620**	**1.09**	**0.40126**	**0.97**	**0.887**	**0.12945**	**0.51**	**2175**	**18**	**2091**	**9**	**-4.7**
	s3178-141.1	**0.43**	**0.000283**	**14.49**	**0.11435**	**2.64**	**8.9545**	**1.17**	**0.44950**	**1.02**	**0.873**	**0.14448**	**0.57**	**2393**	**20**	**2282**	**10**	**-5.8**
	s3178-141.2	**0.45**	**0.000147**	**21.32**	**0.12146**	**2.94**	**8.6711**	**1.15**	**0.42931**	**1.01**	**0.873**	**0.14649**	**0.56**	**2303**	**20**	**2305**	**10**	**+0.1**
	s3178-142.1	0.50	0.000583	18.49	0.13406	4.92	8.1269	1.83	0.40290	1.33	0.730	0.14629	1.25	2182	25	2303	21	+6.2
x	**s3178-149.1**	**0.47**	**0.000100**	**33.34**	**0.14371**	**3.10**	**6.6909**	**1.38**	**0.37898**	**1.16**	**0.841**	**0.12805**	**0.75**	**2072**	**21**	**2071**	**13**	**-0.0**
	s3178-154.1	0.50	0.000115	30.15	0.13954	3.09	8.8122	1.38	0.43567	1.19	0.864	0.14670	0.69	2331	23	2308	12	-1.2
	s3178-155.1	0.87	0.000477	21.33	0.25016	3.56	7.0430	2.03	0.39734	1.44	0.713	0.12856	1.42	2157	26	2078	25	-4.4
*	**s3178-156.1**	**0.79**	**0.000122**	**40.83**	**0.22431**	**3.33**	**10.1291**	**1.72**	**0.46903**	**1.45**	**0.842**	**0.15663**	**0.93**	**2479**	**30**	**2420**	**16**	**-3.0**
*	**s3178-156.2**	**0.37**	**0.000328**	**25.82**	**0.10399**	**5.93**	**10.0478**	**2.98**	**0.47293**	**1.47**	**0.494**	**0.15409**	**2.59**	**2496**	**30**	**2392**	**44**	**-5.3**

	s3178																	
	-157.1	0.49	0.000020	50.00	0.13613	2.10	9.3741	1.10	0.45685	1.01	0.921	0.14882	0.43	2426	20	2332	7	-4.8
	s3178																	
	-158.1	**0.37**	**0.000031**	**50.00**	**0.10263**	**2.95**	**8.5140**	**1.43**	**0.42521**	**1.10**	**0.768**	**0.14522**	**0.92**	**2284**	**21**	**2290**	**16**	**+0.3**
	s3178																	
	-168.1	0.84	0.000294	17.96	0.24292	2.27	8.9124	1.36	0.43878	1.13	0.834	0.14732	0.75	2345	22	2315	13	-1.6
	s3178																	
	-169.1	0.46	0.000240	18.82	0.12636	2.90	9.0675	1.25	0.44398	1.07	0.855	0.14812	0.65	2368	21	2324	11	-2.3
	s3178																	
	-174.1	**0.19**	**0.000074**	**33.33**	**0.05153**	**4.59**	**7.1612**	**1.87**	**0.39816**	**1.76**	**0.944**	**0.13044**	**0.61**	**2161**	**32**	**2104**	**11**	**-3.2**
	s3178																	
	-179.1	**0.44**	**0.000568**	**17.21**	**0.12822**	**4.72**	**7.2267**	**1.78**	**0.38974**	**1.29**	**0.722**	**0.13448**	**1.23**	**2122**	**23**	**2157**	**22**	**+1.9**
	s3178			100.0														
	-184.1	0.87	0.000010	0	0.24797	2.08	9.1314	1.31	0.44733	1.17	0.895	0.14805	0.58	2383	23	2324	10	-3.1
	s3178																	
*	**-188.1**	**0.17**	**0.000168**	**26.73**	**0.04913**	**6.47**	**8.8870**	**1.72**	**0.42695**	**1.21**	**0.704**	**0.15096**	**1.22**	**2292**	**23**	**2357**	**21**	**+3.3**
	s3178																	
	-197.2	0.67	0.000426	18.61	0.18808	3.42	6.6081	1.70	0.37437	1.26	0.742	0.12802	1.14	2050	22	2071	20	+1.2
	s3178																	
	-198.1	0.54	0.000032	50.00	0.15093	2.49	8.9977	1.25	0.44419	1.12	0.896	0.14691	0.55	2369	22	2310	10	-3.1
	s3177																	
14KA095	-001.1	0.52	0.000238	25.00	0.14728	7.44	5.9083	1.61	0.34742	1.25	0.777	0.12334	1.02	1922	21	2005	18	+4.8
	s3177																	
	-002.1	0.62	0.000136	27.74	0.16939	2.78	8.3979	1.39	0.41219	1.20	0.866	0.14776	0.70	2225	23	2320	12	+4.9
	s3177																	
	-004.1	**0.47**	**0.000117**	**23.57**	**0.13621**	**2.47**	**8.5087**	**1.14**	**0.41892**	**1.00**	**0.879**	**0.14731**	**0.54**	**2256**	**19**	**2315**	**9**	**+3.0**
	s3177																	
	-006.1	***0.00***	***0.000092***	***25.00***	***0.00072***	***140.15***	***5.7453***	***1.10***	***0.35084***	***0.95***	***0.864***	***0.11877***	***0.55***	***1939***	***16***	***1938***	***10***	***-0.0***
	s3177																	
	-011.2	**0.23**	**0.000171**	**25.82**	**0.06126**	**5.41**	**6.4729**	**1.76**	**0.36941**	**1.55**	**0.883**	**0.12708**	**0.82**	**2027**	**27**	**2058**	**15**	**+1.8**
	s3177																	
	-014.1	**0.39**	**0.000227**	**12.79**	**0.11180**	**3.10**	**6.6640**	**1.05**	**0.40766**	**0.93**	**0.885**	**0.11856**	**0.49**	**2204**	**17**	**1935**	**9**	**-16.5**
	s3177																	
	-015.1	0.61	0.000157	40.83	0.17916	4.26	6.1157	1.84	0.35495	1.36	0.742	0.12496	1.23	1958	23	2028	22	+4.0
	s3177																	
	-015.2	0.60	0.000187	31.63	0.16023	3.94	6.3752	1.75	0.37322	1.37	0.783	0.12389	1.09	2045	24	2013	19	-1.8
	s3177																	
	-017.2	**0.38**	**0.000125**	**25.00**	**0.10563**	**3.08**	**7.4375**	**1.25**	**0.40026**	**1.09**	**0.868**	**0.13477**	**0.62**	**2170**	**20**	**2161**	**11**	**-0.5**
	s3177																	
	-033.1	0.63	0.000529	20.42	0.15320	4.93	6.8635	2.08	0.38329	1.48	0.710	0.12987	1.47	2092	26	2096	26	+0.3
	s3177																	
	-034.1	0.55	0.000306	18.29	0.15779	3.10	8.9152	1.45	0.42985	1.18	0.820	0.15042	0.83	2305	23	2351	14	+2.3
	s3177																	
	-035.1	**0.29**	**0.000338**	**19.00**	**0.07810**	**5.16**	**5.5100**	**1.55**	**0.33415**	**1.19**	**0.768**	**0.11960**	**0.99**	**1858**	**19**	**1950**	**18**	**+5.4**
	s3177																	
	-036.1	0.59	0.000335	27.74	0.16201	4.89	5.9485	2.05	0.34592	1.46	0.712	0.12472	1.44	1915	24	2025	25	+6.3
	s3177																	
	-037.1	0.48	0.000068	40.83	0.13505	3.16	8.4742	1.40	0.41675	1.22	0.874	0.14747	0.68	2246	23	2317	12	+3.6
	s3177																	
	-038.1	0.61	0.000053	30.15	0.17406	1.82	8.4978	1.37	0.42734	1.29	0.946	0.14422	0.44	2294	25	2279	8	-0.8

	s3177 -054.1	0.71	0.000360	17.96	0.18222	3.00	6.6941	1.53	0.37634	1.19	0.779	0.12901	0.96	2059	21	2084	17	+1.4
	s3177 -057.1	**0.37**	**0.000259**	**19.25**	**0.10347**	**3.77**	**8.1877**	**1.38**	**0.40608**	**1.16**	**0.842**	**0.14623**	**0.74**	**2197**	**22**	**2302**	**13**	**+5.4**
	s3177 -059.1	0.94	0.000259	18.98	0.29189	1.98	6.0979	1.36	0.35538	1.09	0.802	0.12445	0.81	1960	18	2021	14	+3.5
x	s3177 -061.1	0.82	0.000155	18.64	0.23750	1.67	6.8951	1.15	0.38854	1.01	0.877	0.12871	0.55	2116	18	2080	10	-2.0
	s3177 -062.2	**0.30**	**0.000051**	**44.72**	**0.09626**	**3.53**	**5.3290**	**2.32**	**0.32667**	**2.21**	**0.954**	**0.11831**	**0.70**	**1822**	**35**	**1931**	**12**	**+6.5**
	s3177 -064.1	0.49	0.000494	22.37	0.13867	5.54	8.9265	2.12	0.43961	1.61	0.760	0.14727	1.38	2349	32	2314	24	-1.8
	s3177 -065.1	0.77	0.000035	50.00	0.21978	2.13	10.9232	1.29	0.48242	1.17	0.906	0.16422	0.55	2538	25	2500	9	-1.9
	s3177 -067.1	**0.45**	**0.000019**	**57.74**	**0.12999**	**2.35**	**9.3239**	**1.17**	**0.45495**	**1.07**	**0.912**	**0.14864**	**0.48**	**2417**	**22**	**2330**	**8**	**-4.5**
	s3177 -067.2r	***0.06***	***0.000172***	***15.88***	***0.01530***	***9.04***	***6.0498***	***1.45***	***0.37385***	***1.19***	***0.817***	***0.11737***	***0.84***	***2047***	***21***	***1917***	***15***	***-8.0***
x	***s3177 -071.1r***	***0.01***	***0.000159***	***19.37***	***0.00228***	***60.45***	***6.0218***	***1.17***	***0.36911***	***0.99***	***0.849***	***0.11832***	***0.62***	***2025***	***17***	***1931***	***11***	***-5.7***
	s3177 -072.1	**0.33**	**0.000224**	**20.41**	**0.06888**	**4.73**	**6.4593**	**1.35**	**0.36215**	**1.11**	**0.822**	**0.12936**	**0.77**	**1992**	**19**	**2089**	**13**	**+5.4**
	s3177 -081.1	**0.20**	**0.000379**	**13.65**	**0.05616**	**5.16**	**6.2743**	**1.63**	**0.36930**	**1.44**	**0.884**	**0.12322**	**0.76**	**2026**	**25**	**2003**	**14**	**-1.3**
	s3177 -083.1	**0.44**	**0.000130**	**17.99**	**0.13063**	**2.04**	**6.1556**	**2.12**	**0.36920**	**1.92**	**0.908**	**0.12092**	**0.89**	**2026**	**33**	**1970**	**16**	**-3.3**
	s3177 -083.2	**0.40**	**0.000185**	**18.84**	**0.11435**	**2.60**	**5.9318**	**1.18**	**0.36765**	**1.00**	**0.847**	**0.11702**	**0.63**	**2018**	**17**	**1911**	**11**	**-6.5**
	s3177 -084.1	0.55	0.000054	37.80	0.15208	2.46	8.7999	1.21	0.42852	1.08	0.891	0.14894	0.55	2299	21	2334	9	+1.8
	s3177 -087.1	0.56	0.000187	26.73	0.15073	3.42	7.6342	1.45	0.37986	1.19	0.821	0.14576	0.83	2076	21	2297	14	+11.3
	s3177 -089.1	0.42	0.000638	20.42	0.12096	6.61	7.7066	2.20	0.39167	1.52	0.691	0.14270	1.59	2131	28	2260	27	+6.7
	s3177 -093.1	**0.52**	**0.000159**	**21.49**	**0.14922**	**2.51**	**8.8292**	**1.71**	**0.43759**	**1.10**	**0.644**	**0.14634**	**1.31**	**2340**	**22**	**2304**	**22**	**-1.9**
	s3177 -096.1	0.46	0.000150	30.15	0.12627	3.82	9.1679	1.50	0.45604	1.26	0.838	0.14580	0.82	2422	25	2297	14	-6.5
	s3177 -100.1	0.48	0.000209	25.82	0.13357	3.77	7.4775	1.51	0.40593	1.21	0.800	0.13360	0.91	2196	23	2146	16	-2.8
x fl	**s3177 -101.1**	**0.29**	**0.000198**	**18.61**	**0.07631**	**3.73**	**7.1763**	**1.23**	**0.39566**	**1.05**	**0.856**	**0.13155**	**0.64**	**2149**	**19**	**2119**	**11**	**-1.7**
*	**s3177 -102.1**	**0.43**	**0.000563**	**21.06**	**0.11892**	**6.42**	**8.4585**	**2.32**	**0.42018**	**1.81**	**0.781**	**0.14600**	**1.45**	**2261**	**35**	**2300**	**25**	**+2.0**
	s3177 -111.1	**0.34**	**0.000172**	**25.82**	**0.09763**	**4.03**	**8.7471**	**1.44**	**0.43122**	**1.23**	**0.855**	**0.14712**	**0.75**	**2311**	**24**	**2313**	**13**	**+0.1**
	s3177 -114.2	**0.40**	**0.000204**	**19.61**	**0.11734**	**3.04**	**5.7489**	**1.30**	**0.35282**	**1.07**	**0.824**	**0.11818**	**0.74**	**1948**	**18**	**1929**	**13**	**-1.2**

	s3177 -116.1	**0.12**	**0.000100**	**26.73**	**0.03515**	**5.76**	**6.5673**	**1.52**	**0.37843**	**1.06**	**0.698**	**0.12586**	**1.09**	**2069**	**19**	**2041**	**19**	**-1.6**
	s3177 -119.1	0.65	0.000184	25.00	0.19506	2.70	8.0793	1.41	0.39664	1.19	0.845	0.14773	0.76	2154	22	2320	13	+8.4
x	**s3177 -121.1**	**0.47**	**0.000060**	**37.80**	**0.13742**	**2.69**	**7.5887**	**1.29**	**0.39507**	**1.11**	**0.862**	**0.13931**	**0.65**	**2146**	**20**	**2219**	**11**	**+3.8**
	s3177 -122.1	**0.37**	**0.000069**	**50.00**	**0.10026**	**4.55**	**7.0090**	**1.52**	**0.38976**	**1.24**	**0.815**	**0.13043**	**0.88**	**2122**	**22**	**2104**	**15**	**-1.0**
	s3177 -125.1	0.95	0.000455	22.95	0.25716	5.94	8.6844	2.44	0.42942	1.60	0.657	0.14668	1.84	2303	31	2308	32	+0.2
x	**s3177 -128.1**	**0.35**	**0.000509**	**20.86**	**0.10479**	**6.44**	**6.8406**	**2.06**	**0.38672**	**1.43**	**0.697**	**0.12829**	**1.48**	**2108**	**26**	**2075**	**26**	**-1.9**
x	**s3177 -130.1**	**0.17**	**0.000404**	**18.07**	**0.04130**	**9.12**	**7.0740**	**1.54**	**0.39098**	**1.18**	**0.764**	**0.13122**	**1.00**	**2127**	**21**	**2114**	**17**	**-0.7**
	s3177 -132.1	0.51	0.000190	22.36	0.17158	4.46	7.6322	1.32	0.38821	1.12	0.847	0.14259	0.70	2115	20	2259	12	+7.5
x	**s3177 -133.2**	**0.36**	**0.000062**	**31.62**	**0.10477**	**2.67**	**9.1030**	**1.13**	**0.44990**	**1.01**	**0.898**	**0.14675**	**0.50**	**2395**	**20**	**2308**	**9**	**-4.5**
*	**s3177 -134.1**	**0.14**	**0.000197**	**26.73**	**0.03494**	**9.13**	**9.0760**	**1.57**	**0.44229**	**1.33**	**0.845**	**0.14883**	**0.84**	**2361**	**26**	**2333**	**14**	**-1.5**
	s3177 -141.1	**0.54**	**0.000181**	**22.49**	**0.14335**	**2.87**	**6.0228**	**1.31**	**0.34504**	**1.08**	**0.823**	**0.12660**	**0.74**	**1911**	**18**	**2051**	**13**	**+7.9**
	s3177 -145.1	**0.27**	**0.000259**	**12.17**	**0.07970**	**2.71**	**5.7699**	**1.21**	**0.35212**	**0.95**	**0.785**	**0.11884**	**0.75**	**1945**	**16**	**1939**	**13**	**-0.3**
x	**s3177 -153.1**	**0.46**	**0.000032**	**57.74**	**0.12446**	**3.18**	**8.7168**	**1.95**	**0.42907**	**1.66**	**0.850**	**0.14734**	**1.03**	**2302**	**32**	**2315**	**18**	**+0.7**
	s3177 -158.1	**0.39**	**0.000240**	**19.94**	**0.10468**	**3.39**	**8.1268**	**1.28**	**0.41820**	**1.08**	**0.838**	**0.14094**	**0.70**	**2252**	**20**	**2239**	**12**	**-0.7**
	s3177 -169.1	**0.45**	**0.000084**	**31.62**	**0.12971**	**2.83**	**6.9936**	**1.27**	**0.38757**	**1.10**	**0.868**	**0.13087**	**0.63**	**2112**	**20**	**2110**	**11**	**-0.1**
*	**s3177 -171.1**	**0.35**	**0.000310**	**27.74**	**0.11455**	**5.69**	**6.0167**	**1.94**	**0.34843**	**1.39**	**0.717**	**0.12524**	**1.35**	**1927**	**23**	**2032**	**24**	**+6.0**
	s3177 -178.1	**0.45**	**0.000111**	**27.74**	**0.12258**	**5.96**	**6.6449**	**1.28**	**0.37397**	**1.10**	**0.857**	**0.12887**	**0.66**	**2048**	**19**	**2083**	**12**	**+1.9**
x	s3177 -195.1	0.67	0.000080	26.73	0.18942	1.89	8.7494	1.15	0.42830	1.04	0.905	0.14816	0.49	2298	20	2325	8	+1.4
	s3177 -196.1	**0.29**	**0.000321**	**18.68**	**0.07467**	**5.24**	**5.8631**	**1.45**	**0.31859**	**1.15**	**0.791**	**0.13347**	**0.89**	**1783**	**18**	**2144**	**16**	**+19.3**
	s3177 -203.1	0.51	0.000099	30.15	0.13495	2.89	10.8259	1.31	0.46695	1.17	0.894	0.16815	0.59	2470	24	2539	10	+3.3
	s3177 -206.1	**0.47**	**0.000144**	**25.82**	**0.15524**	**2.76**	**7.8878**	**1.80**	**0.39866**	**1.66**	**0.926**	**0.14350**	**0.68**	**2163**	**31**	**2270**	**12**	**+5.5**
*	**s3177 -212.1**	**0.58**	**0.000368**	**37.80**	**0.15132**	**7.28**	**6.9616**	**2.78**	**0.39238**	**1.87**	**0.673**	**0.12868**	**2.05**	**2134**	**34**	**2080**	**36**	**-3.0**
	s3177 -217.1	1.05	0.000263	20.85	0.28011	2.25	8.4739	1.47	0.42580	1.23	0.833	0.14433	0.81	2287	24	2280	14	-0.4
	s3177 -230.1	0.78	0.000027	44.72	0.21130	1.73	7.3193	1.13	0.40328	1.03	0.908	0.13163	0.47	2184	19	2120	8	-3.6
*	**s3177 -239.1**	**0.34**	**0.000417**	**27.74**	**0.07914**	**9.09**	**7.2638**	**2.36**	**0.40045**	**1.69**	**0.717**	**0.13156**	**1.64**	**2171**	**31**	**2119**	**29**	**-2.9**

s3177																	
-243.1	**0.31**	**0.000098**	**35.36**	**0.08180**	**7.32**	**5.7252**	**1.92**	**0.34654**	**1.74**	**0.907**	**0.11982**	**0.81**	**1918**	**29**	**1954**	**14**	**+2.1**
s3177																	
-244.1	**0.49**	**0.000320**	**20.85**	**0.12495**	**4.11**	**8.8632**	**1.54**	**0.44832**	**1.22**	**0.791**	**0.14338**	**0.94**	**2388**	**24**	**2268**	**16**	**-6.3**
s3177																	
-247.1	0.62	0.000109	35.36	0.18000	3.05	6.8659	1.51	0.38055	1.26	0.837	0.13085	0.83	2079	22	2109	14	+1.7

Table A.1 (see Stern, 1997):
Spot name follows the convention x-y.z; where x = sample number, y = grain number and z = spot number. Multiple analyses in an individual spot are labelled as x-y.z.z
Uncertainties reported at 1σ and are calculated by using SQUID 2.50.11.10.15, rev. 15 Oct 2011
Discordance relative to origin = 100 * ((207/206 age -206/238 age)/(207Pb/206Pb age))
Analytical details
20 µm spot size, U-Pb calibration error, 0.8%
Measured age of secondary standard Temora2 = 419.6 ± 9 Ma (n=33); Intraelement mass fractionation correction of 0.3% applied to unknowns.
Key to Table:
r=rim
bold=evidence of alteration in CL
italic=Th/U<0.1
x=recrystallization?
*=very bright centres in CL - metamorphic?
fl=featureless centres

APPENDIX B: SAMPLE PHOTOS AND ZIRCON IMAGES

Figure B.1 Photos of samples collected for this study.

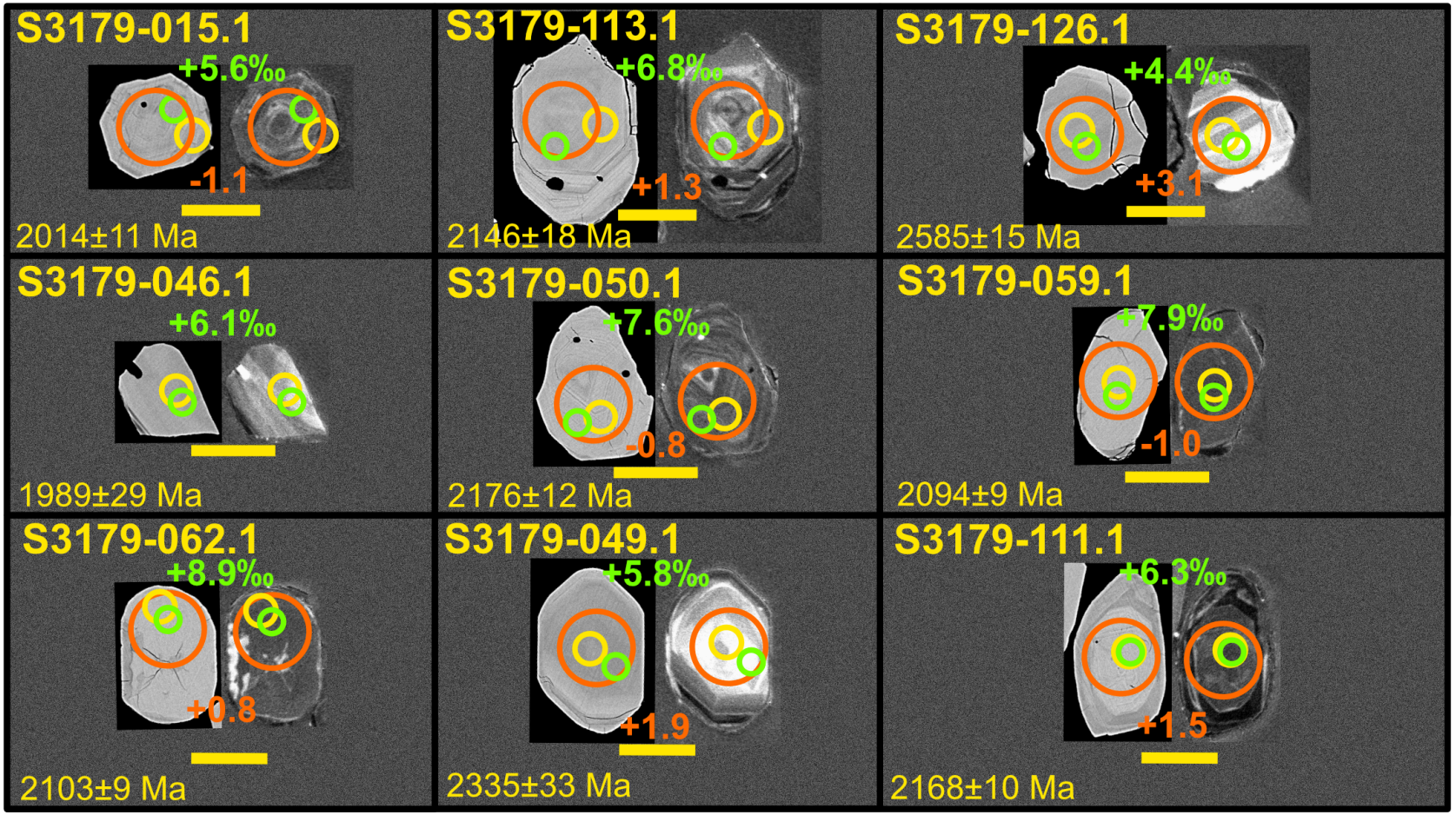
S3179-015.1
+5.6‰
-1.1
2014±11 Ma
S3179-113.1
+6.8‰
+1.3
2146±18 Ma
S3179-126.1
+4.4‰
+3.1
2585±15 Ma
S3179-046.1
+6.1‰
1989±29 Ma
S3179-050.1
+7.6‰
-0.8
2176±12 Ma
S3179-059.1
+7.9‰
-1.0
2094±9 Ma
S3179-062.1
+8.9‰
+0.8
2103±9 Ma
S3179-049.1
+5.8‰
+1.9
2335±33 Ma
S3179-111.1
+6.3‰
+1.5
2168±10 Ma

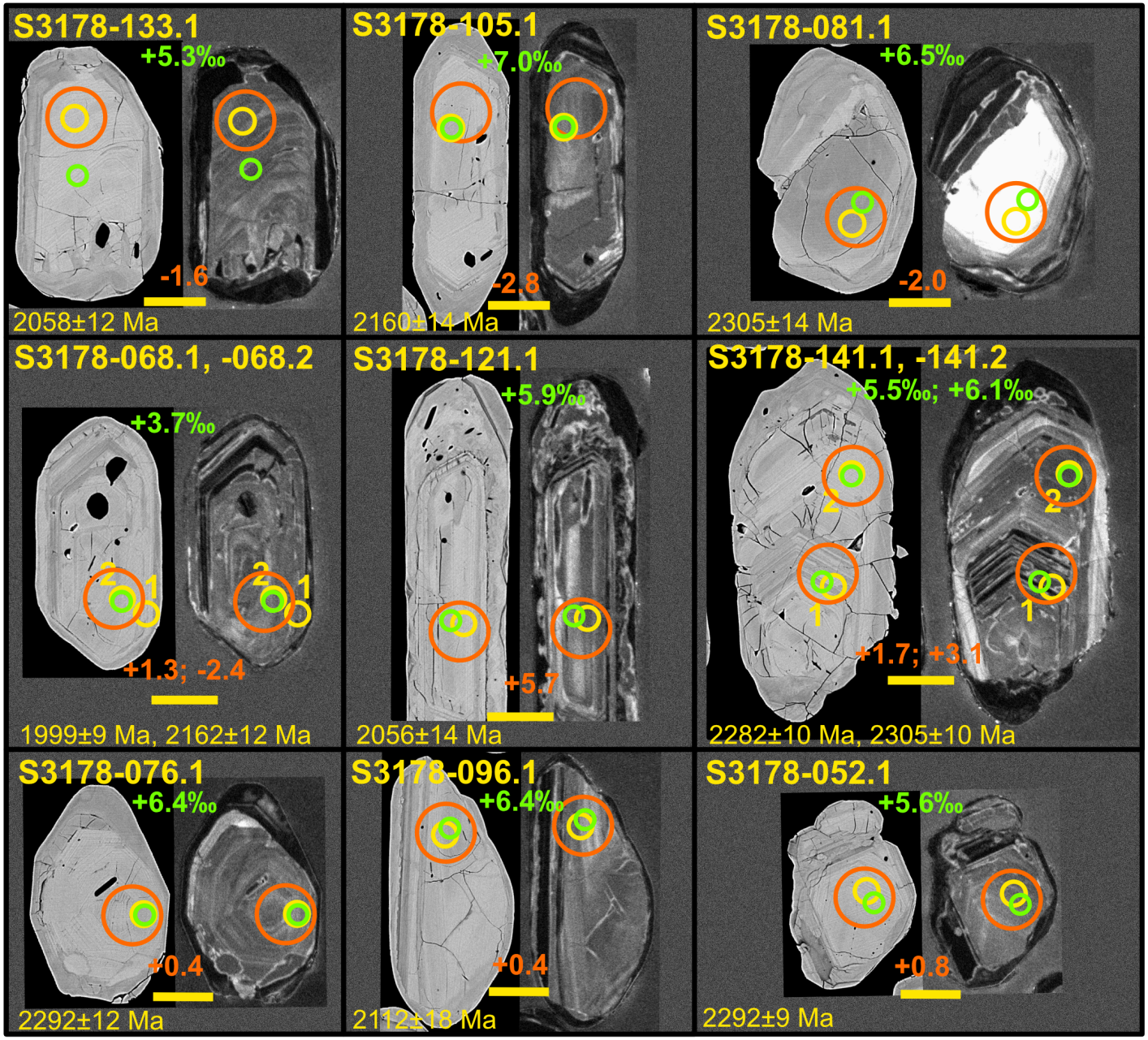
S3178-133.1
+5.3‰
-1.6
2058±12 Ma
S3178-105.1
+7.0‰
-2.8
2160±14 Ma
S3178-081.1
+6.5‰
-2.0
2305±14 Ma
S3178-068.1, -068.2
+3.7‰
+1.3; -2.4
1999±9 Ma, 2162±12 Ma
S3178-121.1
+5.9‰
+5.7
2056±14 Ma
S3178-141.1, -141.2
+5.5‰; +6.1‰
+1.7; +3.1
2282±10 Ma, 2305±10 Ma
S3178-076.1
+6.4‰
+0.4
2292±12 Ma
S3178-096.1
+6.4‰
+0.4
2112±18 Ma
S3178-052.1
+5.6‰
+0.8
2292±9 Ma

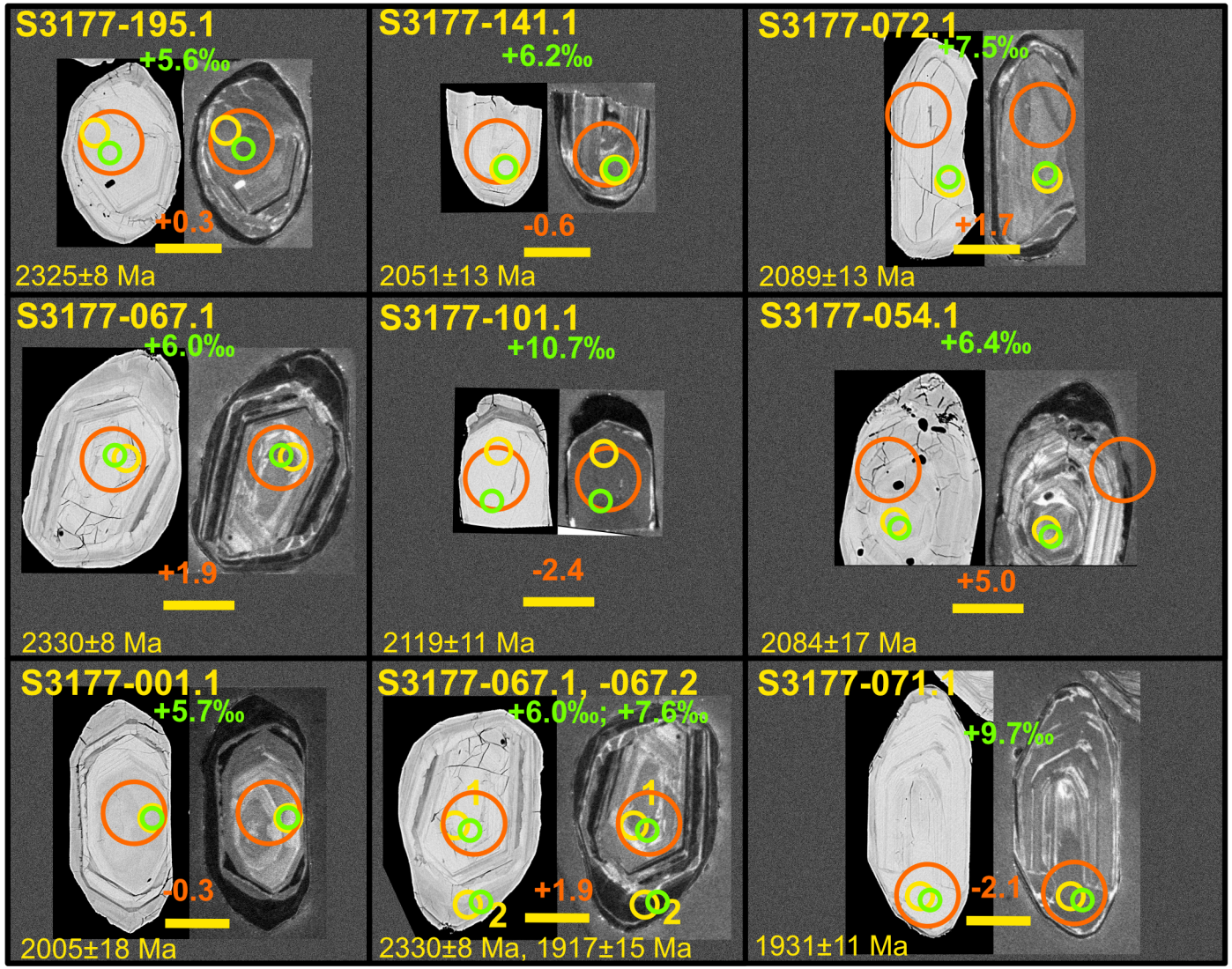

Figure B.2 BSE (left) and CL (right) of select detrital zircons used in this study. Scale bars are each 50µm. Spots targeted for U-Pb analysis are shown in yellow (20µm spot size), $\delta^{18}O$ spots are in green (15µm spot size), and Hf isotope analysis spots are in orange (49µm spot size).

APPENDIX C: HF AND O ISOTOPE DATA

Table C.1 Zircon εHf, $\delta^{18}O$, and U-Pb age data from the upper Murmac Bay Group. Beam size of 49μm was used for all Hf analyses except where indicated by bold text, which used a beam size of 40μm

Sample	$^{176}Hf/^{177}Hf$	Error (2SE)	$^{176}Lu/^{177}Hf$	Error (2SE)	$^{176}Yb/^{177}Hf$	Error (2SE)	Th/U	$^{207}Pb/^{206}Pb$ Age (Ma)	1σ Error (Ma)	Disc. %	T_{DM} Hf (Ma)	εHf (t)	Error (2SE)	$\delta^{18}O$ ‰	2σ Error ‰
s3179-001.1	0.281550	0.000025	0.001476	0.000074	0.034708	0.002211	0.14	2335	16	-1.2	2777	-2.0	0.8	8.91	0.22
s3179-010.1	0.281379	0.000022	0.000679	0.000006	0.016599	0.000198	0.20	2044	18	-2.2	2556	-2.6	0.9	9.06	0.28
s3179-013.1	0.281418	0.000024	0.000738	0.000005	0.018620	0.000155	0.61	2190	29	+1.3	2354	5.0	1.0	4.90	0.26
s3179-015.1	**0.281483**	**0.000032**	**0.000972**	**0.000014**	**0.026259**	**0.000395**	**1.01**	**2014**	**11**	**-6.1**	**2735**	**-0.7**	**1.5**	**5.55**	**0.23**
s3179-019.1	0.281506	0.000026	0.001121	0.000086	0.029391	0.002335	0.71	2702	13	+5.6	2715	5.2	0.8	6.28	0.21
s3179-021.1	0.281446	0.000031	0.001046	0.000043	0.028376	0.001230	0.38	2517	19	+5.1	2694	2.5	1.5	6.53	0.23
s3179-049.1	0.281452	0.000022	0.000739	0.000025	0.017250	0.000548	0.77	2273	33	-7.6	2696	1.9	0.6	5.82	0.23
s3179-050.1	0.281373	0.000026	0.000975	0.000088	0.025089	0.002308	0.54	2176	12	+4.5	2867	-0.8	1.1	6.01	0.21
s3179-059.1	**0.281437**	**0.000019**	**0.000867**	**0.000032**	**0.023275**	**0.001157**	**0.54**	**2094**	**9**	**-2.2**	**2517**	**-1.0**	**1.3**	**7.54**	**0.19**
s3179-062.1	0.281370	0.000026	0.000888	0.000068	0.023338	0.001848	0.14	2103	9	-1.0	2433	0.8	1.0	8.85	0.25
s3179-073.1	0.281436	0.000020	0.000674	0.000019	0.018219	0.000628	0.15	2072	12	+3.3	2535	-1.7	0.9	8.09	0.16
s3179-076.1	**0.281626**	**0.000030**	**0.002383**	**0.000105**	**0.060972**	**0.002775**	**0.40**	**2113**	**21**	**+0.1**	**2415**	**1.3**	**1.4**	**6.70**	**0.31**
s3179-085.1	0.281341	0.000022	0.001360	0.000014	0.035014	0.000384	0.28	2293	15	-3.9	2835	-3.9	1.2	8.05	0.17
s3179-094.1	0.281343	0.000023	0.001117	0.000031	0.027736	0.000887	0.34	2242	20	-4.0	2512	1.5	0.9	6.55	0.21
s3179-095.1	**0.281626**	**0.000026**	**0.000884**	**0.000038**	**0.020484**	**0.000952**	**0.64**	**2169**	**21**	**-7.4**	**2609**	**-1.5**	**1.5**	**7.52**	**0.28**
s3179-110.1	0.281382	0.000029	0.001434	0.000071	0.037495	0.001952	0.72	2021	28	+36.1	2658	0.2	1.0	5.53	0.24
s3179-111.1	0.281615	0.000035	0.001387	0.000055	0.034909	0.001342	0.36	2168	10	-2.4	2651	1.5	1.1	6.27	0.23
s3179-113.1	0.281535	0.000025	0.000969	0.000082	0.024478	0.002197	0.50	2146	18	-1.9	2576	-1.3	0.7	6.83	0.22
s3179-126.1	0.281403	0.000024	0.000892	0.000067	0.023218	0.001784	0.46	2585	15	+0.6	3089	0.1	1.2	4.38	0.28
s3179-128.1	0.281377	0.000023	0.001790	0.000088	0.043300	0.002158	0.27	2336	12	+0.1	2750	-1.5	1.1	7.14	0.21
s3177-001.1	0.281387	0.000022	0.000930	0.000029	0.023309	0.000748	0.52	2005	18	+4.8	2695	-0.3	0.9	5.69	0.24
s3177-002.1	0.281517	0.000024	0.000666	0.000068	0.018453	0.001808	0.62	2320	12	+4.9	2736	1.8	0.8	5.26	0.25
s3177-004.1	0.281569	0.000025	0.001792	0.000104	0.048943	0.002947	0.47	2315	9	+3.0	2629	3.0	0.9	5.64	0.19
s3177-006.1	0.281560	0.000025	0.002433	0.000068	0.063849	0.001771	*0.00*	1938	10	-0.0	2518	-3.5	1.1	10.03	0.23
s3177-011.2	0.281562	0.000026	0.000783	0.000005	0.019288	0.000125	0.23	2058	15	+1.8	2726	-0.3	0.9	6.49	0.21
s3177-014.1	0.281328	0.000022	0.000611	0.000016	0.015203	0.000410	0.39	1935	9	-16.5	3056	-5.0	1.1	5.81	0.24
s3177-015.1	0.281431	0.000030	0.001062	0.000038	0.027360	0.000977	0.61	2028	22	+4.0	2529	-2.3	0.8	7.06	0.19

s3177-017.2	0.281366	0.000021	0.000754	0.000058	0.019418	0.001652	0.38	2161	11	-0.5	2650	-2.4	0.9	6.71	0.22
s3177-033.1	0.281353	0.000023	0.000658	0.000030	0.016659	0.000783	0.63	2096	26	+0.3	2546	-1.5	0.7	7.98	0.20
s3177-034.1	0.281407	0.000026	0.001038	0.000070	0.026584	0.001881	0.55	2351	14	+2.3	2754	1.9	0.9	6.31	0.25
s3177-035.1	0.281412	0.000023	0.001145	0.000030	0.029370	0.000848	0.29	1950	18	+5.4	3025	-4.5	0.7	6.15	0.20
s3177-036.1	0.281413	0.000022	0.001236	0.000010	0.032926	0.000306	0.59	2025	25	+6.3	2540	1.6	1.1	6.17	0.23
s3177-037.1	0.281311	0.000021	0.000610	0.000010	0.015571	0.000213	0.48	2317	12	+3.6	2956	-0.7	0.8	6.25	0.21
s3177-038.1	0.281454	0.000027	0.000938	0.000008	0.026129	0.000318	0.61	2279	8	-0.8	2964	-1.1	0.8	6.42	0.24
s3177-054.1	0.281604	0.000019	0.001037	0.000098	0.027323	0.002800	0.71	2084	17	+1.4	2283	5.0	0.9	6.42	0.24
s3177-057.1	0.281283	0.000022	0.000451	0.000018	0.011378	0.000530	0.37	2302	13	+5.4	2625	0.3	1.0	6.82	0.24
s3177-059.1	0.281344	0.000027	0.001170	0.000111	0.029155	0.002537	0.94	2021	14	+3.5	2459	2.4	1.3	5.97	0.24
s3177-061.1	0.281380	0.000026	0.000656	0.000014	0.016758	0.000292	0.82	2080	10	-2.0	2376	1.5	0.9	6.57	0.21
s3177-064.1	0.281436	0.000025	0.000845	0.000023	0.022404	0.000588	0.49	2314	24	-1.8	2538	2.2	0.8	7.27	0.22
s3177-065.1	0.281306	0.000037	0.001126	0.000056	0.029574	0.001681	0.77	2500	9	-1.9	2677	4.0	0.8	5.13	0.19
s3177-067.1	0.281466	0.000020	0.001535	0.000085	0.042355	0.002516	0.45	2330	8	-4.5	2735	1.9	0.8	6.03	0.19
s3177-071.1	0.281376	0.000019	0.000691	0.000025	0.017306	0.000650	*0.01*	1931	11	-5.7	2438	-2.1	0.9	9.74	0.24
s3177-072.1	0.281364	0.000021	0.000893	0.000034	0.022519	0.000754	0.33	2089	13	+5.4	2372	1.7	0.9	7.50	0.20
s3177-081.1	0.281230	0.000034	0.001124	0.000017	0.030172	0.000488	0.20	2003	14	-1.3	2459	-1.3	0.9	7.80	0.25
s3177-083.1	0.281501	0.000033	0.001136	0.000028	0.029950	0.000939	0.44	1970	16	-3.3	2620	0.2	0.9	5.56	0.26
s3177-084.1	0.281429	0.000018	0.000757	0.000040	0.019869	0.001240	0.55	2334	9	+1.8	2869	0.4	0.8	6.32	0.22
s3177-087.1	0.281315	0.000019	0.000657	0.000037	0.016537	0.000961	0.56	2297	14	+11.3	2654	2.6	1.1	6.16	0.25
s3177-089.1	0.281431	0.000024	0.000988	0.000043	0.026633	0.001099	0.42	2260	27	+6.7	2613	-0.1	0.7	6.63	0.23
s3177-093.1	0.281552	0.000022	0.000785	0.000003	0.020399	0.000080	0.52	2304	22	-1.9	2837	0.6	0.8	6.07	0.17
s3177-096.1	0.281432	0.000025	0.000994	0.000062	0.024888	0.001033	0.46	2297	14	-6.5	2728	1.7	0.9	6.03	0.21
s3177-100.1	0.281447	0.000022	0.000584	0.000041	0.015758	0.001166	0.48	2146	16	-2.8	2597	-1.7	0.8	8.42	0.23
s3177-101.1	0.281348	0.000027	0.001033	0.000040	0.026214	0.001037	0.29	2119	11	-1.7	2610	-2.4	0.8	10.65	0.19
s3177-102.1	0.281433	0.000025	0.001030	0.000045	0.029096	0.001525	0.43	2300	25	+2.0	2689	-0.9	0.7	7.92	0.17
s3177-111.1	0.281263	0.000025	0.000723	0.000054	0.018175	0.001405	0.34	2313	13	+0.1	2543	3.9	0.9	5.33	0.23
s3177-114.2	0.281506	0.000031	0.001198	0.000063	0.034141	0.001775	0.40	1929	13	-1.2	2303	0.4	0.7	6.56	0.22
s3177-116.1	0.281386	0.000028	0.001253	0.000046	0.033669	0.001446	0.12	2041	19	-1.6	2816	-7.6	0.8	6.93	0.22

s3177-119.1	0.281414	0.000028	0.001746	0.000086	0.048223	0.002818	0.65	2320	13	+8.4	2914	-0.2	1.0	5.76	0.21
s3177-121.1	0.281373	0.000022	0.000918	0.000030	0.024938	0.000766	0.47	2219	11	+3.8	2861	-0.4	0.9	6.22	0.24
s3177-122.1	0.281374	0.000037	0.000852	0.000027	0.022602	0.000714	0.37	2104	15	-1.0	2543	-1.3	0.9	7.49	0.24
s3177-125.1	0.281436	0.000026	0.000858	0.000023	0.024081	0.000398	0.95	2308	32	+0.2	3043	-1.7	1.3	6.38	0.24
s3177-128.1	0.281359	0.000041	0.000977	0.000275	0.027743	0.008066	0.35	2075	26	-1.9	2547	-1.9	0.7	8.31	0.19
s3177-132.1	0.281400	0.000039	0.000714	0.000034	0.017995	0.001151	0.51	2259	12	+7.5	2825	0.3	0.7	5.67	0.26
s3177-133.2	0.281401	0.000025	0.000767	0.000015	0.019674	0.000347	0.36	2308	9	-4.5	2828	0.7	0.7	5.32	0.24
s3177-134.1	**0.281352**	**0.000027**	**0.000802**	**0.000014**	**0.022168**	**0.000468**	**0.14**	**2333**	**14**	**-1.5**	**2871**	**-2.4**	**2.4**	**9.03**	**0.16**
s3177-141.1	0.281345	0.000023	0.000781	0.000010	0.020541	0.000256	0.54	2051	13	+7.9	2751	-0.6	1.2	6.16	0.19
s3177-145.1	0.281386	0.000022	0.001112	0.000037	0.029609	0.000974	0.27	1939	13	-0.3	2602	-5.2	0.6	7.20	0.21
s3177-153.1	0.281371	0.000024	0.000777	0.000047	0.018478	0.001003	0.46	2315	18	+0.7	2940	-0.5	0.7	6.44	0.21
s3177-158.1	0.281328	0.000025	0.000570	0.000005	0.014276	0.000138	0.39	2239	12	-0.7	2717	1.4	0.8	5.85	0.23
s3177-169.1	0.281363	0.000031	0.000808	0.000050	0.021616	0.001016	0.45	2110	11	-0.1	2472	3.0	0.8	6.05	0.22
s3177-171.1	0.281358	0.000023	0.000971	0.000011	0.025304	0.000378	0.35	2032	24	+6.0	2584	-3.3	0.9	7.35	0.26
s3177-178.1	0.281321	0.000025	0.001329	0.000027	0.037085	0.000845	0.45	2083	12	+1.9	2510	-1.0	0.8	7.03	0.21
s3177-195.1	0.281399	0.000032	0.001178	0.000091	0.030587	0.002539	0.67	2325	8	+1.4	2879	0.3	1.0	5.95	0.23
s3177-196.1	0.281363	0.000019	0.000588	0.000020	0.015100	0.000565	0.29	2144	16	+19.3	2549	-0.8	0.9	7.66	0.26
s3177-203.1	0.281158	0.000026	0.000593	0.000041	0.013804	0.001017	0.51	2539	10	+3.3	2827	2.6	0.9	6.12	0.20
s3177-212.1	0.281415	0.000025	0.001533	0.000033	0.042172	0.001015	0.58	2080	36	-3.0	2447	0.1	1.1	7.05	0.32
s3177-217.1	0.281325	0.000027	0.000717	0.000018	0.020412	0.000493	1.05	2280	14	-0.4	2844	0.3	1.0	4.64	0.26
s3177-230.1	0.281413	0.000029	0.001074	0.000118	0.029310	0.003327	0.78	2120	8	-3.6	2644	-3.0	1.0	7.82	0.21
s3177-239.1	0.281483	0.000023	0.001131	0.000047	0.030094	0.001197	0.34	2119	29	-2.9	2660	-3.3	0.8	7.99	0.24
s3177-244.1	0.281421	0.000018	0.000611	0.000006	0.015490	0.000158	0.49	2268	16	-6.3	2843	0.2	1.3	5.79	0.21
s3177-247.1	0.281403	0.000015	0.001045	0.000050	0.029046	0.001701	0.62	2109	14	+1.7	2541	-1.2	0.9	7.32	0.27
s3178-004.1	**0.281350**	**0.000021**	**0.000436**	**0.000012**	**0.011360**	**0.000243**	**0.56**	**2261**	**11**	**+4.2**	**2917**	**-2.3**	**1.4**	**5.71**	**0.19**
s3178-010.1	0.281366	0.000022	0.000978	0.000026	0.025896	0.000817	0.65	2283	20	+2.9	2721	1.7	1.4	6.14	0.26
s3178-013.1	0.281397	0.000021	0.000686	0.000033	0.015767	0.000426	0.64	2134	8	-6.4	2916	-1.8	0.9	5.48	0.21
s3178-014.1	0.281367	0.000024	0.000594	0.000009	0.015589	0.000242	0.49	2176	26	+3.0	2672	-2.6	1.0	6.56	0.23
s3178-016.1	0.281411	0.000018	0.000553	0.000023	0.014338	0.000560	0.61	2307	18	+3.4	2639	0.1	0.8	7.02	0.24

s3178-018.1	0.281369	0.000019	0.000829	0.000027	0.020998	0.000701	0.37	2147	12	-1.8	2991	-2.5	0.8	6.28	0.23
s3178-026.1	0.281419	0.000021	0.000741	0.000013	0.018652	0.000250	0.58	2324	20	+8.7	2769	1.5	0.8	5.98	0.28
s3178-027.1	0.281335	0.000020	0.000689	0.000038	0.017210	0.000882	0.60	2317	13	+1.4	2888	0.1	0.9	6.30	0.21
s3178-031.1	**0.281302**	**0.000048**	**0.000973**	**0.000044**	**0.026208**	**0.001447**	**0.29**	**1846**	**9**	**+2.8**	**3395**	**-1.5**	**1.9**	**5.94**	**0.25**
s3178-032.1	0.281527	0.000027	0.002010	0.000108	0.053315	0.002948	0.36	2268	9	+0.5	2910	-0.6	0.8	6.07	0.16
s3178-039.1	0.281438	0.000033	0.001209	0.000157	0.032101	0.004263	0.45	2262	9	+6.1	3083	-2.6	0.9	6.46	0.32
s3178-048.1	**0.281393**	**0.000020**	**0.000771**	**0.000037**	**0.021690**	**0.001211**	**0.68**	**2307**	**8**	**-1.5**	**2759**	**-0.2**	**1.3**	**6.18**	**0.25**
s3178-052.1	0.281694	0.000029	0.001635	0.000144	0.040285	0.003860	0.55	2292	9	-1.9	2809	0.8	0.7	5.59	0.23
s3178-053.1	0.281473	0.000020	0.000695	0.000006	0.018072	0.000128	0.32	2369	32	+2.7	3357	-4.8	0.9	5.54	0.24
s3178-056.1	0.281348	0.000022	0.000551	0.000004	0.014190	0.000116	0.77	2255	8	+5.1	2823	0.3	0.9	2.93	0.27
s3178-058.1	0.281167	0.000021	0.000556	0.000005	0.014731	0.000144	0.89	2315	7	-1.0	2918	-0.3	1.0	6.35	0.22
s3178-065.2	0.281436	0.000019	0.000825	0.000048	0.020069	0.001091	0.40	2149	16	+0.6	2900	-1.5	1.0	6.47	0.20
s3178-068.2	0.281446	0.000017	0.000577	0.000006	0.014147	0.000174	0.38	1999	9	-7.2	2669	-2.4	0.8	3.71	0.15
s3178-069.1	0.281436	0.000019	0.000490	0.000013	0.012051	0.000332	0.39	2091	13	+1.4	2889	-1.8	0.6	5.51	0.17
s3178-074.1	0.281317	0.000032	0.000630	0.000016	0.016529	0.000530	0.60	2299	11	-7.3	2737	1.6	0.5	5.57	0.18
s3178-075.1	0.281442	0.000019	0.000752	0.000017	0.018162	0.000459	0.44	2336	12	-5.5	2775	1.5	0.8	5.70	0.28
s3178-076.1	0.281413	0.000024	0.000957	0.000006	0.025407	0.000246	0.46	2296	12	+4.3	2849	0.4	0.8	6.42	0.19
s3178-077.1	0.281429	0.000024	0.000768	0.000010	0.020464	0.000219	0.24	2289	11	+7.5	2719	1.8	0.8	5.80	0.24
s3178-079.1	0.281395	0.000017	0.000623	0.000021	0.015931	0.000539	0.65	2305	14	+6.4	2782	1.2	0.8	6.39	0.17
s3178-081.1	0.281447	0.000018	0.000876	0.000084	0.023102	0.002330	0.74	2094	46	-0.9	2570	-2.0	0.6	6.54	0.23
s3178-086.1	0.281329	0.000020	0.000988	0.000051	0.025901	0.001450	0.66	2306	16	+5.4	2808	0.9	0.7	5.74	0.22
s3178-088.1	0.281485	0.000024	0.001191	0.000071	0.030632	0.001955	0.56	2290	16	+0.3	2658	2.5	0.8	5.83	0.18
s3178-089.1	0.281356	0.000025	0.000862	0.000034	0.021689	0.000928	0.46	2304	10	+0.9	2897	-0.1	0.7	6.27	0.16
s3178-095.1	**0.281413**	**0.000021**	**0.000589**	**0.000010**	**0.014827**	**0.000232**	**0.68**	**2315**	**10**	**-1.2**	**2731**	**-0.7**	**1.0**	**6.62**	**0.20**
s3178-096.1	0.281320	0.000029	0.000773	0.000090	0.022246	0.002842	0.32	2112	18	-1.4	2704	0.4	0.9	6.44	0.23
s3178-105.1	**0.281347**	**0.000032**	**0.001176**	**0.000095**	**0.031759**	**0.002644**	**0.39**	**2160**	**14**	**+4.1**	**2549**	**-2.8**	**1.4**	**7.01**	**0.23**
s3178-110.2	0.281367	0.000018	0.000786	0.000008	0.019306	0.000213	0.30	2313	15	+8.7	2716	2.0	0.7	6.38	0.23
s3178-121.1	0.281474	0.000019	0.001363	0.000064	0.037725	0.001872	0.64	2056	14	-4.2	2196	5.7	1.0	5.90	0.21
s3178-123.2	0.281376	0.000016	0.000791	0.000013	0.020854	0.000327	0.49	2127	11	+8.1	2690	0.7	0.7	5.48	0.21

s3178-126.1	0.281374	0.000024	0.000885	0.000014	0.022962	0.000392	0.32	2311	10	-2.1	2613	0.7	0.8	7.68	0.25
s3178-127.1	0.281240	0.000025	0.000698	0.000024	0.018100	0.000722	0.31	2413	21	-5.0	3268	-3.4	0.7	5.93	0.18
s3178-128.1	0.281565	0.000019	0.001053	0.000089	0.025139	0.002103	0.40	2089	9	-2.9	2871	-1.6	0.7	5.22	0.22
s3178-133.1	0.281348	0.000025	0.000747	0.000059	0.018226	0.001309	0.43	2058	12	-4.3	2848	-1.6	0.6	5.30	0.26
s3178-135.1	0.281304	0.000023	0.001640	0.000040	0.044873	0.001252	0.42	2088	15	+0.7	2828	-1.1	0.7	5.12	0.24
s3178-139.1	**0.281410**	**0.000026**	**0.000111**	**0.000005**	**0.003419**	**0.000154**	**0.32**	**2258**	**19**	**-2.2**	**3006**	**0.3**	**1.1**	**5.83**	**0.21**
s3178-140.1	0.281568	0.000028	0.001051	0.000029	0.026189	0.000703	0.46	2091	9	-4.7	2842	-1.3	0.7	5.07	0.17
s3178-141.1	0.281517	0.000042	0.001043	0.000046	0.026378	0.001212	0.43	2282	10	-5.8	2717	1.7	0.9	5.50	0.21
s3178-141.2	0.281232	0.000023	0.000737	0.000030	0.018895	0.000833	0.45	2305	10	+0.1	2609	3.1	0.9	6.13	0.24
s3178-142.1	0.281279	0.000042	0.000817	0.000046	0.021901	0.001112	0.50	2303	21	+6.2	2701	2.1	0.6	6.48	0.21
s3178-149.1	0.281402	0.000017	0.000467	0.000013	0.011896	0.000356	0.47	2071	13	-0.0	2864	-1.7	0.6	5.42	0.22
s3178-154.1	0.281409	0.000030	0.000999	0.000035	0.025504	0.000943	0.50	2308	12	-1.2	2953	-0.7	0.7	6.46	0.25
s3178-155.1	0.281456	0.000038	0.000941	0.000024	0.026040	0.000926	0.87	2078	25	-4.4	2775	-0.6	0.9	5.70	0.16
s3178-156.2	0.281466	0.000028	0.000112	0.000009	0.004041	0.000292	0.37	2392	44	-5.3	2743	2.3	0.9	5.53	0.26
s3178-157.1	0.281427	0.000026	0.000369	0.000064	0.011726	0.001897	0.49	2332	7	-4.8	2600	3.5	0.7	5.74	0.21
s3178-158.1	0.281512	0.000040	0.001070	0.000020	0.028485	0.000767	0.37	2290	16	+0.3	2690	-1.1	1.0	7.42	0.24
s3178-168.1	**0.281247**	**0.000033**	**0.000912**	**0.000057**	**0.024733**	**0.001371**	**0.84**	**2315**	**13**	**-1.6**	**2914**	**-0.3**	**2.4**	**5.77**	**0.22**
s3178-169.1	0.281421	0.000024	0.000671	0.000045	0.018022	0.001006	0.46	2324	11	-2.3	2784	1.3	0.7	5.45	0.22
s3178-174.1	0.281396	0.000042	0.001016	0.000022	0.027398	0.000488	0.19	2104	11	-3.2	2510	-0.7	0.7	7.73	0.22
s3178-179.1	0.281561	0.000028	0.001604	0.000047	0.043177	0.001213	0.44	2157	22	+1.9	2970	-2.2	0.6	6.34	0.21
s3178-184.1	0.281485	0.000032	0.001103	0.000097	0.029063	0.002310	0.87	2324	10	-3.1	2777	1.4	0.9	6.34	0.17
s3178-188.1	0.281406	0.000021	0.000739	0.000056	0.020342	0.001583	0.17	2357	21	+3.3	2810	-2.3	0.9	6.61	0.28
s3178-197.2	0.281146	0.000033	0.000409	0.000021	0.011214	0.000539	0.67	2071	20	+1.2	2515	2.2	0.7	5.79	0.20
s3178-198.1	0.281274	0.000032	0.000657	0.000021	0.018066	0.000569	0.54	2310	10	-3.1	2629	0.4	0.9	6.60	0.18

Table C.2 Ages, locations, εHf, and εNd values for potential source rocks for upper MBG detrital zircons. εNd is converted to εHf* using the equation for the Terrestrial Array: εHf*=1.55*εNd +1.21 (Vervoort et al., 2011). Asterisks (*) indicate results from this study.

Unit	Drill / Rock Name	Latitude	Longitude	U/Pb Age (Ma)	εNd	εHf	T_{DM} Nd (Ga)	Reference
Rae Craton								
Upper Murmac Bay Group	Pelite-Psammopelite	~ 59.5	~ -108.6	<1999 ± 13 to >1930		-7.6 to +5.7*		Shiels et al., 2016; This Study*
Lower Murmac Bay Group	Quartzite	59.55611	-108.44002	<2333	-7.50	-10.42		Hartlaub et. al., 2004
North Shore Plutons	Hayter Bay monzogranite	59.48676	-108.17383	2297 ± 10	-6.70	-9.18		Hartlaub et al., 2007
North Shore Plutons	Hayter Bay monzogranite	59.48676	-108.17383	2297 ± 10		-12.8 to -3.40		Hartlaub et al., 2007; Partin et. al., 2014b
North Shore Plutons	Gunnar monzogranite	59.38538	-108.85306	2321 ± 3	-4.30	-5.46		Hartlaub et al., 2007
North Shore Plutons	Gunnar monzogranite	59.38538	-108.85306	2321 ± 3		-6.20 to -2.40		Hartlaub et al., 2007; Partin et. al., 2014b
North Shore Plutons	Geebee Lake tonalite	59.54179	-108.38858	2320 ± 44		-11.5 to -8.00		Hartlaub et al., 2007; Partin et. al., 2014b
North Shore Plutons	Macintosh Bay monzogranite	59.46456	-108.30698	2330 ± 5	-1.50	-1.12		Hartlaub et al., 2007
North Shore Plutons	Macintosh Bay monzogranite	59.46456	-108.30698	2330 ± 5		-3.60 to -0.50		Hartlaub et al., 2007; Partin et. al., 2014b
Beaverlodge domain	Cornwall Bay granite	59.45806	-108.46377	2999 ± 7	+1.70	+3.85		Hartlaub et. al., 2004
Beaverlodge domain	Cornwall Bay granite	59.45806	-108.46377	3060 ± 40	+1.20	+3.07		Hartlaub et. al., 2004
Snowbird Lake area	Chipman tonalite	60.36134	-103.13693	3385 ± 16	+2.43	+4.98	3.36	Martel et. al., 2008
Snowbird Lake area	Zebra tonalite	56.60705	-103.93993	2735 ± 6	-0.61	+0.26	2.99	Martel et. al., 2008
Snowbird Lake area	Camp granodiorite	60.86182	-103.37161	2661 ± 12	+0.97	+2.71	2.76	Martel et. al., 2008
Snowbird Lake area	Super Mario megacrystic granite	55.60583	-103.56280	2668 +9/ -6	+1.96	+4.25	2.71	Martel et. al., 2008

Snowbird Lake area	Rambo granodiorite	60.34338	-103.37916	2547 ± 5	-0.54	0.37	2.79	Martel et. al., 2008
Snowbird Lake area	metapsammite	60.33855	-103.42883	2.07 - 1.92	-4.65	-6.00	2.67	Martel et. al., 2008
Hearne Craton								
Snowbird Lake area	Kasba rhyolite	60.25640	-102.39236	2724 ± 12	1.97	4.26	2.76	Martel et. al., 2008
Taltson								
Taltson Basement Complex	Cornwall Lake syenogranite gneiss	59.53830	-110.52290	2138 ± 2	-1.80	-1.58	2.72	McNicoll et al., 2000
Taltson Basement Complex	Cornwall Lake hornblende granite gneiss	59.54117	-110.68075	2393 +12/ -20	-12.50	-18.17	3.19	McNicoll et al., 2000
Taltson Basement Complex	Potts Lake banded mafic gneiss	60.12410	-110.45310	2295 +6/ -5	-9.20	-13.05	3.34	McNicoll et al., 2000
Taltson Basement Complex	Mercredi Lake granodiorite gneiss	59.80490	-110.71270	2382 ± 5	-5.70	-7.63	2.84	McNicoll et al., 2000
Taltson Basement Complex	Andrew Lake tonalite gneiss	59.11099	-110.48869	2562 ± 6	-5.90	-7.94	2.83	McNicoll et al., 2000
Taltson Basement Complex	Andrew Lake migmatitic tonalite gneiss	59.47250	-110.40580	3076 +5/ -15	-14.30	-20.96	3.73	McNicoll et al., 2000
Taltson Basement Complex	Leland Lake granodiorite gneiss	59.74134	-111.11521	3186 +17/ -13	-9.90	-14.14	3.29	McNicoll et al., 2000
Taltson Arc Subsurface	Imperial Wolverine syenogranite	55.59715	-112.65475	2174 +54/ -43	-5.00	-6.54	2.66	Thériault and Ross, 1991; Villeneuve et. al., 1993
Taltson Arc Subsurface	Merrill Arab Chard syenogranite	55.80078	-110.85624	1973 ± 5	-3.70	-4.53		Thériault and Ross, 1991; Villeneuve et. al., 1993
Taltson Arc Subsurface	ROC Watchusk Lake monzogranite	56.17898	-110.43705	1948 ± 4	-9.70	-13.83		Thériault and Ross, 1991; Villeneuve et. al., 1993
Taltson Arc Subsurface	Bear Vampire #1 monzogranite	56.57167	-111.84943	1932	-6.30	-8.56	2.69	Thériault and Ross, 1991; Villeneuve et. al., 1993
Taltson Arc Subsurface	California Standard Mikkwa granite	57.52065	-113.30702	1937 +61/ -45	-5.30	-7.01	2.57	Thériault and Ross, 1991; Villeneuve et. al., 1993

Slave Craton								
Blatchford Lake Intrusive Suite	Nechalacho Layered Suite	62.09796	-112.59515	2164 ± 11	+1.00 to +2.50	+2.76 to +5.09		Mumford, 2013
Blatchford Lake Intrusive Suite	Grace Lake granite	62.12723	-112.58301	2176 ± 1.3	+1.00 to +1.71	+2.76 to +3.85		Sinclair et. al., 1994; Mumford, 2013
Blatchford Lake Intrusive Suite	Thor Lake leucosyenite	62.08420	-112.52225	2177 ± 1.6	+1.70 to +2.40	+3.85 to +4.93		Mumford, 2013
Yellowknife Supergroup	Burwash Formation turbidites	~ 62.5	~ -114	2600	-5.98 to -3.18	-8.06 to -3.72		Mumford, 2013; Yamashita & Creaser, 1999
Yellowknife Supergroup	Morose granite			2586	-3.00 to -0.25	-3.44 to +0.82		Mumford, 2010; 2013
Yellowknife Supergroup	Defeat granodiorite	62.41217	-114.19050	2621 +5/ -8	-5.90 to -2.90	-7.94 to -3.29		Yamashita et. al., 1999; Mumford et. al., 2010
Buffalo Head Terrane								
Buffalo Head Subsurface	Imperial Pelican Hills gneiss	55.63712	-113.86476	2017 +2/ -1	-6.00	-8.09	2.74	Thériault and Ross, 1991; Villeneuve et. al., 1993
Buffalo Head Subsurface	IOE Sylvia granitoid	55.30318	-114.72360	2317 +27/ -15	+1.00	+2.76	2.65	Thériault and Ross, 1991
Buffalo Head Subsurface	IOE Sylvia granitoid	55.30318	-114.72360	2317 +27/ -15	-1.00	-0.34	2.65	Villeneuve et. al., 1993
Buffalo Head Subsurface	Imperial Joussard gneiss	55.30366	-115.87676	2324 ± 1	-1.30	-0.81	2.82	Thériault and Ross, 1991; Villeneuve et. al., 1993
Buffalo Head Subsurface	Chevron Hunt Creek	56.88838	-114.91789	1991 +225/ -41	-4.30	-5.46	2.83	Thériault and Ross, 1991; Villeneuve et. al., 1993
Buffalo Head Subsurface	Imperial Virginia Hills	54.49231	-115.68059	1998 +5/ -4	-3.20	-3.75	2.69	Thériault and Ross, 1991; Villeneuve et. al., 1993
Buffalo Head Subsurface	Dome et al Peavine leucogranite	55.48858	-117.03125	2072 ± 6	-0.40	+0.59	2.51	Thériault and Ross, 1991; Villeneuve et. al., 1993
Buffalo Head Subsurface	Canhunter et al Golden granitoid	56.47006	-116.23162	1990 +13/ -12	-6.30	-8.56	2.81	Thériault and Ross, 1991; Villeneuve et. al., 1993
Buffalo Head Subsurface	Chevron Irving Cadotte mafic gneiss	56.56452	-117.34875	2165 +5/ -4	-1.10	-0.50	2.67	Thériault and Ross, 1991; Villeneuve et. al., 1993

Buffalo Head Subsurface	Fina Keg River monzonite augen gneiss	57.88453	-117.34911	1993 +10 /-5	-2.30	-2.36	2.54	Thériault and Ross, 1991; Villeneuve et. al., 1993
Buffalo Head Subsurface	H.B. East Virginia Hills metagabbro	54.66691	-114.90582	2332 +202/ -133	-3.40	-4.06	2.75	Thériault and Ross, 1991; Villeneuve et. al., 1993
Buffalo Head Subsurface	Clear Hills felsic metavolcanics	56.62277	-118.22928	2257 +25/ -21	+0.20	+1.52	2.67	Thériault and Ross, 1991; Villeneuve et. al., 1993
Chinchaga Domain								
Chinchaga Subsurface	Scurry Rainbow Cariibou Banff alkali porpyritic granite	58.73828	-117.08976	2088 +23/ -21	-0.40	-0.59	2.46	Thériault and Ross, 1991; Villeneuve et. al., 1993
Chinchaga Subsurface	Chevron et al Sheldon monzonite augen gneiss	55.45976	-117.56881	2159 +11/ -10	-1.80	-1.58	2.68	Thériault and Ross, 1991; Villeneuve et. al., 1993
Chinchaga Subsurface	Two Creek quartzofeldspathic gneiss	54.43427	-116.31065	2186 +68/ -51	+0.60	+2.14	2.57	Thériault and Ross, 1991; Villeneuve et. al., 1993